UNIVERSITATSKLINIKUM HAMBURG-EPPENDORF

II. Medizinische Klinik und Poliklinik
Onkologie, Hämatologie, Knochenmarktransplantation mit der Sektion Pneumologie

Prof. Dr. med. Carsten Bokemeyer

Bedeutung der GLI-Transkriptionsfaktoren in der Resistenzentwicklung gegenüber Chemotherapie und deren Inhibition in der akuten myeloischen Leukämie

Dissertation

zur Erlangung des Grades eines Doktors der Medizin
an der Medizinischen Fakultät der Universität Hamburg.

vorgelegt von:

Fabian Freisleben
aus Friedrichshafen

Hamburg 2023

Angenommen von der
Medizinischen Fakultät der Universität Hamburg am: 11.03.2024

Veröffentlicht mit Genehmigung der
Medizinischen Fakultät der Universität Hamburg.

Prüfungsausschuss, der/die Vorsitzende: Prof. Dr. Boris Fehse

Prüfungsausschuss, zweite/r Gutachter/in: PD Dr. Jasmin Wellbrock

Inhaltsverzeichnis

1. Originalarbeiten

1.1. Originalarbeit 1: Freisleben et al., Int. J. Mol. Sci. 2020, 21(14), 5084

International Journal of
Molecular Sciences

MDPI

Article

Downregulation of GLI3 Expression Mediates Chemotherapy Resistance in Acute Myeloid Leukemia

Fabian Freisleben, Lena Behrmann, Vanessa Thaden, Jana Muschhammer, Carsten Bokemeyer, Walter Fiedler and Jasmin Wellbrock *

Department of Oncology, Hematology and Bone Marrow Transplantation with Section Pneumology, Hubertus Wald University Cancer Center, University Medical Center Hamburg-Eppendorf, 20251 Hamburg, Germany; freisleben.fabian@gmail.com (F.F.); le.behrmann@uke.de (L.B.); v.thaden@uke.de (V.T.); j.muschhammer@uke.de (J.M.); c.bokemeyer@uke.de (C.B.); fiedler@uke.de (W.F.)
* Correspondence: j.wellbrock@uke.de; Tel.: +49-40-7410-55606

Received: 26 June 2020; Accepted: 17 July 2020; Published: 18 July 2020

Abstract: Aberrant activation of the hedgehog (HH) pathway is observed in many neoplasms, including acute myeloid leukemia (AML). The glioma-associated oncogene homolog (GLI) transcription factors are the main downstream effectors of the HH signaling cascade and are responsible for the proliferation and maintenance of leukemic stem cells, which support chemotherapy resistance and leukemia relapse. Cytarabine (Ara-C)-resistant variants of AML cell lines were established through long-term cultivation with successively increasing Ara-C concentrations. Subsequently, differences in *GLI* expression were analyzed by RT-qPCR. *GLI3* mRNA levels were detectable in parental Kasumi-1, OCI-AML3, and OCI-AML5 cells, whereas *GLI3* expression was completely silenced in all resistant counterparts. Therefore, we generated GLI3-knockdown cell lines using small hairpin RNAs (shRNA) and evaluated their sensitivity to Ara-C in vitro. The knockdown of GLI3 partly abolished the effect of Ara-C on colony formation and induction of apoptosis, indicating that *GLI3* downregulation results in Ara-C resistance. Moreover, we analyzed the expression of several genes involved in Ara-C metabolism and transport. Knockdown of GLI3 resulted in the upregulation of SAM and HD domain-containing protein 1 (*SAMHD1*), cytidine deaminase (*CDA*), and ATP-binding cassette C11 (*ABCC11*)/multidrug resistance-associated protein 8 (*MRP8*), each of which has been identified as a predictive marker for Ara-C response in acute myeloid leukemia. Our results demonstrate that *GLI3* downregulation is a potential mechanism to induce chemotherapy resistance in AML.

Keywords: AML; GLI3; HH; cytarabine; Ara-C; resistance; *SAMHD1*; *CDA*; *ABCC11*

1. Introduction

Attaining sustained long-term remission in acute myeloid leukemia (AML) patients presents a notable therapeutic challenge. Despite high initial response rates to chemotherapy, the majority of patients suffer from a relapse, ultimately leading to death in most cases [1,2]. Growing evidence indicates that relapse is caused by a small population of leukemic stem cells (LSCs) resistant to chemotherapy, which serve as reservoir for leukemic blasts [3,4]. In the bone marrow niche, hematopoietic stem cells (HSC) maintain their stemness and survival by bidirectional crosstalk with the bone marrow microenvironment [5]. LSCs are able to infiltrate the niche and alter homeostatic processes to maintain their quiescence, survival, and resistance to chemotherapy [6]. The interaction of LSC with the microenvironment involves a variety of stem cell signaling pathways, including the hedgehog (HH) signaling pathway [7].

The HH signaling pathway is a highly conserved signaling cascade that plays a critical role during embryogenesis and is strongly involved in many basic cellular functions, including cell differentiation and proliferation and stem cell maintenance [8]. It is well established that aberrant hedgehog signaling is associated with a wide variety of neoplasms [9], which results in the activation of the GLI transcription factors, the main downstream effectors of the HH signaling cascade. In previous work, we could show that *GLI* expression represents a negative prognostic factor in AML [10].

The GLI transcription factors consist of three members with specialized function and distinct regulation mechanisms: GLI1, GLI2, and GLI3. GLI1 and GLI2 represent transcriptional activators, whereas GLI3 occurs predominantly in its repressor form and functions as a strong repressor of GLI-mediated transcription [11–13]. In the canonical HH pathway, SMO regulates the level of GLI activity by shifting the balance between transcriptional stimulation through activated GLI2 and inhibition through GLI3 in its repressor form (GLI3R), while GLI1 is not expressed in resting cells [13–15]. However, GLI transcription factors represent central hubs in the oncogenic signaling network and can get activated non-canonically by cross-talk with a variety of pathways, including FLT3, PI3K-AKT, RAS–RAF–MEK, or TGFβ [16,17]. In AML cells, HH activation is largely independent of SMO activity but is strongly suppressed by GLI3R protein expression [18]. Analysis of The Cancer Genome Atlas AML data set has shown that *GLI3* expression is epigenetically silenced in the majority of AML patient samples [18]. Consistent with these findings, we could show that *GLI3* expression is absent in most AML patients as determined by qPCR analysis [10].

Several studies have supported the role of activated GLI signaling in the development of resistance to chemotherapy in multiple cancers, including AML, gastric cancer, and ovarian cancer [19–21]. While it has been shown that chemotherapy resistance can be caused by aberrant activation of the transcriptional activators GLI1 or GLI2 [22,23], changes in *GLI3* expression have never been described in this context in AML. We hypothesized that the transcriptional repressor GLI3 may represent a major switch involved in sensitivity to chemotherapy.

2. Results

2.1. GLI3 Expression Silenced in Cytarabine (Ara-C)-Resistant Cell Lines

To better understand the role of the hedgehog pathway in the development of drug resistance and relapse in AML, we generated Ara-C-resistant variants of the AML cell lines Kasumi-1, OCI-AML3, and OCI-AML5 through long-term cultivation with successively increasing Ara-C concentrations. Ara-C resistance was characterized by an IC80 value (80% inhibitory concentration) for cell growth above 10,000 nM (refer to Figure 1 for relative number of viable cells and Figure A1 for cell viability, respectively).

Subsequently, *GLI* expression was analyzed in resistant variants and compared to that in their respective parental cell lines. We could not detect consistently significant changes in *GLI1* and *GLI2* mRNA expression (Appendix A, Figure A2). However, RT-qPCR analysis revealed that *GLI3* expression was completely silenced in Ara-C-RCL Kasumi-1, OCI-AML3, and OCI-AML5, whereas *GLI3* mRNA levels were detectable in their parental counterparts (Figure 2a). Moreover, we could show that resistant OCI-AML3 and OCI-AML5 cells had lower protein levels of both full length GLI3 and its repressor form compared to their parental cell line, using western blot analysis (Figure 2b).

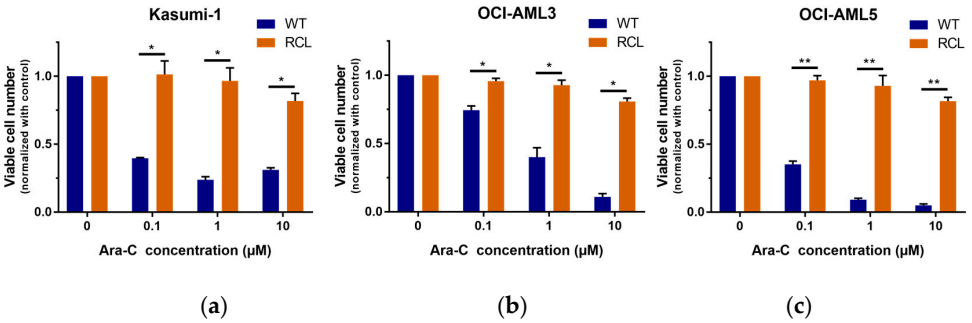

Figure 1. Number of viable cells in resistant vs. parental cell lines following treatment with increasing cytarabine (Ara-C) concentrations. Resistant cell lines (RCL) and wildtype (WT) variants of acute myeloid leukemia (AML) cell lines Kasumi-1 (**a**), OCI-AML3 (**b**), OCI-AML5 (**c**) were plated with different concentrations of Ara-C ranging from 100 nM to 10,000 nM. Cell counts were normalized to the those in untreated controls. The average number of viable cells (Ø) in the untreated control samples was 1.00×10^6 (Kasumi-1), 1.54×10^6 (OCI-AML3), and 1.43×10^6 (OCI-AML3) for WT cells and 1.96×10^6 (Kasumi-1), 1.92×10^6 (OCI-AML3), and 1.75×10^6 (OCI-AML3) for RCL; * $p < 0.05$ and ** $p < 0.01$ in Welch's *t*-test.

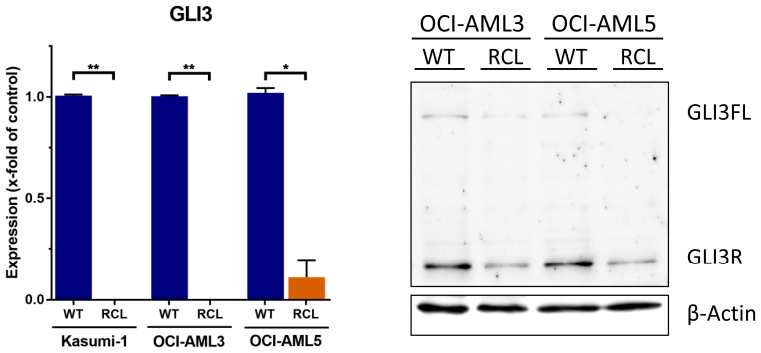

Figure 2. Downregulation of GLI3 in Ara-C resistant cell lines. (**a**) WT and Ara-C-RCL Kasumi-1, OCI-AML3, and OCI-AML5 were analyzed for *GLI3* mRNA levels by RT-qPCR analysis; * $p < 0.05$ and ** $p < 0.01$ in Welch's *t*-test. (**b**) Western blot of full length GLI3 (GLI3FL) and its repressor form (GLI3R) in WT and RCL variants of OCI-AML3 and OCI-AML5.

2.2. GLI3 Knockdown Promotes Resistance to Chemotherapy

For shRNA experiments, we chose the AML cell lines THP-1 and OCI-AML3 that express the highest levels of *GLI3* (Figure A3). To investigate whether GLI3 silencing alone imparted drug resistance, we generated GLI3-knockdown cells by lentiviral transduction of two distinct *GLI3*-specific shRNAs. AML cells with GLI3 knockdown were compared with control cells containing nontargeting shRNA. Compared with the control, *GLI3* expression was reduced to 39.6% (± 31.1%) in THP-1 cells and to 53.7% (± 31.4%) in OCI-AML3 cells (Figure 3).

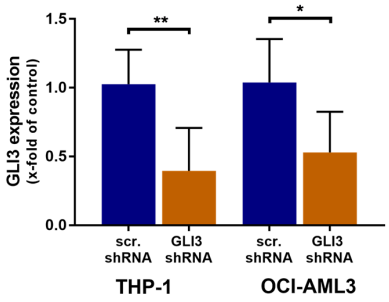

Figure 3. Efficiency of GLI3 knockdown in AML cell lines THP-1 and OCI-AML3. *GLI3* mRNA levels were measured by RT-qPCR following lentiviral transduction with two distinct shRNA targeting *GLI3*. The expression of *GLI3* was normalized to that in control cells transduced with a scrambled control shRNA; * $p < 0.05$ and ** $p < 0.01$ in Welch's *t*-test.

We performed colony formation assays to investigate whether GLI3 knockdown affects the ability of leukemic cells to form colonies upon exposure to Ara-C. GLI3-knockdown and scrambled shRNA control AML cell lines THP-1 and OCI-AML3 were treated with Ara-C concentrations ranging from 25 to 100 nM. Colony numbers were counted on day 7 and normalized to the untreated control. For both GLI3-knockdown cell lines, Ara-C treatment reduced the colony numbers significantly compared to the control cells (Figure 4a,b).

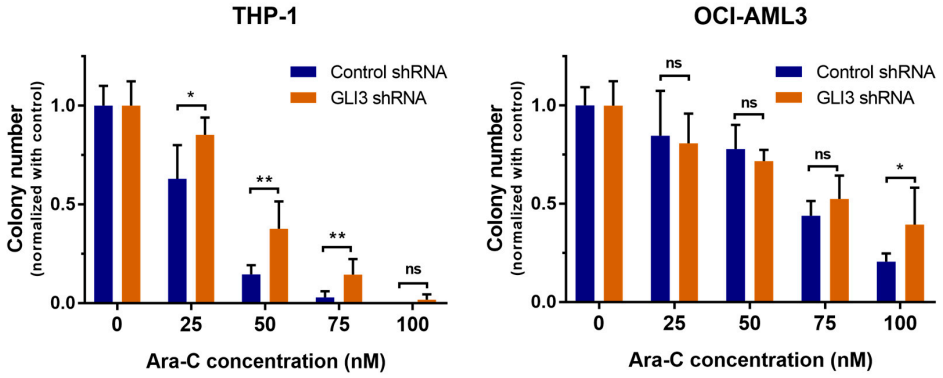

(**a**) (**b**)

Figure 4. GLI3 knockdown partially protects AML cells against the cytotoxic effect of Ara-C. AML cell lines THP-1 (**a**) and OCI-AML3 (**b**) after GLI3 knockdown and treatment with scrambled shRNA control were subjected to different Ara-C concentrations for 7 days. Colony numbers were counted and normalized to those of the untreated controls. The average number of colonies (Ø) in the untreated control samples was 84 (scrambled shRNA) and 62 (GLI3 shRNA) for THP-1 and 72 (scrambled shRNA) and 83 (GLI3 shRNA) for OCI-AML3; * $p < 0.05$ and ** $p < 0.01$ in Welch's *t*-test; ns, statistically not significant.

THP-1 cells transduced with either GLI3-targeted shRNA or non-targeting control shRNA were investigated for apoptosis induction upon Ara-C treatment. Cells were treated with Ara-C concentration ranging from 1 µM to 10 µM, and apoptosis rates were determined by flow cytometry. GLI3 knockdown had the most pronounced effect on apoptosis rates in the presence of high concentrations of Ara-C, with significant differences observed at 2.5 and 5 µM (Figure 5).

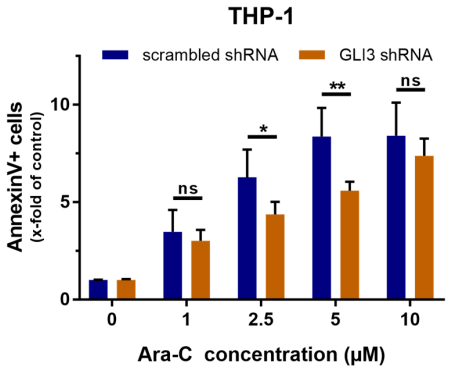

Figure 5. GLI3 knockdown suppresses apoptosis induction upon treatment with Ara-C. THP-1 cells transduced with GLI3-targeted shRNA or scrambled shRNA control were treated with the indicated concentrations of Ara-C, and induction of apoptosis was measured after 48 h by flow cytometry using Annexin V and propidium iodide. In the untreated (control) samples, the majority of cells transduced with scrambled shRNA (Ø 5.9% Annexin V-positive) or GLI3 shRNA (Ø 6.9% Annexin V-positive) were viable. Representative flow cytometry plots are shown in Figure A4 (Appendix A). Error bars represent the mean values ± standard deviation; * $p < 0.05$, ** $p < 0.01$ in the Welch's *t*-test; ns, statistically not significant.

2.3. GLI3 Knockdown Impacts the Expression of Ara-C Resistance Genes

Because GLI3 knockdown reduced the sensitivity of AML cells to Ara-C, we next assessed whether gene knockdown was associated with expression changes of several genes involved in Ara-C metabolism and transport. RT-qPCR analysis revealed that *SAMHD1*, *CDA*, and *ABCC11* (*MRP8*) were upregulated in GLI3-knockdown cells compared to cells transduced with control shRNA (Figure 6).

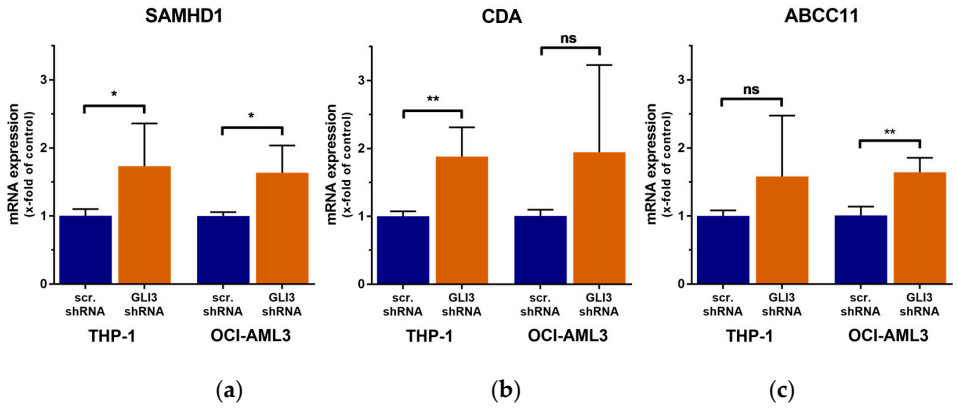

Figure 6. Knockdown of GLI3 results in the upregulation of genes involved in Ara-C metabolism and transport. Expression levels of *SAMHD1* (**a**), *CDA* (**b**), and *ABCC11* (**c**) in GLI3-knockdown cell lines THP-1 and OCI-AML3 were quantified by RT-qPCR and compared to their expression levels in control cells transduced with a scrambled shRNA. Error bars represent the mean values ± standard deviation; * $p < 0.05$, ** $p < 0.01$ in the Welch's *t*-test; ns, not significant.

SAMHD1 and CDA are two key enzymes of the Ara-C metabolism that strongly reduce the intracellular level of the active Ara-C metabolite by promoting the conversion of Ara-C to an inactive state. In addition, GLI3 knockdown increased the expression of ABCC11, a membrane transporter with the ability to efflux nucleoside analogues, such as Ara-C, inhibiting their intracellular accumulation (Figure 7).

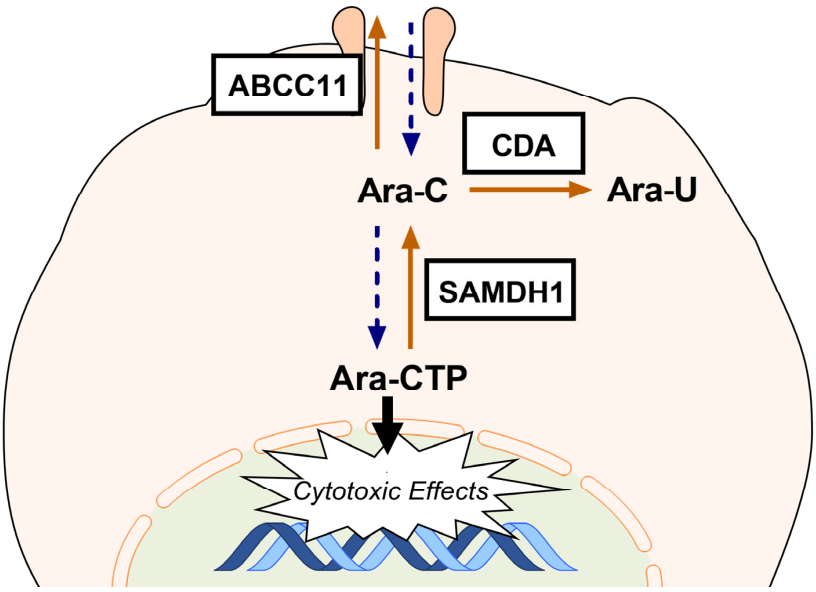

Figure 7. Role of SAMHD1, CDA, and ABCC11 in Ara-C metabolism. ATP-binding cassette C11 (ABCC11) functions as a nucleotide efflux pump and reduces the intracellular levels of Ara-C; cytidine deaminase (CDA) irreversibly deaminates Ara-C to its inactive uracil derivative uracil arabinoside (Ara-U); the phosphohydrolase SAMHD1 reduces active Ara-CTP levels through hydrolyzing Ara-CTP into inactive Ara-C.

3. Discussion

Despite high responses to initial chemotherapy, the vast majority of AML patients relapses after remission due to persistent subpopulation of LSC, because of their drug-resistant phenotype. The LSC hypothesis is of substantial clinical relevance, offering an explanation for minimal residual disease, relapse, and therapy failure and highlighting the need to target these cells in order to achieve long-lasting remissions [24,25].

In mammals, three GLI transcription factors function as central mediators of HH signaling. GLI1 only functions as a transcriptional activator [26], while GLI2 and GLI3 can function both as activating and as inhibitory regulators [27]. Full-length GLI3 (GLI3FL), after phosphorylation and nuclear translocation, acts as a weak transcriptional activator [28]. The proteolytically processing of GLI2FL to its repressor form is not present in cultured cell lines or, at best, is inefficient. The majority of GLI2FL is degraded completely by the proteasome. In contrast, GLI3FL is efficiently processed to the truncated GLI3-repressor form that acts as a strong negative regulator of GLI-mediated transcription [11]. In the absence of HH signaling, GLI3 is predominantly in its repressor form and functions as a strong repressor of GLI-mediated transcription. The level of GLI signaling activity is largely determined by the balance between the transcriptional activators GLI1 and GLI2 and the repressor GLI3R [14,15].

To investigate the molecular changes underlying resistance to chemotherapy, we generated Ara-C-resistant strains of several AML cell lines and performed gene expression analysis of the HH pathway members using RT-qPCR and western blot. We showed that *GLI3* expression was silenced in AML cells with acquired Ara-C resistance. A tumor suppressor role for GLI3R has been demonstrated in a medulloblastoma mouse model driven by GLI2ΔN expression. GLI2ΔN is a constitutively active GLI2 isoform. In the absence of cilia, GLI2ΔN induces medulloblastoma early in life by elimination of GLI3R [29]. The primary cilium is required for proteolytical processing of GLI3 to its repressor form [30]. Interestingly, it has been shown that primary cilia are absent in a high proportion of AML cells, possibly resulting in reduced intracellular GLI3R levels in most cases [31]. In line with this hypothesis, we could observe the absence of *GLI3* expression in 74% of AML patient samples [10]. Consistent with these

results, genetic analysis of The Cancer Genome Atlas AML dataset by Chaudhry et al. demonstrated that *GLI3* expression is epigenetically silenced in most AML patients [18]. In agreement with these findings, when analyzing AML cell lines by RT-qPCR, *GLI3* expression could not be detected in HL-60 cells, while low expression was found in MOLM-13 and OCI-AML5 AML cell lines. The highest *GLI3* mRNA levels could be detected in Kasumi-1, THP-1, and OCI-AML3 cells (Appendix A, Figure A3). As previously mentioned, *GLI3* is epigenetically silenced in a large number of AML cells, which suggests that *GLI3* expression was also downregulated through epigenetic mechanisms in the Ara-C-resistant subclones. Accordingly, it has been demonstrated that *GLI3* expression could be restored in AML cells treated with decitabine, a hypomethylating agent [18].

We showed that downregulation of *GLI3* using shRNA reduced cell sensitivity towards Ara-C treatment. This effect was especially obvious in clonogenic assays of AML cells. This indicates that *GLI3* downregulation might specifically protect leukemic stem or progenitor cells from the cytotoxic effects of Ara-C. Even though GLI3 silencing has never been described in the context of Ara-C resistance in AML, the association of HH pathway activity with chemotherapy resistance is well established in leukemia and other cancers. Queiroz and colleagues showed that activation of the HH pathway was associated with a multidrug-resistant phenotype of myeloid leukemia cells by upregulation of *p*-glycoprotein, a drug efflux pump [32]. Several studies demonstrated that the combination of Ara-C with the SMO inhibitor cyclopamine or the GLI inhibitor GANT-61 significantly enhanced the sensitivity of AML cell lines and primary $CD34^+$ AML cells to Ara-C [21,33,34]. In a recent study, *GLI1* expression was significantly higher in refractory patients compared to non-refractory cases. In addition, high expression of *GLI1* was associated with rapid and repeated relapse. The authors could reverse resistance in the multiple drug-resistant HL-60 AML cell line using the SMO inhibitor NVP-LDE225, resulting in decreased protein expression of MRP1, which is a membrane drug transporter protein responsible for drug resistance and a poor prognosis in AML patients [35]. Furthermore, activated GLI signaling results in the upregulation of several drug transporters, including the ABC transporters *ABCB1*, *ABCB2*, and *ABCG2*, DNA repair mechanisms, and drug-modifying enzymes of the UDP glucuronosyltransferase (*UGT1A*) family [22,36–38]. However, while the role of GLI signaling in drug resistance is well established, the involvement of *GLI3* gene expression in the development of chemotherapy resistance has not been investigated.

We could show that GLI3 downregulation resulted in increased expression of *SAMHD1*, *CDA*, and *ABCC11* (*MRP8*). ATP-binding cassette C11 (*ABCC11*) is a member of the multidrug resistance-associated protein (MRP) family of ATP-binding cassette transporters, which functions as a nucleotide efflux pump and has been shown to reduce the intracellular levels of several clinically relevant nucleotide analogs, including the anticancer fluoropyrimidines and antiviral agents [39]. The expression of the efflux transporter *ABCC11* correlates with poor prognosis in AML. Cells transfected with ABCC11 were resistant to Ara-C and showed reduced intracellular levels of Ara-C and its metabolites [40]. Intracellularly, Ara-C is activated through three phosphorylation steps leading to its active metabolite cytidine-5′-triphosphate (Ara-CTP), with phosphorylation of Ara-C to Ara-CMP by deoxycytidine kinase (DCK) being the rate-limiting step in its activation [41]. *SAMHD1* is a phosphohydrolase that cleaves deoxynucleoside triphosphates (dNTP) into inorganic triphosphate and deoxyribonucleosides [42]. In leukemic cells exposed to Ara-C, SAMHD1 drastically reduces Ara-CTP levels through hydrolyzing Ara-CTP into inactive Ara-C [43]. Schneider et al. showed that inactivation of SAMHD1 strongly sensitizes AML cells to the cytotoxic effects of Ara-C in vitro and in vivo. Moreover, they showed that *SAMHD1* expression is a negative predictor of the response to Ara-C-based treatment in AML patients [44]. In the activation of Ara-C, DCK competes with cytidine deaminase (CDA), which irreversibly deaminates Ara-C to its inactive uracil derivative uracil arabinoside (Ara-U) [45]. Ohta et al. showed that high CDA activity mediates the resistance of U937 monocytoid leukemia cells to Ara-C [46]. In an ex vivo cytotoxicity assay of AML patient samples, *CDA* expression was significantly lower in the Ara-C-sensitive group compared with intermediately sensitive or resistant samples and was found to be a strong predictor of Ara-C response [47]. In AML

patients, high activity and expression of *CDA* was associated with poor initial response and predictive of remission duration [48,49].

In conclusion, we describe that loss of GLI3R through *GLI3* gene silencing in AML cells results in acquired Ara-C resistance. GLI3R functions as a strong repressor of GLI-mediated transcription, and its downregulation by shRNA significantly reduces the effect of Ara-C in AML cells by modulating key enzymes involved in Ara-C metabolism.

4. Materials and Methods

4.1. Cell Lines and Cell Culture

The cell lines used in this study were either purchased from the DSMZ (Deutsche Sammlung von Mikroorganismen und Zellkulturen GmbH, Braunschweig, Germany) or authenticated by the Multiplex human Cell Authentication test (Multiplexion GmbH, Heidelberg, Germany). THP1 cells were maintained in RPMI 1640 medium (Gibco, Thermo Fisher Scientific, Waltham, MA, USA) supplemented with 10% fetal bovine serum (FBS Superior, Biochrom GmbH, Berlin, Germany). Kasumi-1 cells were cultured in RPMI 1640 medium supplemented with 20% FBS. OCI-AML3 cells were maintained in α-MEM medium (Gibco, Thermo Fisher Scientific, Waltham, MA, USA) supplemented with 20 % FBS. OCI-AML5 cells were cultured in α-MEM mediumsupplemented with 20 % FBS and 10 ng/mL GM-CSF (PeproTech GmbH, Hamburg, Germany). All cells were maintained in a humidified incubator with 5 % CO_2 at 37 °C.

4.2. Generation of Ara-C-Resistant Cell Lines

Kasumi-1, OCI-AML3, and OCI-AML5 cells were cultivated with their respective IC95 Ara-C concentration continuously for several months. Cell viability was measured twice a week on day 3 and day 7, and Ara-C dose was adjusted according to cellular IC95 rates. Cells were routinely tested for Ara-C resistance in proliferation assays with Ara-C concentration up to 10,000 nM. Resistance was defined as IC80 > 10,000 nM Ara-C. All cell lines (resistant and parental) were routinely checked to ensure there was no mycoplasma contamination, using MycoAlert Mycoplasma Detection kit (Lonza Group AG, Basel, Swiss).

4.3. Lentiviral Transduction of AML Cell Lines with GLI3-Specific shRNA

Two different pLKO.1-puro vectors encoding GLI3 (#1, TRCN0000416117, sequence 5′-CCGGACAAGAGGTCCAAGATCAAACCTCGAGGTTTGATCTTGGACCTCTTGTTTTTTTG-3′ and #2, TRCN0000020506, sequence 5′-CCGGGCCATCCACATGGAATATCTTCTCGAGAAGATATTC CATGTGGATGGCTTTTT-3′) or scrambled shRNA (SHC002, non-target shRNA vector) were purchased from Sigma-Aldrich (Taufkirchen, Germany). We used the Lentiviral Gene Ontology Vector (LeGO) system for cloning and transfection into the AML cell lines (LeGO-C/Zeo and LeGO-G/Puro, respectively) [50]. Lentiviral particle-containing supernatants were generated in HEK293T cells co-transfected with the plasmids LeGO-C/Zeo + GLI3 shRNA (#1), LeGO-G/Puro + GLI3 shRNA (#2), or LeGO-G/Puro + scrambled shRNA in combination with pMD2.G-VSV-G and psPAX2-Gag-Pol, using calcium phosphate co-precipitation. THP-1 or OCI-AML3 were transduced either with non-targeting shRNA (negative control) or with two shRNA against *GLI3*, simultaneously. On day 3 after transduction, the transduced cells were selected by treatment with puromycin (2 µg/mL; Sigma-Aldrich, Taufkirchen, Germany) and/or zeocin (500 µg/mL; Thermo Fisher Scientific, Waltham, MA, USA) for 7 days prior to functional assays. The knock-down efficiency for *GLI3* was determined using quantitative PCR analysis after 7 days of zeocin and/or puromycin selection. All work with lentiviral particles was done in an S2 facility after approval according to German law.

4.4. Proliferation Assay

Ara-C-resistant and parental cells of the AML cell lines Kasumi-1, OCI-AML3, and OCI-AML5 were plated in 24-well plates at a density of 150,000 cells/well in 500 µL of cell culture medium and cultured with increasing concentrations of Ara-C for 3 days. The number of viable cell was determined after 3 days with the Trypan Blue dye exclusion method, using the cell viability analyzer Vi-Cell ™ XR (Beckman Coulter, Brea, CA, USA).

4.5. Apoptosis Assay

THP-1 cells were seeded in 96-well plates at a density of 200,000 cells/well in 200 µL of cell culture medium and incubated with increasing concentrations of Ara-C for 48 h. For shRNA experiments, *GLI3*-knockdown AML cells were compared to the negative control containing non-targeting shRNA. Induction of apoptosis was measured after 48 h by flow cytometry using APC (allophycocyanin)-conjugated Annexin-V (MabTag GmbH, Friesoythe, Germany) and propidium iodide. Data analysis was performed using the FACS Calibur (BD Biosciences, San Jose, CA, USA) and FlowJo X (Version 10.0.7, BD Life Sciences, FlowJo, LLC, Ashland, OR, USA) Software.

4.6. Colony Formation Assay

Cell lines were seeded in cell culture dishes (35 × 10 mm, Sarstedt AG & Co. KG, Nümbrecht, Germany) at a density of 250 cells/mL in 1 mL of methylcellulose-based semi-solid medium (Methocult H4230, Stemcell Technologies, Vancouver, BC, Canada) supplemented with different concentrations of Ara-C. For shRNA experiments, the colony formation capacity of AML cell lines with *GLI3* knockdown were compared to that of the negative controls containing non-targeting shRNA. After 7 days, the number of colonies was counted using an inverted microscope (Axiovert 25, Zeiss, Jena, Germany).

4.7. Protein Isolation and Western Blot Analysis

Proteins of OCI-AML3 and OCI-AML5 cells were extracted using the trichloroacetic acid method. Protein concentration was determined using the DC Protein Assay (Bio-Rad Laboratories, Inc., Hercules, CA, USA). For each sample, a total of 20 µg of protein was separated using a 4–12% tris-glycine SDS-polyacrylamide gel (Thermo Fisher Scientific, Waltham, MA, USA). The proteins were transferred to a nitrocellulose membrane, and the membrane was incubated with either polyclonal goat IgG anti-human/mouse GLI3 (AF3690, 1:2000, R&D Systems) or mouse anti-human β-ACTIN (sc-47778, 1:5000, Santa Cruz Biotechnology, Dallas, TX, USA) at 4 °C overnight. HRP-linked anti-goat immunoglobulins (P0449, 1:10,000) and anti-mouse IgG (NXA931, 1:10,000) secondary antibodies were purchased from Dako (Glostrup, Denmark) and GE Healthcare (Chicago, IL, USA), respectively. Membranes were incubated with secondary antibodies for 1 h at room temperature. Imaging was performed using the Amersham ECL Prime Western Blotting Detection Reagent (GE Healthcare, Chicago, IL, USA) and the Fusion SL 4 3500 WL chemiluminescence system (Vilber Lourmat, Eberhardzell, Germany).

4.8. Reverse Transcription and Quantitative PCR

Exon-spanning primers were designed with Primer 3 software (Whitehead Institute for Biomedical Research, Boston, MA, USA) or obtained from the GETPrime qPCR primer database [51]. RNA was extracted using innuPREP RNA Mini Kit 2.0 (Analytik Jena, Jena, Germany) and reverse-transcribed into cDNA using PrimeScript™ RT Master Mix (TaKaRa Bio Inc., Kusatsu, Japan). RT-qPCR analyses were carried out on the LightCycler 1.2 (Roche, Basel, Swiss) using the TB Green Premix Ex Taq II (TaKaRa Bio Inc., Kusatsu, Japan) over 40 PCR cycles. The relative expression of the target genes was normalized to that of the reference gene glyceraldehyde 3-phosphate dehydrogenase (*GAPDH*) and calculated using the Pfaffl method [52]. Primers are listed in Appendix A (Table A1).

4.9. Statistical Analysis

Data from the in vitro assays were statistically analyzed by the Welch's *t*-test using GraphPad Prism 7 (GraphPad Software, Inc., San Diego, CA, USA). A p value < 0.05 was considered to be statistically significant.

Author Contributions: Conceptualization, F.F., W.F., and J.W.; Investigation, F.F., V.T., and J.M.; Methodology, F.F., V.T., and J.M.; Supervision, L.B., C.B., and J.W.; Writing—original draft, F.F., W.F., and J.W.; Writing—review & editing, L.B., V.T., J.M., and C.B. All authors have read and agreed to the published version of the manuscript.

Funding: This research was kindly supported by the Deutsche José Carreras Leukämie-Stiftung (Grant number PSD 04/2017).

Acknowledgments: The LeGO Vectors were kindly provided by Kristoffer Riecken, Department for Stem Cell Transplantation at the University Medical Center Hamburg-Eppendorf.

Conflicts of Interest: W. Fiedler has an advisory and consulting role for Amgen, Morphosys; has an advisory role for ARIAD/Incyte, Novartis, Pfizer; Celgene, Jazz Pharmaceuticals, Daiichi Sankyo; has royalties for Amgen; received support for meeting attendance from Amgen, Gilead, Servier, BMS, Daiichi Sankyo; and received research funding from Amgen, Pfizer, outside the submitted work. Bokemeyer reports personal fees from Sanofi Aventis, personal fees from Merck KgA, personal fees from Bristol-Myers Squibb, personal fees from Merck Sharp & Dohme, personal fees from Lilly Imclone, personal fees from Bayer Healthcare, personal fees from GSO Contract Research, personal fees from AOK Rheinland-Hamburg, personal fees from Novartis, outside the submitted work. No potential conflicts of interest were disclosed by the other authors. The funders had no role in the design of the study; in the collection, analyses, or interpretation of data; in the writing of the manuscript, or in the decision to publish the results.

Abbreviations

AML	acute myeloid leukemia
LSC	leukemic stem cells
HSC	hematopoietic stem cells
HH	hedgehog (signaling pathway)
GLI	glioma-associated oncogene homolog family zinc finger protein
GLI3FL	GLI3, full length
GLI3R	GLI3, repressor form
Ara-C	cytarabine, cytosine arabinoside
Ara-U	uracil arabinoside
Ara-CTP	aracytidine-5′-triphosphate
SAMHD1	SAM and HD domain-containing protein 1
CDA	cytidine deaminase
ABCC11	ATP-binding cassette C11
MRP8	multidrug resistance-associated protein 8
WT	wildtype
RCL	resistant cell line
shRNA	small hairpin RNA
APC	allophycocyanin

Appendix A

Table A1. Primers used in this study.

Gene	Sense	Anti-Sense
GAPDH	GTCAGTGGTGGACCTGACCT	TGCTGTAGCCAAATTCGTTG
GLI1	CTACATCAACTCCGGCCAAT	CGGCTGACAGTATAGGCAGA
GLI2	GGCCATCCACATGGAATATC	TGAAGAGCTGCTACGGGAAT
GLI3	GGCCATCCACATGGAATATC	TGAAGAGCTGCTACGGGAAT
SAMHD1	ATTGAAAGACGCACGAGAG	AAGAGATTCATAGTCCTCCCT
CDA	GAGAATCTTCAAAGGGTGCA	TTGTACCCTTCTGAGACGG
ABCC11	CCTACTTCATTATTGGATACACTGC	CTTGTCATGAATACCGCCAG

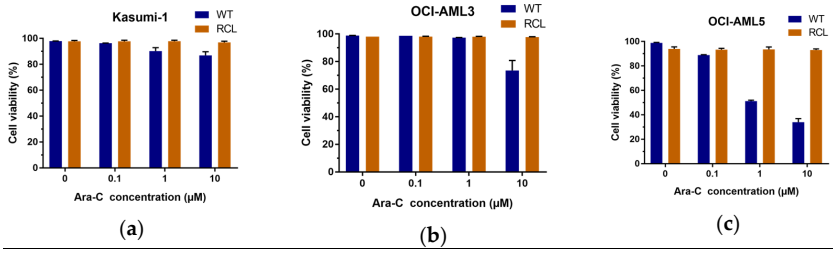

Figure A1. Cell viability of resistant and parental cell lines following treatment with increasing Ara-C concentrations. Resistant (RCL) and wildtype (WT) variants of AML cell lines Kasumi-1 (**a**), OCI-AML3 (**b**), OCI-AML5 (**c**) were plated with different concentrations of Ara-C ranging from 100 nM to 10,000 nM. Cell viability was determined after 3 days with the Trypan Blue dye exclusion method.

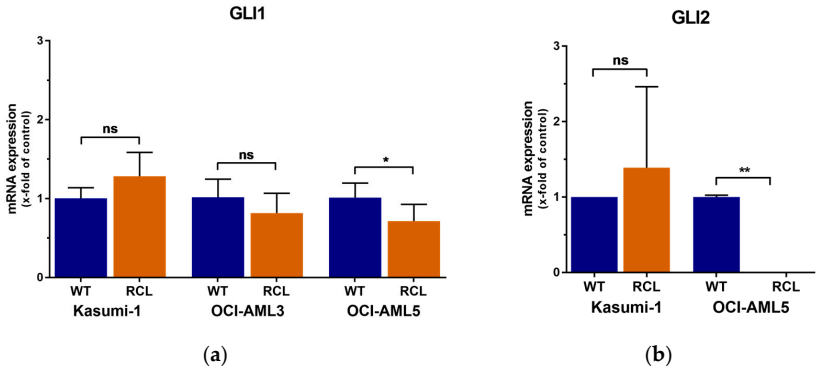

Figure A2. No consistently significant changes in *GLI1* and *GLI2* mRNA expression in Ara-C-resistant cell lines. (**a**) WT and Ara-C RCL Kasumi-1, OCI-AML3, and OCI-AML5 were analyzed for *GLI1* and *GLI*2 mRNA levels by RT-qPCR. Relative *GLI2* expression could not be analyzed for OCI-AML3, as the *GLI2* expression levels were below the detection level. Error bars represent the mean values ± standard deviation; * $p < 0.05$, ** $p < 0.01$ in the Welch's *t*-test; ns, not significant.

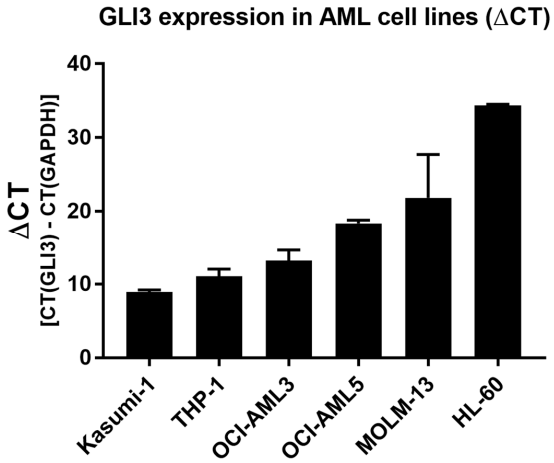

Figure A3. Expression levels of *GLI3* in different AML cell lines. *GLI3* expression in AML cell lines Kasumi-1, THP-1, OCI-AML3, OCI-AML5, MOLM-13, and HL-60 was quantified by RT-qPCR. ΔCT values were calculated with the following formula: $\Delta CT = CT(GLI3) - CT(GAPDH)$. Small ΔCT values indicate high *GLI3* expression. If no expression was found, the CT values were equated with the total cycle number (50 cycles). No *GLI3* expression was found in HL-60 cells. Error bars represent the mean values ± standard deviation.

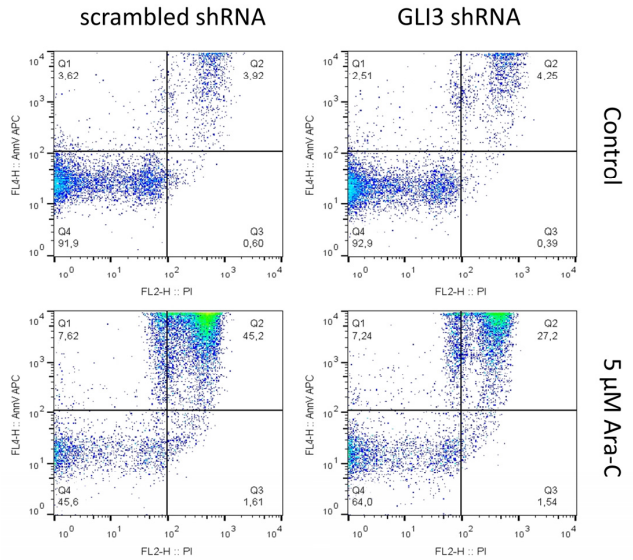

Figure A4. Representative flow cytometry plots for the treatment of THP-1 cells transduced with *GLI3*-targeted shRNA or scrambled shRNA control with 5 µM Ara-C. Induction of apoptosis was measured after 48 h by flow cytometry using Annexin V-APC and propidium iodide.

References

1. Löwenberg, B.; Downing, J.R.; Burnett, A. Acute Myeloid Leukemia. *N. Engl. J. Med.* **1999**, *341*, 1051–1062. [CrossRef] [PubMed]
2. Shipley, J.L.; Butera, J.N. Acute myelogenous leukemia. *Exp. Hematol.* **2009**, *37*, 649–658. [CrossRef] [PubMed]
3. Gentles, A.J.; Plevritis, S.K.; Majeti, R.; Alizadeh, A.A. Association of a leukemic stem cell gene expression signature with clinical outcomes in acute myeloid leukemia. *JAMA J. Am. Med. Assoc.* **2010**, *304*, 2706–2715. [CrossRef] [PubMed]
4. Lapidot, T.; Sirard, C.; Vormoor, J.; Murdoch, B.; Hoang, T.; Caceres-Cortes, J.; Minden, M.; Paterson, B.; Caligiuri, M.A.; Dick, J.E. A cell initiating human acute myeloid leukaemia after transplantation into SCID mice. *Nature* **1994**, *367*, 645–648. [CrossRef] [PubMed]
5. Dick, J.E. Stem cell concepts renew cancer research. *Blood* **2008**, *112*, 4793–4807. [CrossRef]
6. Lane, S.W.; Scadden, D.T.; Gilliland, D.G. The leukemic stem cell niche: Current concepts and therapeutic opportunities. *Blood* **2009**, *114*, 1150–1157. [CrossRef]
7. Irvine, D.A.; Copland, M. Targeting hedgehog in hematologic malignancy. *Blood* **2012**, *119*, 2196–2204. [CrossRef]
8. Hui, C.; Angers, S. Gli Proteins in Development and Disease. *Annu. Rev. Cell Dev. Biol.* **2011**, *27*, 513–537. [CrossRef]
9. Teglund, S.; Toftgård, R. Hedgehog beyond medulloblastoma and basal cell carcinoma. *Biochim. Biophys. Acta Rev. Cancer* **2010**, *1805*, 181–208. [CrossRef]
10. Wellbrock, J.; Latuske, E.; Kohler, J.; Wagner, K.; Stamm, H.; Vettorazzi, E.; Vohwinkel, G.; Klokow, M.; Uibeleisen, R.; Ehm, P.; et al. Expression of hedgehog pathway mediator GLI represents a negative prognostic marker in human acute myeloid leukemia and its inhibition exerts Antileukemic effects. *Clin. Cancer Res.* **2015**, *21*, 2388–2398. [CrossRef]
11. Pan, Y.; Wang, B. A novel protein-processing domain in Gli2 and Gli3 differentially blocks complete protein degradation by the proteasome. *J. Biol. Chem.* **2007**, *282*, 10846–10852. [CrossRef]
12. Kinzler, K.W.; Vogelstein, B. The GLI gene encodes a nuclear protein which binds specific sequences in the human genome. *Mol. Cell. Biol.* **1990**, *10*, 634–642. [CrossRef]
13. Niewiadomski, P.; Niedziółka, S.M.; Markiewicz, Ł.; Uśpieński, T.; Baran, B.; Chojnowska, K. Gli Proteins: Regulation in Development and Cancer. *Cells* **2019**, *8*, 147. [CrossRef] [PubMed]

14. Lipinski, R.J.; Gipp, J.J.; Zhang, J.; Doles, J.D.; Bushman, W. Unique and complimentary activities of the Gli transcription factors in Hedgehog signaling. *Exp. Cell Res.* **2006**, *312*, 1925–1938. [CrossRef]
15. Petrova, R.; Garcia, D.R.; Joyner, A.L. Titration of GLI3 repressor activity by sonic hedgehog signaling is critical for maintaining multiple adult neural stem cell and astrocyte functions. *J. Neurosci.* **2013**, *33*, 17490–17505. [CrossRef] [PubMed]
16. Gu, D.; Xie, J. Non-canonical Hh signaling in cancer—Current understanding and future directions. *Cancers* **2015**, *7*, 1684–1698. [CrossRef] [PubMed]
17. Latuske, E.M.; Stamm, H.; Klokow, M.; Vohwinkel, G.; Muschhammer, J.; Bokemeyer, C.; Jücker, M.; Kebenko, M.; Fiedler, W.; Wellbrock, J. Combined inhibition of GLI and FLT3 signaling leads to effective anti-leukemic effects in human acute myeloid leukemia. *Oncotarget* **2017**, *8*, 29187–29201. [CrossRef] [PubMed]
18. Chaudhry, P.; Singh, M.; Triche, T.J.; Guzman, M.; Merchant, A.A. GLI3 repressor determines Hedgehog pathway activation and is required for response to SMO antagonist glasdegib in AML. *Blood* **2017**, *129*, 3465–3475. [CrossRef]
19. Zhang, W.; Yu, F.; Wang, Y.; Zhang, Y.; Meng, L.; Chi, Y. Rab23 promotes the cisplatin resistance of ovarian cancer via the Shh-Gli-ABCG2 signaling pathway. *Oncol. Lett.* **2018**, *15*, 5155–5160. [CrossRef]
20. Yoon, C.; Park, D.J.; Schmidt, B.; Thomas, N.J.; Lee, H.J.; Kim, T.S.; Janjigian, Y.Y.; Cohen, D.J.; Yoon, S.S. CD44 expression denotes a subpopulation of gastric cancer cells in which Hedgehog signaling promotes chemotherapy resistance. *Clin. Cancer Res.* **2014**, *20*, 3974–3988. [CrossRef]
21. Kobune, M.; Takimoto, R.; Murase, K.; Iyama, S.; Sato, T.; Kikuchi, S.; Kawano, Y.; Miyanishi, K.; Sato, Y.; Niitsu, Y.; et al. Drug resistance is dramatically restored by hedgehog inhibitors in CD34+ leukemic cells. *Cancer Sci.* **2009**, *100*, 948–955. [CrossRef] [PubMed]
22. Zahreddine, H.A.; Culjkovic-Kraljacic, B.; Assouline, S.; Gendron, P.; Romeo, A.A.; Morris, S.J.; Cormack, G.; Jaquith, J.B.; Cerchietti, L.; Cocolakis, E.; et al. The sonic hedgehog factor GLI1 imparts drug resistance through inducible glucuronidation. *Nature* **2014**, *511*, 90–93. [CrossRef] [PubMed]
23. Yu, B.; Gu, D.; Zhang, X.; Liu, B.; Xie, J. The role of GLI2-ABCG2 signaling axis for 5Fu resistance in gastric cancer. *J. Genet. Genom.* **2017**, *44*, 375–383. [CrossRef] [PubMed]
24. Terwijn, M.; Zeijlemaker, W.; Kelder, A.; Rutten, A.P.; Snel, A.N.; Scholten, W.J.; Pabst, T.; Verhoef, G.; Löwenberg, B.; Zweegman, S.; et al. Leukemic stem cell frequency: A strong biomarker for clinical outcome in acute myeloid leukemia. *PLoS ONE* **2014**, *9*, e107587. [CrossRef]
25. Jordan, C.T. The leukemic stem cell. *Best Pr. Res. Clin. Haematol.* **2007**, *20*, 13–18. [CrossRef]
26. Carpenter, R.L.; Lo, H.W. *Identification, Functional Characterization, and Pathobiological Significance of GLI1 Isoforms in Human Cancers*; Elsevier: Amsterdam, The Netherlands, 2012; Volume 88, ISBN 9780123946225.
27. Sasaki, H.; Nishizaki, Y.; Hui, C.C.; Nakafuku, M.; Kondoh, H. Regulation of Gli2 and Gli3 activities by an amino-terminal repression domain: Implication of Gli2 and Gli3 as primary mediators of Shh signaling. *Development* **1999**, *126*, 3915–3924.
28. Niewiadomski, P.; Kong, J.H.; Ahrends, R.; Ma, Y.; Humke, E.W.; Khan, S.; Teruel, M.N.; Novitch, B.G.; Rohatgi, R. Gli protein activity is controlled by multisite phosphorylation in vertebrate hedgehog signaling. *Cell Rep.* **2014**, *6*, 168–181. [CrossRef]
29. Han, Y.G.; Kim, H.J.; Dlugosz, A.A.; Ellison, D.W.; Gilbertson, R.J.; Alvarez-Buylla, A. Dual and opposing roles of primary cilia in medulloblastoma development. *Nat. Med.* **2009**, *15*, 1062–1065. [CrossRef]
30. Laclef, C.; Anselme, I.; Besse, L.; Catala, M.; Palmyre, A.; Baas, D.; Paschaki, M.; Pedraza, M.; Métin, C.; Durand, B.; et al. The role of primary cilia in corpus callosum formation is mediated by production of the Gli3 repressor. *Hum. Mol. Genet.* **2015**, *24*, 4997–5014. [CrossRef]
31. Singh, M.; Chaudhry, P.; Merchant, A.A. Primary cilia are present on human blood and bone marrow cells and mediate Hedgehog signaling. *Exp. Hematol.* **2016**, *44*, 1181–1187. [CrossRef]
32. Queiroz, K.C.S.; Ruela-De-Sousa, R.R.; Fuhler, G.M.; Aberson, H.L.; Ferreira, C.V.; Peppelenbosch, M.P.; Spek, C.A. Hedgehog signaling maintains chemoresistance in myeloid leukemic cells. *Oncogene* **2010**, *29*, 6314–6322. [CrossRef] [PubMed]
33. Liang, H.; Zheng, Q.L.; Fang, P.; Zhang, J.; Zhang, T.; Liu, W.; Guo, M.; Robinson, C.L.; Chen, S.B.; Chen, X.P.; et al. Targeting the PI3K/AKT pathway via GLI1 inhibition enhanced the drug sensitivity of acute myeloid leukemia cells. *Sci. Rep.* **2017**, *7*. [CrossRef] [PubMed]

34. Long, B.; Wang, L.X.; Zheng, F.M.; Lai, S.P.; Xu, D.R.; Hu, Y.; Lin, D.J.; Zhang, X.Z.; Dong, L.; Long, Z.J.; et al. Targeting GLI1 suppresses cell growth and enhances chemosensitivity in CD34 + enriched acute myeloid leukemia progenitor cells. *Cell. Physiol. Biochem.* **2016**, *38*, 1288–1302. [CrossRef] [PubMed]
35. Huang, K.; Sun, Z.; Ding, B.; Jiang, X.; Wang, Z.; Zhu, Y.; Meng, F. Suppressing hedgehog signaling reverses drug resistance of refractory acute myeloid leukemia. *Onco Targets. Ther.* **2019**, *12*, 7477–7488. [CrossRef] [PubMed]
36. Zhou, X.T.; Ding, J.; Li, H.Y.; Zuo, J.L.; Ge, S.Y.; Jia, H.L.; Wu, J. Hedgehog signalling mediates drug resistance through targeting TAP1 in hepatocellular carcinoma. *J. Cell. Mol. Med.* **2020**, *24*, 4298–4311. [CrossRef]
37. Meng, E.; Hanna, A.; Samant, R.S.; Shevde, L.A. The impact of hedgehog signaling pathway on DNA repair mechanisms in human cancer. *Cancers* **2015**, *7*, 1333–1348. [CrossRef]
38. Chen, Y.; Bieber, M.M.; Teng, N.N.H. Hedgehog signaling regulates drug sensitivity by targeting ABC transporters ABCB1 and ABCG2 in epithelial ovarian cancer. *Mol. Carcinog.* **2014**, *53*, 625–634. [CrossRef]
39. Guo, Y.; Kotova, E.; Chen, Z.S.; Lee, K.; Hopper-Borge, E.; Belinsky, M.G.; Kruh, G.D. MRP8, ATP-binding cassette C11 (ABCC11), is a cyclic nucleotide efflux pump and a resistance factor for fluoropyrimidines 2′,3′-dideoxycytidine and 9′-(2′-phosphonylmethoxyethyl)adenine. *J. Biol. Chem.* **2003**, *278*, 29509–29514. [CrossRef]
40. Guo, Y.; Kock, K.; Ritter, C.A.; Chen, Z.S.; Grube, M.; Jedlitschky, G.; Illmer, T.; Ayres, M.; Beck, J.F.; Siegmund, W.; et al. Expression of ABCC-type nucleotide exporters in blasts of adult acute myeloid leukemia: Relation to long-term survival. *Clin. Cancer Res.* **2009**, *15*, 1762–1769. [CrossRef]
41. Lamba, J.K. Genetic factors influencing cytarabine therapy. *Pharmacogenomics* **2009**, *10*, 1657–1674. [CrossRef]
42. Franzolin, E.; Pontarin, G.; Rampazzo, C.; Miazzi, C.; Ferraro, P.; Palumbo, E.; Reichard, P.; Bianchi, V. The deoxynucleotide triphosphohydrolase SAMHD1 is a major regulator of DNA precursor pools in mammalian cells. *Proc. Natl. Acad. Sci. USA* **2013**, *110*, 14272–14277. [CrossRef] [PubMed]
43. Hollenbaugh, J.A.; Shelton, J.; Tao, S.; Amiralaei, S.; Liu, P.; Lu, X.; Goetze, R.W.; Zhou, L.; Nettles, J.H.; Schinazi, R.F.; et al. Substrates and inhibitors of SAMHD1. *PLoS ONE* **2017**, *12*, e0169052. [CrossRef] [PubMed]
44. Schneider, C.; Oellerich, T.; Baldauf, H.M.; Schwarz, S.M.; Thomas, D.; Flick, R.; Bohnenberger, H.; Kaderali, L.; Stegmann, L.; Cremer, A.; et al. SAMHD1 is a biomarker for cytarabine response and a therapeutic target in acute myeloid leukemia. *Nat. Med.* **2017**, *23*, 250–255. [CrossRef] [PubMed]
45. Cohen, S. The mechanisms of lethal action of arabinosyl cytosine (araC) and arabinosyl adenine (araA). *Cancer* **1977**, *40*, 509–518. [CrossRef]
46. Ohta, T.; Hori, H.; Ogawa, M.; Miyahara, M.; Kawasaki, H.; Taniguchi, N.; Komada, Y. Impact of cytidine deaminase activity on intrinsic resistance to cytarabine in carcinoma cells. *Oncol. Rep.* **2004**, *12*, 1115–1120. [CrossRef]
47. Abraham, A.; Varatharajan, S.; Karathedath, S.; Philip, C.; Lakshmi, K.M.; Jayavelu, A.K.; Mohanan, E.; Janet, N.B.; Srivastava, V.M.; Shaji, R.V.; et al. RNA expression of genes involved in cytarabine metabolism and transport. *Pharmacogenomics* **2015**, *16*, 877–890. [CrossRef]
48. Jahns-streubel, G.; Reuter, C.; Auf der Landwehr, U.; Unterhalt, M.; Schleyer, E.; Wörmann, B.; Büchner, T.; Hiddemann, W. Activity of Thymidine Kinase and of Polymerase a as Well as Activity and Gene Expression of Deoxycytidine Deaminase in Leukemic Blasts Are Correlated With Clinical Response in the Setting of Granulocyte- Macrophage Colony-Stimulating Factor—Based Priming. *Blood* **1997**, *90*, 1968–1976. [CrossRef]
49. Schröder, J.K.; Kirch, C.; Seeber, S.; Schütte, J. Structural and functional analysis of the cytidine deaminase gene in patients with acute myeloid leukaemia. *Br. J. Haematol.* **1998**, *103*, 1096–1103. [CrossRef]
50. Weber, K.; Mock, U.; Petrowitz, B.; Bartsch, U.; Fehse, B. Lentiviral gene ontology (LeGO) vectors equipped with novel drug-selectable fluorescent proteins: New building blocks for cell marking and multi-gene analysis. *Gene Ther.* **2010**, *17*, 511–520. [CrossRef]

51. David, F.P.A.; Rougemont, J.; Deplancke, B. GETPrime 2.0: Gene- and transcript-specific qPCR primers for 13 species including polymorphisms. *Nucleic Acids Res.* **2017**, *45*, D56–D60. [CrossRef]
52. Pfaffl, M.W. A new mathematical model for relative quantification in real-time RT–PCR. *Nucleic Acids Res.* **2001**, *29*, 2002–2007. [CrossRef] [PubMed]

International Journal of
Molecular Sciences

MDPI

Article

Mebendazole Mediates Proteasomal Degradation of GLI Transcription Factors in Acute Myeloid Leukemia

Fabian Freisleben [1], Franziska Modemann [1,2], Jana Muschhammer [1], Hauke Stamm [1], Franziska Brauneck [1], Alexander Krispien [1], Carsten Bokemeyer [1], Karl N. Kirschner [3], Jasmin Wellbrock [1,†] and Walter Fiedler [1,*,†]

[1] Department of Oncology, Hematology and Bone Marrow Transplantation with Section Pneumology, Hubertus Wald University Cancer Center, University Medical Center Hamburg-Eppendorf, 20251 Hamburg, Germany; fabian.freisleben@stud.uke.uni-hamburg.de (F.F.); f.modemann@uke.de (F.M.); j.muschhammer@uke.de (J.M.); hauke.stamm@astrazeneca.com (H.S.); f.brauneck@uke.de (F.B.); alexander.krispien@stud.uke.uni-hamburg.de (A.K.); c.bokemeyer@uke.de (C.B.); j.wellbrock@uke.de (J.W.)
[2] Mildred Scheel Cancer Career Center, University Cancer Center Hamburg, 20251 Hamburg, Germany
[3] Department of Computer Science, University of Applied Sciences Bonn-Rhein-Sieg, 53757 Sankt Augustin, Germany; karl.kirschner@h-brs.de
* Correspondence: fiedler@uke.de; Tel.: +49-40-7410-23051
† These authors contributed equally to the study.

Abstract: The prognosis of elderly AML patients is still poor due to chemotherapy resistance. The Hedgehog (HH) pathway is important for leukemic transformation because of aberrant activation of GLI transcription factors. MBZ is a well-tolerated anthelmintic that exhibits strong antitumor effects. Herein, we show that MBZ induced strong, dose-dependent anti-leukemic effects on AML cells, including the sensitization of AML cells to chemotherapy with cytarabine. MBZ strongly reduced intracellular protein levels of GLI1/GLI2 transcription factors. Consequently, MBZ reduced the GLI promoter activity as observed in luciferase-based reporter assays in AML cell lines. Further analysis revealed that MBZ mediates its anti-leukemic effects by promoting the proteasomal degradation of GLI transcription factors via inhibition of HSP70/90 chaperone activity. Extensive molecular dynamics simulations were performed on the MBZ-HSP90 complex, showing a stable binding interaction at the ATP binding site. Importantly, two patients with refractory AML were treated with MBZ in an off-label setting and MBZ effectively reduced the GLI signaling activity in a modified plasma inhibitory assay, resulting in a decrease in peripheral blood blast counts in one patient. Our data prove that MBZ is an effective GLI inhibitor that should be evaluated in combination to conventional chemotherapy in the clinical setting.

Keywords: GLI; AML; MBZ; mebendazole; HSP90; HSP70

Citation: Freisleben, F.; Modemann, F.; Muschhammer, J.; Stamm, H.; Brauneck, F.; Krispien, A.; Bokemeyer, C.; Kirschner, K.N.; Wellbrock, J.; Fiedler, W. Mebendazole Mediates Proteasomal Degradation of GLI Transcription Factors in Acute Myeloid Leukemia. *Int. J. Mol. Sci.* **2021**, *22*, 10670. https://doi.org/10.3390/ijms221910670

Academic Editor: Tsuyoshi Shimo

Received: 22 August 2021
Accepted: 24 September 2021
Published: 1 October 2021

1. Introduction

The Hedgehog (HH) signaling pathway is a highly conserved signaling cascade that plays a critical role during embryogenesis and is strongly involved in many basic cellular functions, including cell differentiation, proliferation and stem cell maintenance [1]. The main receptor for HH ligands is Patched (Ptch), a 12-pass transmembrane protein. Upon ligand binding Ptch releases SMO, a seven-transmembrane domain G-protein coupled receptor-like protein, which then activates the GLI transcription factors representing the main effectors of the HH signaling pathway. In addition to this canonical HH pathway, numerous signaling cascades result in non-canonical activation of the GLI transcription factors, including *FLT3/STAT5*, *RTK/RAF/MEK/ERK* and *PI3K/AKT/mTOR* [2,3].

It is well established that aberrant activation of HH signaling is associated with a wide variety of neoplasms [4]. Activated GLI transcription factors drive a transcriptional program that promotes survival, growth, migration and stemness [2,4,5]. Expression of GLI1 is associated with a poor prognosis in a wide variety of cancers [6,7]. Moreover, GLI

transcription factors play a fundamental role in the maintenance of leukemia, initiating cells that are responsible for therapy failure and tumor relapse due to their chemotherapy resistance [2]. In a previous work, we showed that a high GLI1 and GLI2 expression represents a negative prognostic marker in AML, and that targeted inhibition of GLI1 and GLI2 mediates anti-leukemic effects in vitro and in vivo [7].

Current treatment strategies aim to inhibit GLI signaling by targeting SMO in cancer cells. SMO inhibitors have been tested in AML, where Glasdegib is an approved treatment in conjunction with low-dose cytarabine [8]. However, due to the frequent non-canonical activation of the HH pathway, the inhibition of GLI transcription factors may represent a better choice.

For decades the synthetic benzimidazole Mebendazole (MBZ) has been an approved anthelminthic drug, effective against a broad spectrum of intestinal helminthiasis with a favorable toxicity profile. Indications include short-term and low-dose treatments, as well as high-dose long-term treatments (e.g., 50 mg/kg bodyweight for several months) [9,10]. Besides its anthelmintic activity, MBZ exhibits strong anti-tumor effects in different cancer entities [9]. MBZ's mechanisms of action are manifold—including anti-angiogenic properties, and inhibition of microtubule depolymerisation and signaling cascades (e.g., BRAF, MEK) [9]. Walf-Vorderwülbecke et al. proposed that MBZ induced c-MYB degradation by inhibiting protein folding through blockade of HSP70 in AML [11]. Herein, we show that MBZ mediates strong anti-leukemic effects by promoting the degradation of GLI transcription factors through inhibition of HSP70/90 chaperone activity, and that MBZ sensitizes AML cells to chemotherapy. Furthermore, two patients with refractory AML were treated with MBZ in an off-label setting, and the clinically achievable MBZ plasma concentrations effectively reduced the GLI signaling activity in a modified plasma inhibitory assay. Our data prove that MBZ is an effective GLI inhibitor that should be evaluated in combination to conventional chemotherapy in the clinical setting.

2. Results

2.1. MBZ Inhibits SMO Independent Non-Canonical GLI Signaling Predominant in AML

Since the 1987 discovery of GLI1 in human glioma cells [12], the role of the three members GLI1, GLI2 and GLI3 in a variety of cancers has become increasingly apparent [4], with GLI1 expression specifically identified as a negative prognostic factor in numerous cancers [6,7]. Previously, we demonstrated that the treatment of GLI reporter AML cell lines with SMO-inhibitor cyclopamine did not lead to a reduction in GLI promoter activity [3]. We hypothesized that this might be due to the predominant expression of the GLI2ΔN isoform in AML cells. GLI2ΔN represents a constitutively active GLI2 isoform that lacks the amino-terminal repressor domain [13] and has the ability to induce target genes several fold stronger in comparison to the GLI2 full length (GLI2FL) [14]. Expression of GLI2ΔN results in a constitutively active GLI signaling cascade even in the presence of SMO inhibitors, providing an important mechanism for resistance to SMO inhibitors in cancer [15]. Consequently, we analyzed the expression of GLI2ΔN and GLI2FL in samples from 47 newly diagnosed AML patients by qPCR. GLI2 expression was detected in 16 of the 47 samples (34%). *GLI2ΔN* mRNA expression was 29.5-fold higher than the expression of *GLI2FL* mRNA (with a range of 0.8- to 111.5-fold; Figure 1A). Moreover, protein levels of GLI2ΔN were considerably higher than those of GLI2FL in the AML cell lines used herein as determined by western blot (Figures 2C and 3B, Supplementary Materials Figure S1I). This indicates that GLI2ΔN is the predominantly expressed isoform, relative to GLI2FL, in AML.

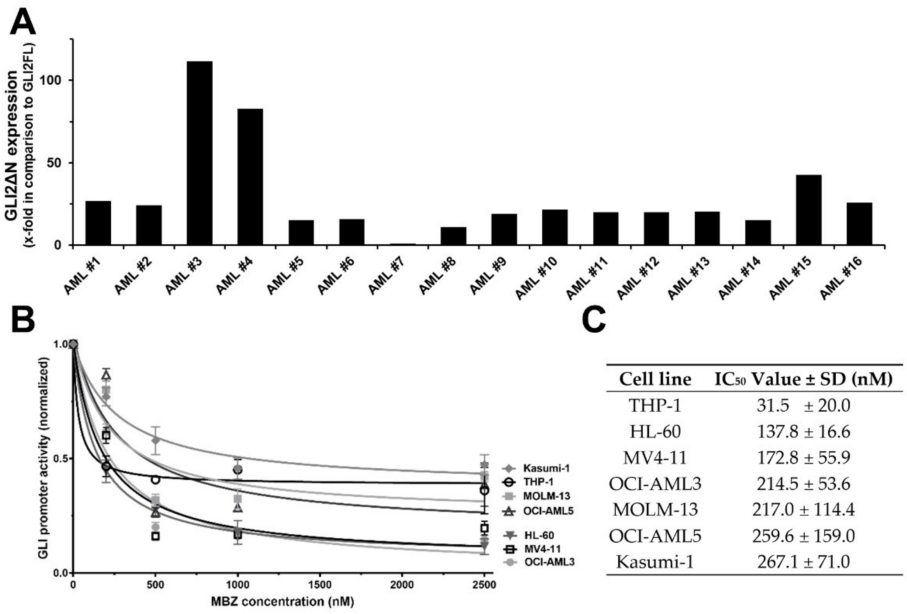

Figure 1. MBZ inhibits SMO independent non-canonical GLI signaling predominant in AML. (**A**) Pre-treatment samples of 16 different AML patients with detectable GLI2 expression were analyzed for *GLI2FL* and *GLI2ΔN* expression using RT-qPCR. *GLI2ΔN* expression was normalized to *GLI2FL* expression. (**B**) The AML reporter cell lines MV4-11, MOLM-13, HL60, THP-, Kasumi-1, OCI-AML3 and OCI-AML5 were treated with increasing MBZ concentrations or DMSO as solvent control. The GLI promoter activity was measured after 48 h. (**C**) The IC50 of MBZ on the GLI promoter activity of the different GLI reporter cell lines was calculated from the data shown in (**B**) using a nonlinear regression (curve fit) for inhibitor vs. response with three parameters in GraphPad Prism 7.04.

The anthelmintic MBZ has shown to exhibit strong anti-tumor effects in preclinical studies [9]. In order to investigate if MBZ inhibits the GLI cascade, we treated seven AML GLI reporter cell lines with increasing MBZ concentrations for 48 h. Endogenous expression of GLI transcription factors has been detected in leukemic blasts from a large proportion of AML patients and cell lines [7,16] and was also found in all AML cell lines used herein. Treatment with MBZ led to a strong dose-dependent reduction in all analyzed AML reporter cell lines (Figure 1C). The MBZ concentration required to inhibit the GLI promoter activity was within clinically achievable concentrations, with an IC50 ranging from 32 ± 20 to 267 ± 71 nM after 48 h in the AML cell lines tested (Figure 1C). In contrast to MBZ, the active metabolite of albendazole (i.e., Albendazole sulfoxide (ABZ-S)), a closely related benzimidazole-derived anthelmintic agent [17], had no effect on the GLI reporter activity (Supplementary Materials, Figure S2).

2.2. MBZ Promotes Proteasomal Degradation of GLI

To analyze the effects of MBZ on GLI expression, AML cell lines MV4-11, MOLM-13, THP-1 and OCI-AML3 were treated with MBZ in increasing concentrations from 100 nM to 500 nM, followed by western blot and RT-qPCR analyses. We found that GLI1 and GLI2 protein levels were clearly reduced in 24 h after MBZ exposure (Figure 2A–C), whereas *GLI1* and *GLI2* mRNA levels did not decrease (Supplementary Materials Figure S1A–H). Incubation of AML cells with MBZ for 48 h strongly affected GLI2ΔN protein levels and thus could overcome SMO inhibitor resistance (Supplementary Materials Figure S1I).

We hypothesized that MBZ decreases the GLI protein levels by promoting their proteasomal degradation. Therefore, we evaluated the influence of the 26S proteasome inhibitor Bortezomib (BTZ) on GLI protein levels and signaling activity after MBZ treatment. AML GLI reporter cell lines THP-1 and OCI-AML3 were treated with 5 or 10 nM BTZ for 24 h. As

anticipated, MBZ inhibited GLI signaling activity in a dose-dependent manner. However, BTZ fully reversed MBZ-mediated inhibition of the GLI promoter activity (Figure 2D,E). Consistent with these results, 10 nM BTZ abolished MBZ's effect on GLI1 and GLI2 protein levels in THP-1 and OCI-AML3 cells in western blot analysis (Figure 2A–C). Taken together, these results strongly suggest that MBZ mediates proteasomal degradation of GLI1 and GLI2.

2.3. MBZ Promotes Degradation of GLI Transcription Factors via Inhibition of HSP70/90-Chaperone Activity

The heat shock proteins 70 (HSP70) and 90 (HSP90) tightly cooperate in the protein stabilization of a wide spectrum of client substrates, including transcription factors. Inhibition of either HSP70 or HSP90 disrupts this chaperone machinery and leaves a client protein prone to misfolding, resulting in its ubiquitination and proteasomal degradation. Walf-Vorderwülbecke et al. reported that MBZ promotes proteasomal degradation of transcription factor c-MYB by interaction with HSP70 [11]. However, GLI protein stability has never been associated with heat shock proteins. Inhibition of either HSP70 or HSP90 with small-molecule inhibitors VER-155008 and PU-H71, respectively, resulted in significant reduction in GLI1 and GLI2 protein levels in western blot analysis. Inhibition of both HSP70 and HSP90 by combination of both agents increased the effect considerably (Figure 3A,B). In accordance with the effects mediated by MBZ, GLI1 and GLI2 mRNA levels did not decrease (Supplementary Materials Figure S3).

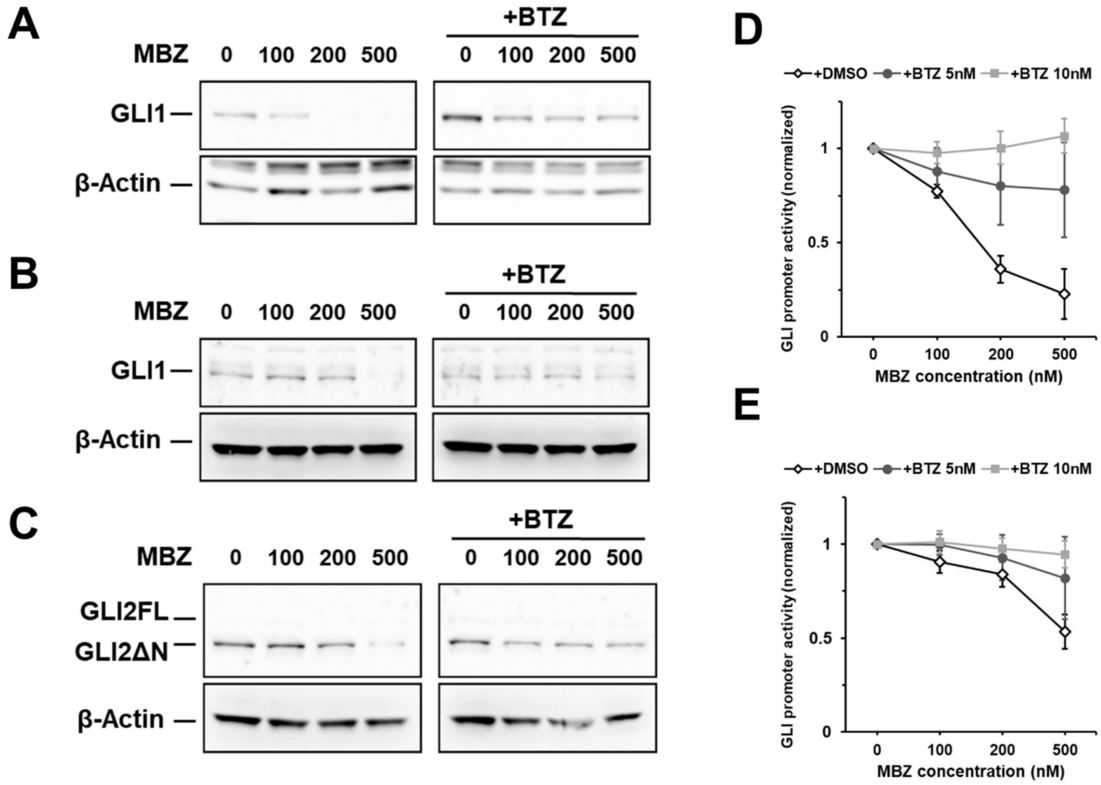

Figure 2. Decreased GLI1 and GLI2FL/GLI2ΔN protein levels upon MBZ treatment. Cell lines THP-1 (**A**) and OCI-AML3 (**B**,**C**) were treated with the indicated concentrations of MBZ alone or in combination with 10 nM BTZ for 24 h. GLI1 (**A**,**B**) and GLI2 (**C**) protein expression was examined by western blot analysis. THP-1 (**D**) and OCI-AML3 (**E**) GLI luciferase reporter cells were treated with MBZ alone or in combination with 5 nM or 10 nM BTZ. The GLI promoter activity was measured after 24 h. Error bars represent the mean values ± standard deviation from at least three independent experiments.

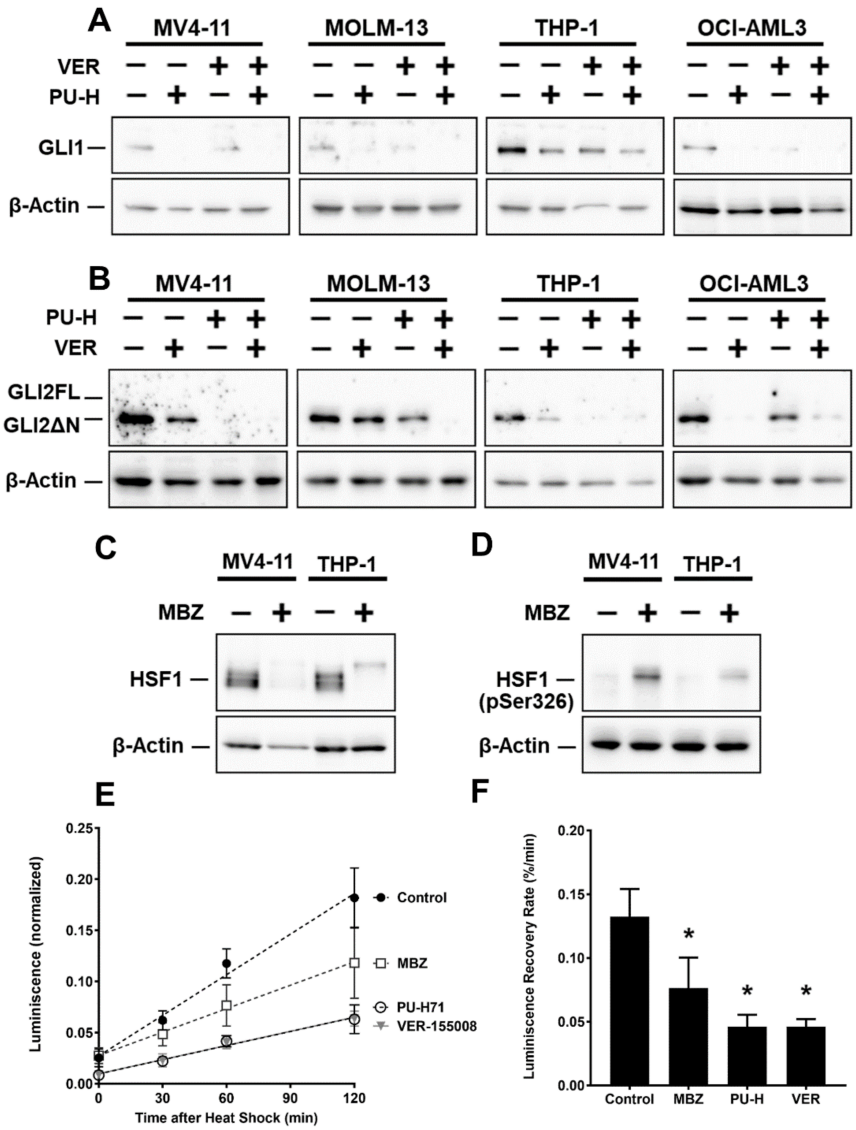

Figure 3. MBZ promotes degradation of GLI Transcription Factors via Inhibition of HSP70/90-Chaperone Activity. AML cell lines MV4-11, MOLM-13, THP-1 and OCI-AML3 have been treated with 1 μM PU-H71 (PU-H) and 25 μM VER-155008 (VER) for 24 h. Subsequently expression of GLI1 (**A**) and GLI2 (**B**) was examined by western blot analysis. (**C**,**D**) AML cell lines MV4-11 and THP-1 were treated with 500 nM MBZ or DMSO as a solvent control for 24 h and protein levels of HSF-1 and phosphorylated HSF-1 (Ser-326) were determined by western blot analysis. Phosphorylated HSF-1 (Ser-326) represents the active state of HSF-1. (**E**) MOLM-13^{luc+} cell line constitutively expressing a firefly luciferase were incubated with 10 μM MBZ, 1 μM PU-H71 (PU-H), 25 μM VER-155008 (VER) or a solvent control. Following a heat-shock, recovery of the intracellular luciferase activity was measured on different time points and normalized to the luciferase activity of the non-heat-shock native control. (**F**) The luminescence recovery rate derived from (**E**) as the slope of the luminescence increases after treatment with MBZ, PU-H71 (PU-H), VER-155008 (VER) or a solvent control. Error bars represent the mean values ± standard deviation from at least three independent experiments. * $p < 0.05$ in the Welch's *t*-test.

We also demonstrated that treatment with 500 nM MBZ did not alter HSP70/HSP90 protein expression in MV4-11, MOLM-13, THP-1 and OCI-AML3 after 24 h using western

blot analysis (Supplementary Materials Figure S4). However, HSF-1, the major transcription factor of the heat shock response genes, was heavily phosphorylated on Serine 326 in MBZ-treated MV4-11 and THP-1 cells—reflecting an active state of HSF-1 (Figure 3C). Interestingly, the total HSF-1 protein levels were reduced by MBZ treatment compared to control (Figure 3D).

To further investigate if MBZ directly inhibits the enzymatic activity of the HSP chaperone machinery in AML cells, we generated a MOLM-13 cell line constitutively expressing a firefly luciferase (MOLM-13^{luc+}). Following heat-shock, refolding of heat-denatured firefly luciferase depends on cooperative chaperone activity of both HSP70 and HSP90. We treated MOLM-13^{luc+} cells with 10 µM MBZ, 25 µM VER-155008, 1 µM PU-H71 or DMSO as a solvent control. The luciferase signal was recovered without an inhibitor in MOLM-13^{luc+} following a heat-shock, but incubation of AML cells with MBZ or specific HSP inhibitors significantly impaired recovery of the signal (Figure 3E,F), suggesting a direct inhibition of HSP70/HSP90-mediated luciferase refolding.

2.4. In Silico Modeling of MBZ Bound to HSP90

Six molecular models were created to explore how MBZ might bind to HSP90 based on the inhibition data shown above. Using three different HSP90 protein crystal structures to diversify the starting coordinates, MBZ was placed into their ATP binding site. MD simulations were subsequently performed under physiological conditions, allowing MBZ to sample different interactions within the binding pocket (Figure 4). A total of nine poses were identified with distinct orientations and significant populations (Figure 4). Throughout all simulations MBZ remained in the ATP binding site, forming nonbonded interactions with 10-16 amino acids, with the residues Asn51, Ala55, Ile96, Gly97, Met98, Asn106, Leu107, Phe138, Thr184 and Val186 being most frequently involved. A free energy analysis revealed two poses that are mostly likely for being experimentally observed. An extensive analysis of the nine binding poses can be found in reference [18] Manuscript is in preparation, which includes an examination of water involvement, how MZB binding effects amino acid motion and a thorough quantum mechanical study of the possible conformations that MBZ can adopt.

2.5. Mebendazole and the GLI Inhibitor GANT-61 Exhibit Synergistic Anti-Leukemic Effects

We treated AML cell lines and primary AML samples with different MBZ concentrations, resulting in a dose-dependent effect on the proliferation, colony formation and apoptosis (Figure 5A–D).

To evaluate the anti-leukemic activity of MBZ upon combined inhibition of GLI, we also investigated its usage with the small molecule GLI inhibitor GANT-61. We treated the AML cell lines MV4-11, MOLM-13, THP-1 and OCI-AML3 with combinations of MBZ and GANT-61, and analyzed cell proliferation and colony formation. In all cell lines tested, MBZ treatment alone already resulted in decreased proliferation and colony forming capacity in a dose dependent manner (Figure 5A–C). The combination of MBZ with the GLI inhibitor GANT-61 synergistically increased MBZ's anti-proliferative effects on all three AML cell lines (Figure 6A). Therapeutic synergy between MBZ and GANT-61 was indicated by a combination index < 1 calculated using the Chou-Talalay-Method (Figure 6A). In colony formation assays, treatment with high MBZ concentrations, in particular, resulted in significant reduction in colony numbers of MV4-11, MOLM-13 and THP-1 cells. Furthermore, GLI inhibition by GANT-61 increased the effect of MBZ on colony formation significantly (Figure 6B). Moreover, inhibition of HH signaling using shRNA targeting *GLI1* sensitized THP-1 cells to anti-proliferative effects by MBZ compared to control cells transduced with a scrambled shRNA (Figure 6C). Freshly isolated primary AML cells from 13 patients were investigated for anti-proliferative effects of MBZ treatment alone and in combination with GANT-61. MBZ mediated a strong and significant inhibitory impact on primary AML cell growth (Figure 5A), which was further increased by combination with GANT-61 (Figure 6D). Additionally, we treated the GLI luciferase reporter AML cell line THP-1 with

MBZ or GANT-61 alone and in combination for 24 h and measured the GLI promoter activity. As expected, MBZ and GANT-61 reduced the GLI promoter activity compared to the untreated control. The inhibitor combination resulted in a more pronounced decrease relative to the single agent treatment (Figure 6E).

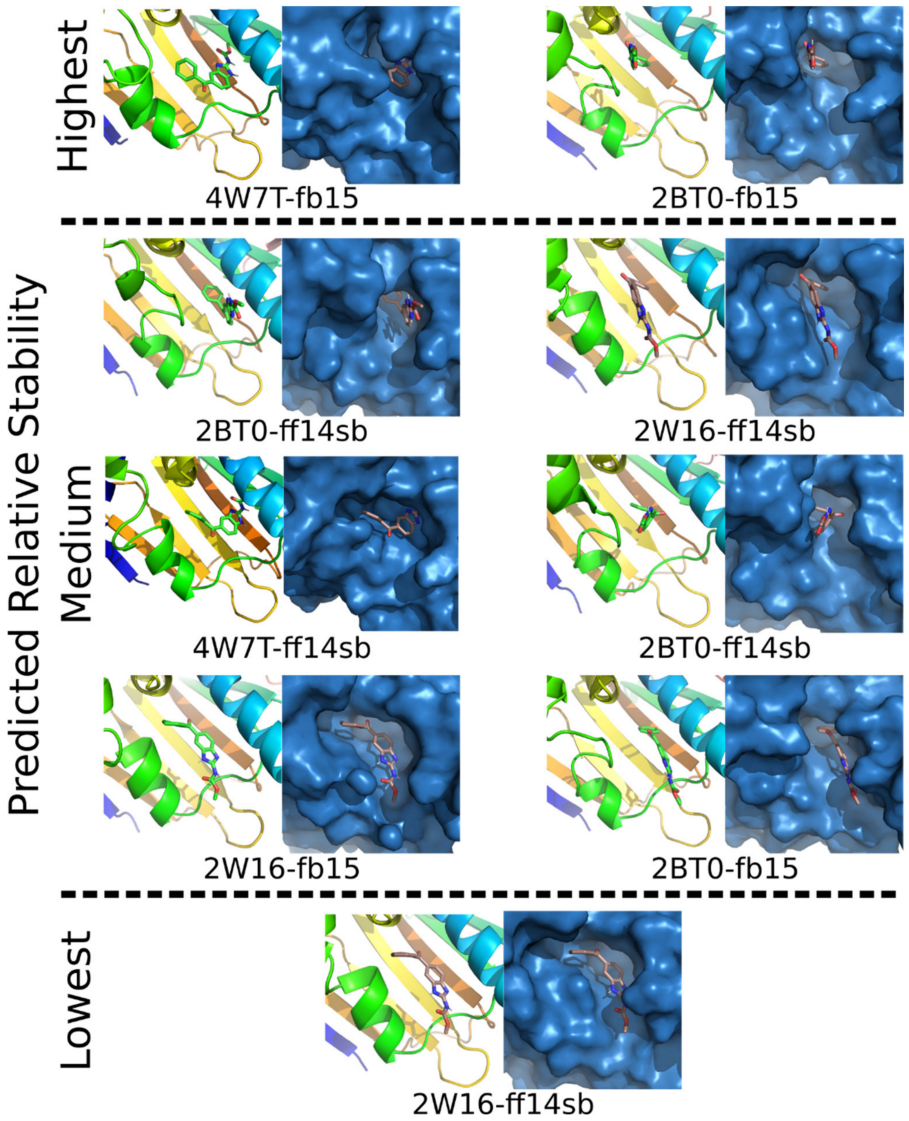

Figure 4. The nine binding poses of MBZ bound to HSP90's ATP binding site as identified through hierarchical clustering of the molecular dynamics simulations (600 ns in total). Each pose is shown with the protein rendered as a cartoon and surface. The poses are grouped according to the results of MM/PBSA calculations, with the highest (i.e., 0.0–0.3 kcal/mol), medium (4.6–8.9 kcal/mol) and lowest (12.6 kcal/mol) relative stabilities group together. The source of the poses are noted according to the protein crystal structure and force field used in the modeling. Only the poses identified with populations of >10% in the simulations are shown. Note that clustering a single model's data can yield multiple poses.

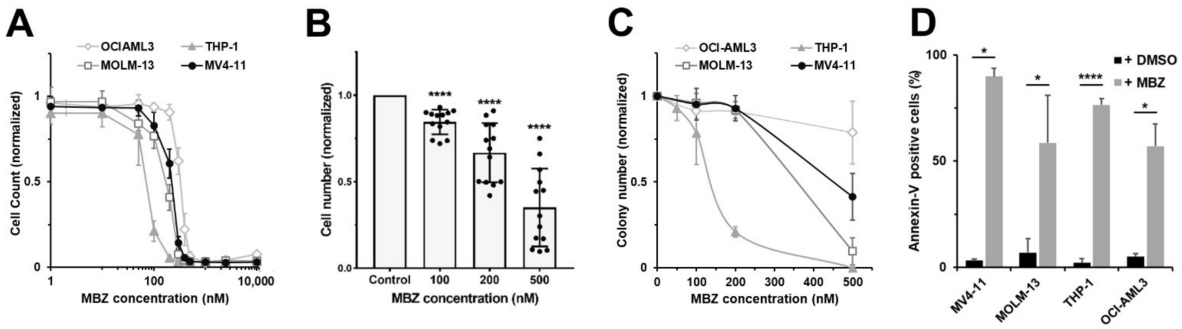

Figure 5. MBZ induces apoptosis and growth inhibition of AML cells. (**A**) Effects of increasing MBZ doses on AML cell lines MV4-11, MOLM-13, THP-1, and OCI-AML3 were analyzed for proliferation after three days. (**B**) Cell growth of primary AML cells (n = 13) was determined after 7 days of MBZ treatment. (**C**) Clonogenicity of AML cell lines MV4-11, MOLM-13 and THP-1 with increasing MBZ doses was investigated in colony formation assays. (**D**) Apoptosis induction was measured at 48 h after MBZ treatment in AML cell lines. Error bars represent the mean values ± standard deviation. * $p < 0.05$, **** $p < 0.0001$ in the Welch's t-test.

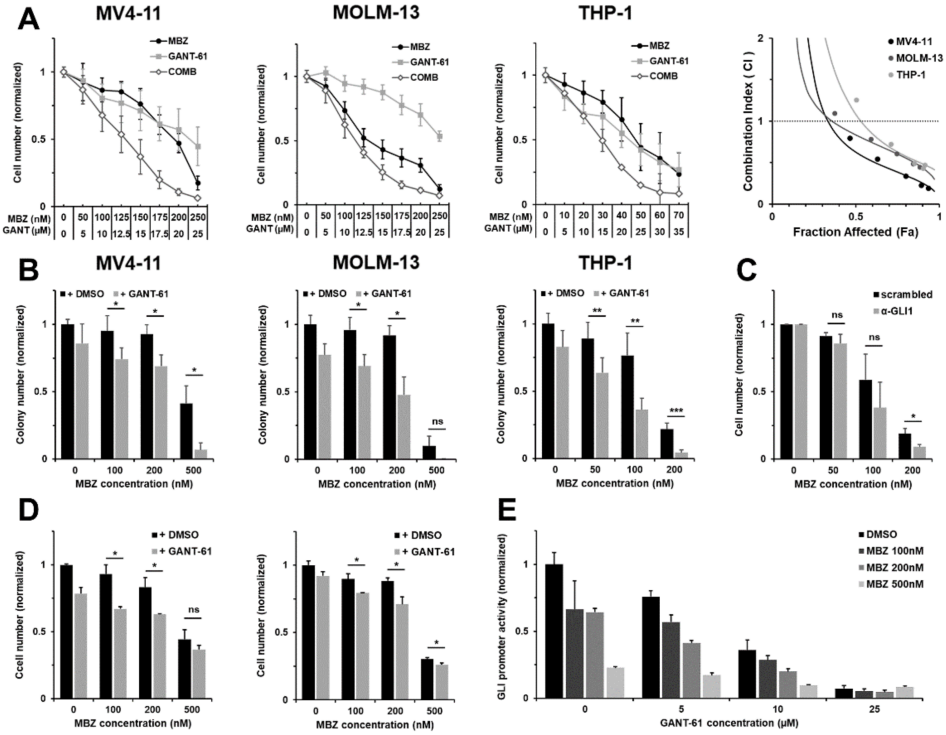

Figure 6. MBZ shows synergistic anti-leukemic effects upon combined treatment with GANT-61. (**A**) MV4-11, MOLM-13 and THP-1 cells were treated with the indicated concentrations of MBZ and GANT-61 alone or in combination and the effect on the proliferation capacity was analyzed after three days. The drug combination was tested for synergy by the method of Chou and Talalay using CompuSyn software. (**B**) The clonogenicity of AML cell lines MV4-11, MOLM-13 and THP-1 under MBZ treatment alone and in combination with GANT-61 was investigated in colony formation assays. (**C**) Effects of MBZ on cell growth of THP-1 cells transduced with shRNA against *GLI1* were analyzed in comparison with control cells transduced with a scrambled shRNA cell growth after 3 days. (**D**) Primary AML cells were treated with MBZ and GANT-61 alone, in combination or a solvent control. The effect on the proliferation capacity was analyzed after three days. Two representative data sets shown out of four AML samples. (**E**) GLI Reporter AML cell line THP-1 was treated with MBZ and GANT-61 alone or in combination. The GLI promoter activity was measured after 24 h. Error bars represent the mean values ± standard deviation. * $p < 0.05$, ** $p < 0.01$ in the Welch's t-test.

2.6. MBZ Sensitizes AML Cells to Chemotherapy

Cumulating evidence suggests that active GLI signaling plays a fundamental role in the maintenance of leukemia initiating cells, which evade chemotherapy due to their high drug resistance against cytotoxic drugs [19]. Consequently, they are associated with residual disease, relapse and therapy failure. Therefore, we examined the combinational effect of cytarabine and MBZ on the cell growth of AML cell lines MV4-11, MOLM-13 and OCI-AML3. As shown in Figure 7A, combined effect of cytarabine and MBZ induced a significant reduction in cell growth compared to each agent alone. To quantify if the combination of MBZ and cytarabine represents a favorable drug combination, data were analyzed using CompuSyn to compute the dose-reduction index (DRI) values for the drug combination tested at a constant dose ratio. DRI values represent the fold decrease in the dose of a drug needed in a combination to achieve the same efficacy as the drug alone. DRI values > 1 are considered favorable with regard to the predicted reduction in toxicity of a drug therapy. These parameters are particularly relevant for the analysis of drug combinations in the context of cancer treatment. When combined with MBZ, cytarabine doses can be reduced by 288.0-, 2.7- and 4.5-fold in MV4-11, MOLM-13 or OCI-AML3, respectively, to meet the same anti-proliferative effect level (Figure 7B). In all three cell lines, the DRI values increased with the rising effect level (Fraction affected (Fa)), suggesting the beneficial effect is particularly pronounced in the relevant effect level of a cancer therapy (Figure 7B,C).

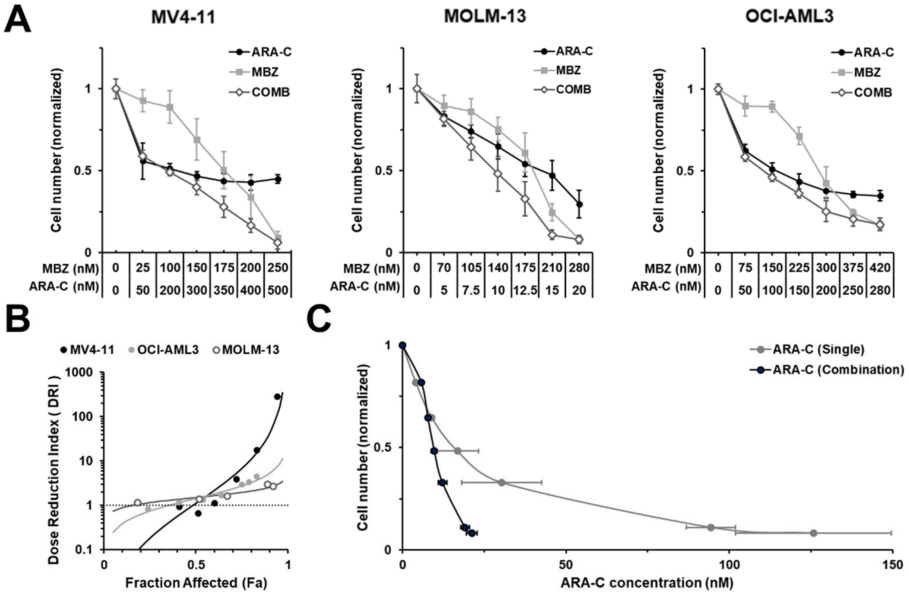

Figure 7. MBZ significantly sensitizes AML cells to cytarabine. (**A**) AML cell lines MV4-11, MOLM-13 and OCI-AML3 were treated with the indicated concentrations of MBZ and cytarabine (ARA-C) alone or in combination and the effect on the proliferation capacity was analyzed after three days. (**B**) Dose reduction index (DRI) of MBZ and GANT-61 combination on proliferation of MV4-11, MOLM-13 and OCI-AML3 cells. Values have been calculated from data of at least three independent experiments (**A**) using CompuSyn Software for Drug Combinations. DRI > 1 indicating a favorable drug combination. (**C**) Effect-dose-relationship of cytarabine (ARA-C) on proliferation of MOLM-13 cells alone or in combination with MBZ, respectively. Values have been calculated from data of at least three independent experiments using CompuSyn Software for Drug Combinations. Error bars represent the mean values ± standard deviation.

2.7. MBZ Effectively Inhibits GLI Signaling in Clinically Achievable Plasma Levels

To further evaluate if MBZ is a suitable therapeutic agent to inhibit GLI, we transferred these findings into the clinical setting by treating two refractory AML patients with MBZ monotherapy in an off-label setting. Using a modified plasma inhibitory assay (PIA) by incubating an indicator cell line carrying the GLI luciferase promoter transgene with the patients' plasma, a reduction in GLI promoter activity was detected for both samples (Figure 8A). Moreover, a 62-year-old male healthy volunteer ingested MBZ at a dose of 50 mg/kg divided over two ingestions at time 0 h and 12 h. Blood was drawn at 4 h and at 24 h. PIA results indicated a biological active plasma concentration (Figure 8A). Two patients with refractory AML received MBZ monotherapy after informed consent: Patient 1, a 66-year-old female, with normal karyotype and *NPM1*, *FLT3-TKD* and *IDH1* mutations (ELN favorable risk). This patient had received 2 induction cycles of cytarabine and daunorubicine followed by three consolidation therapies with cytarabine and in relapsed setting, mitoxantrone, cytarabine and etoposide (MEC) with no response to treatment); Patient 2, a 74-year-old female, had adverse risk (ELN criteria) secondary AML after MDS according with a complex aberrant karyotype (deletion 5, deletion 8 and monosomy 17 with no additional AML specific mutations). This patient has been treated non-intensively with low-dose cytarabine and venetoclax with no response to therapy prior to MBZ treatment. In patient 1, a clear and continuous decrease in leukemic blasts in peripheral blood and a fast reduction in GLI2 levels in peripheral leukemic blood cells could be shown whereas patient 2 did not respond. (Figure 8B,C).

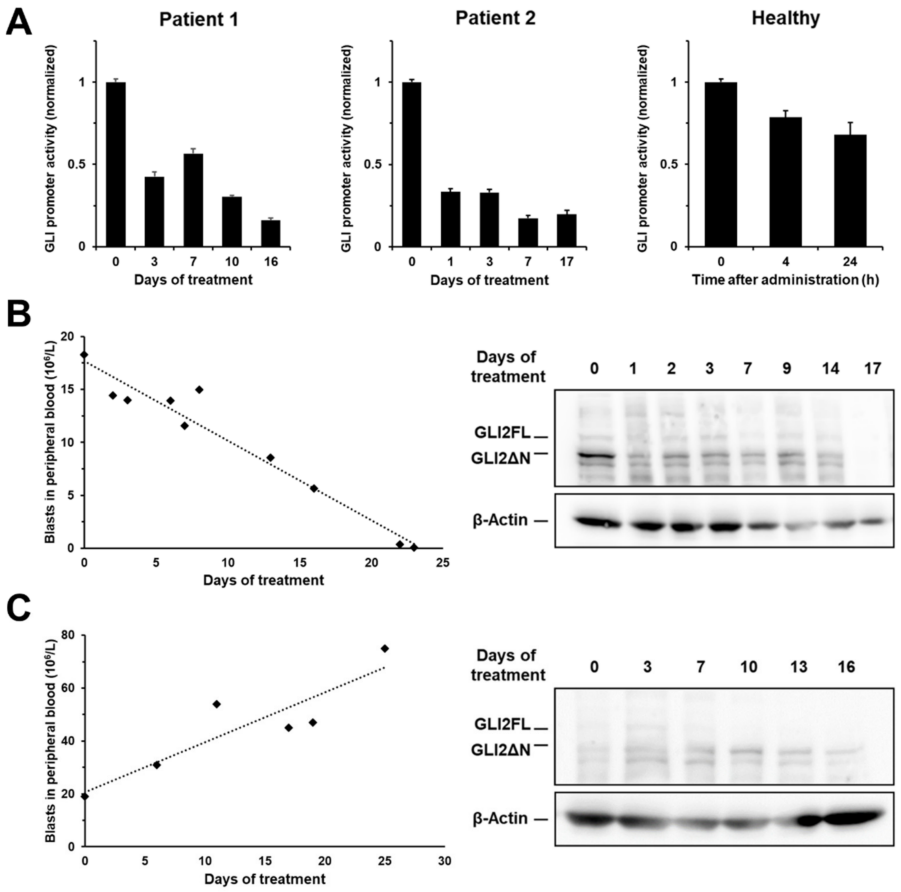

Figure 8. Clinically achievable plasma concentrations of MBZ effectively inhibit GLI signaling. (**A**) Two patients with refractory AML were treated with MBZ monotherapy with a daily dose of up

to 50 mg/kg. Patient blood samples taken at different time points over the period of 16 to 17 days. Isolated plasma samples were incubated GLI luciferase reporter cell line OCI-AML3 for 24 h before GLI promoter activity was measured. A healthy volunteer ingested MBZ at a dose of 50 mg/kg divided into two doses at time 0 h and 12 h. Blood was drawn at 4 h and at 24 h. In a modified Plasma Inhibitory Assay (PIA) MV4-11 GLI luciferase reporter cells were incubated with isolated plasma samples and GLI promoter activity measured after 24 h using the Dual-GLO Luciferase Assay Kit and the Infinite F200 PRO reader. Patient 1 (**B**) and patient 2 (**C**) with refractory AML were treated with MBZ monotherapy as described above. Under MBZ therapy, the blast counts in the peripheral blood of the AML patients were measured. Peripheral mononuclear cells (PBMC) of patient 1 and patient 2 were isolated from several samples throughout the entire treatment period and GLI2 analyzed by western blot analysis. β-Actin was used as a loading control. Error bars represent the mean values ± standard deviation.

3. Discussion

MBZ is a broad spectrum benzimidazole used for several decades in human and veterinary medicine to treat a variety of parasitic worm infections [17]. Lately, MBZ gained attention as a promising candidate for drug repurposing in oncology due to multiple studies reporting substantial in vitro and in vivo anticancer effects [9]. Besides neuroblastoma, hematological malignancies—including leukemia, lymphoma and multiple myeloma—were identified as the most sensitive cancers to treatment with the MBZ analogue flubendazole, as shown in a screen of 321 cell lines from 26 cancer entities [20].

In this study, the anti-leukemic effects of MBZ were confirmed in AML cell lines and primary blasts from AML patients. Most importantly, we revealed that MBZ's anti-leukemic effects were, at a minimum, partly due to a significantly reduced activity of the HH transcription factors GLI1 and GLI2 in AML. Furthermore, our data strongly indicate that MBZ mediates its anti-leukemic effects by promoting the degradation of GLI transcription factors through inhibition of HSP70/90 chaperone activity. Interestingly, MBZ sensitized AML cells to chemotherapy.

We previously demonstrated the importance of GLI1 and GLI2 in AML pathophysiology [7], and showed that inhibition of GLI activity resulted in pronounced anti-leukemic effects in vitro and significantly prolonged survival in a leukemic mouse model. We also showed that high expression of GLI represents a negative prognostic factor in two independent AML patient cohorts [7]. The potent anti-cancer effects mediated by inhibition of GLI transcription factors have also been demonstrated in numerous other studies [21].

Previously, Larsen et al. showed that MBZ inhibits canonical HH signaling in Shh Light2 fibroblasts by inhibiting the formation of the primary cilium [22], which is required for SMO-mediated GLI activation [23]. However, in previous work we could show that the treatment with the SMO inhibitor cyclopamine had no impact on the GLI promoter activity in AML reporter cell lines—leading to the hypothesis that the activation of GLI proteins in AML cells occurs independently of SMO [3]. In line with this theory, Chaudhry et al. also demonstrated that GLI signaling occurs independently of SMO [16]. Another study showed that primary cilia, which are essential for functional SMO signaling, are absent in most AML cells [24]. Mounting evidence implicates SMO-independent, non-canonical ways of GLI activation by alternative oncogenic pathways in AML, including *FLT3-ITD*, *PI3K/AKT/mTOR* and *RAS/RAF/MEK/ERK* signaling cascades [2,3]. These results support our hypothesis that MBZ mediates its inhibitory potential against the HH pathway in an SMO-independent way by inhibiting GLI downstream from SMO.

We could show that the decrease in GLI promoter activity resulted from a reduction in GLI1 and GLI2 protein levels. Inhibition of the 26S proteasome by Bortezomib abolished the effect of MBZ on GLI protein levels, indicating that the reduced GLI protein levels are caused by degradation via this proteasome.

Heat shock proteins act as molecular chaperones that are involved in the folding, activation and assembly of a variety of proteins. HSP70 and HSP90 are believed to act as the core chaperone system regulating stability, trafficking and degradation of signaling

proteins [25,26] and therefore maintaining the activity of a variety of protein kinases, transcription factors and steroid hormone receptors [26]. Based on our hypothesis that MBZ promotes the proteasomal degradation of GLI transcription factors, we investigated the effect of inhibition of HSP70 and HSP90 on GLI transcription factors. Treatment of AML cells with small molecule HSP70 and HSP90 inhibitors resulted in a marked decrease in GLI1 and GLI2 protein levels without reducing mRNA levels. Walf-Vorderwülbecke et al. extensively demonstrated the ability of MBZ to inhibit HSP70 [11]. However, such an effect of MBZ on HSP90 has not yet been demonstrated. Based on the strong effects of MBZ on GLI1 and GLI2 protein levels, which were comparable to dual inhibition with an HSP90 and an HSP70 inhibitor in our experiments, we hypothesized that MBZ might be an inhibitor of HSP70 and HSP90. To further support this hypothesis, in silico molecular models were created by binding MBZ to the ATP binding site. The modeling predicts that MBZ forms short-range nonbonded interaction with at least 10–16 amino acids within the binding site. Thus, the combined experimental and theoretical data strongly support the idea that MBZ binds to heat shock proteins and inhibits their binding to other proteins.

For binding to HSP90, its client proteins require other chaperones and co-chaperones since they are unable to be bound by HSP90 directly. Certain client proteins, such as transcription factors, have to be bound by HSP70 and its co-chaperone HSP40 first before being delivered to HSP90 [26]. Disruption of the HSP70-HSP90 chaperone cascade results in misfolding and degradation of those client proteins [27]. The strong sensitivity to inhibition of HSP70 and HSP90 in our study suggests that GLI transcription factors rely heavily on the HSP70-HSP90 chaperone cascade for protein folding and stability [28].

Similar to inhibitors of HSP70 or HSP90, MBZ was able to inhibit refolding of heat-denatured luciferase in MOLM^{luc+} AML cells. This suggests that MBZ mediates its effect, at least in part, by disrupting the cellular protein folding machinery. In line with our findings, Walf-Vorderwülbecke et al. demonstrated that MBZ is able to interfere with different members of the HSP70-HSP90 chaperone family in AML cells using nematic protein organization technique (NPOT®) analysis and DAVID analysis [11]. They indeed showed that the association of c-MYB with the HSP70 complex was lost after MBZ exposure, leading to misfolding and subsequent proteasomal degradation of MYB [11].

Treatment of AML cell lines with MBZ had no effect on the HSP70 or HSP90 protein expression, as shown by western blot analysis. However, HSF-1, the major transcription factor of the heat shock response genes, was heavily phosphorylated at Serine 326 in MBZ-treated AML cells, a modification that is critical for stress-induced HSF-1 activation [29]. Triggering of the HSF-1 stress response by MBZ could be due to proteotoxic stress that is also caused by other HSP inhibitors [29]. On the other hand, MBZ induced a reduction in total HSF-1 protein levels in AML cells. A possible explanation might be the depletion of factors that stabilize HSF-1 protein levels, such as Bcl-2 interacting cell death suppressor (BIS) [27,30–32].

It should be noted that for MBZ—in addition to the inhibition of HSP70 and HSP90, and subsequent degradation of transcription factors (e.g., GLI1, GLI2, MYB) and other HSP client proteins (e.g., FLT3)—a variety of other mechanisms have been identified that can mediate both inhibitory effects on GLI signaling and generate anticancer effects. Observed MBZ-mediated anticancer effects include the induction of anti-tumor immune response, sensitization to radiation and chemotherapy, inhibition of angiogenesis, induction of apoptosis, and inhibition of proliferation [9]. For instance, MBZ was shown to inhibit several important signaling kinases, including VEGFR2, FAK, GTPases Rho-A and Rac1 [9], ABL, JNK3 and KIT [33]. Furthermore, it was revealed that MBZ inhibits BRAF and MEK by blocking their ATP binding pocket [34]. Furthermore, MBZ inhibits tubulin depolymerization in several tumor models, including non-small cell lung cancer and glioblastoma [35,36]. However, in AML, MBZ did not induce microtubule depolymerization in concentrations of up to 10 μM [11].

We could show that in AML cells, the combination of MBZ with the small-molecule GLI inhibitor GANT-61 leads to synergistic anti-leukemic effects. This could be used as

a potential treatment strategy in the future to enhance the efficacy of a pharmacological HH blockade. Several HH pathway inhibitors are in development for AML treatment and are being considered as a new class of therapeutics [37]. MBZ represents a promising candidate to potentiate the effect of these agents and maximize their therapeutic success. Moreover, MBZ sensitized AML cell lines MV4-11, MOLM-13 and OCI-AML3 to cytarabine as indicated by large positive DRI values. This possible dose reduction could lower the therapy's toxicity while maintaining the same anti-leukemic effect. Consequently, this would be a suitable approach to achieve an improved treatment for the elderly who cannot tolerate higher doses. [38,39]. The prognosis for elderly, unfit patients is still bleak with current treatments. Although, fortunately, in recent years, the prognosis for these patients has brightened-up with the introduction of new targeted agents such as Bcl-2, FLT3 and IDH1/2 inhibitors. Especially the combination of azacitidine and venetoclax has become a wide-spread regimen for elderly, unfit AML patients resulting in an increased overall survival compared to hypomethylating agents alone [40]. However, not all new treatment modalities are curative, and treatment options for patients becoming refractory to these regimens are sparse. Therefore, MBZ may represent a valuable therapeutic option in this setting because of its very favorable toxicity profile, which is well suited for the treatment of elderly patients [38,39].

Long-term, repeated administration of mebendazole results in significantly higher plasma levels compared to a single dose, possibly due to enterohepatic circulation [41]. There is a large interindividual variation in the plasma levels achieved, with one study showing a maximum plasma concentration ranging from 0.017–0.134 μM after a single 1.5 g dose and up to 0.5 μM after repeated administrations of 1 g [42]. In another study, 12 patients with cystic disease were treated with a single or repeated dose of 10 mg/kg. Single dose administration resulted in a maximum plasma concentration of 0.24 μM on average (ranging from 0.06–1.69 μM), while repeated administration resulted in a maximum concentration of 0.47 μM and an Area Under The Curve five times higher than after a single dose [41]. We demonstrated that clinically achievable plasma concentrations of MBZ effectively inhibit GLI signaling in all three subjects (two AML patients and one healthy volunteer). Most notably, one patient with refractory AML treated with MBZ monotherapy in an off-label setting responded with a clear and continuous decrease in leukemic blasts in peripheral blood and a fast reduction in GLI2 levels in peripheral leukemic blood cells. In agreement with previous studies on MBZ plasma levels, repeated administration of the drug resulted in a stronger inhibitory effect than a single dose. Furthermore, and most importantly, MBZ-treatment led to strong anti-leukemic effects in one patient which was consequently accompanied by reduction in GLI2 protein levels in blast lysates. This suggests that oral administration of MBZ is suitable for achieving noticeable therapeutic effects in clinical use.

In summary, our work highlights the exceptional potential of MBZ as a future therapeutic option for the treatment of diverse cancers. Based on the results herein, we are currently pursuing a clinical trial with MBZ and low dose cytarabine for the treatment of elderly, refractory AML patients.

4. Materials and Methods

4.1. Cell Lines and Cell Culture

Cell lines MV4-11, MOLM-13, HL-60, THP1, Kasumi-1, OCI-AML3 and OCI-AML5 were either purchased at the DSMZ (Deutsche Sammlung von Mikroorganismen und Zellkulturen GmbH, Heidelberg, Germany) or at the ATCC (American Type Culture Collection, Manassas, VA, USA) or authenticated by the Multiplex human Cell Authentication test (Multiplexion, Heidelberg, Germany). MV4-11, MOLM-13, HL-60 and THP1 cells were maintained in RPMI 1640 medium (Gibco, Thermo Fisher Scientific, Waltham, MA, USA) supplemented with 10% fetal bovine serum (FBS Superior, Biochrom GmbH, Berlin, Germany). Kasumi-1 cells were cultured in RPMI 1640 medium supplemented with 20% FBS. OCI-AML3 cells were maintained in α-MEM medium (Gibco, Thermo Fisher Scien-

tific, Waltham, MA, USA) supplemented with 20% FBS. OCI-AML5 cells were cultured in α-MEM medium supplemented with 20% FBS and 10 ng/mL GM-CSF (PeproTech GmbH, Hamburg, Germany). All cells were maintained in a humidified incubator with 5% CO_2 at 37 °C. Primary AML cells were obtained after patient's informed consent and approval of the study by the ethics committee (PV3469, Ethik-Kommission der Ärztekammer Hamburg). Cells were isolated from bone marrow using density gradient centrifugation and cultured as described elsewhere [43].

4.2. Inhibitors and Reagents

Mebendazole ((Methyl-N-(5-benzoyl-1H-benzimidazol-2-yl)-carbamat, #M2523) and VER-155008 (#SML027) were purchased from Sigma-Aldrich (St. Louis, MO, USA). Cytarabine (Cytosin-1-β-D-arabinofuranosid) was purchased from Cell Pharm GmbH (Ara-Cell, 06983044, STADA, Bad Vilbel, Germany). GANT-61 (2,20-[[Dihydro-2-(4-pyridinyl)-1,3(2H,4H)-pyrimidinediyl]bis(methylene)]bis[N,N-dimethylbenzenamine], #3191) and PU-H71 (6-Amino-8-[(6-iodo-1,3-benzodioxol-5-yl)thio]-N-(1-methylethyl)-9H-purine-9-propanamine, #3104) were purchased from Tocris Biosience (Bristol, UK).

4.3. Reverse Transcription and Quantitative PCR

Exon-spanning primers were designed with Primer Blast [44] or Primer3web [45]. RNA was extracted using innuPREP RNA Mini Kit 2.0 (845-KS-2040250, Analytik Jena, Jena, Germany) and reverse transcribed into cDNA using PrimeScript™ RT Master Mix (RR036B, TaKaRa Bio Inc., Kusatsu, Japan). RT-qPCR analyses were carried out on the LightCycler 96 (Roche, Basel, Swiss) using the TB Green Premix Ex Taq II (RR820B, TaKaRa Bio Inc., Kusatsu, Japan) over 40 PCR cycles. Relative expression of the target genes was normalized to the reference gene *glyceraldehyde 3-phosphate dehydrogenase* (*GAPDH*) and calculated using the Pfaffl method [46].

Differentiation of *GLI2* and *GLI2ΔN* was performed according to the method of Londoño et al. [47]. The expression of the full-length transcript (*GLI2-FL*) and the C-terminus (*GLI2-C-term*) were determined in relation to total *GLI2* (*GLI2-ALL*). The expression of *GLI2ΔN* was calculated by subtracting the expression of *GLI2-FL* from the expression of *GLI2-C-term*. The difference corresponds to the expression of *GLI2ΔN*.

Primers are listed in Appendix A (Table A1).

4.4. Protein Isolation and Western Blot

Protein isolation and western blots were performed as described before [48]. For analysis of phosphorylated proteins, cells were harvested and lysed with radioimmunoprecipitation assay (RIPA) buffer (89900, Thermo Fisher Scientific, Waltham, MA, USA) supplemented with protease and phosphatase inhibitors (cOmpleteTM Tablets, 11697498001, Roche, Basel, Swiss; Sodium orthovanadate, 13721-39-6, Fivephoton Biochemicals, San Diego, CA, USA). Antibodies against rabbit anti-GLI1 monoclonal antibody (C68H3, 1:1000, Cell Signaling Technology, Inc., Danvers, MA, USA), mouse anti-GLI-2 (Dilution, C-10: sc-271786, Santa Cruz Biotechnology, Dallas, TX, USA), rabbit Anti-HSF1-phospho(S326) antibody (1:5000, EP1713Y, abcam, Cambridge, UK), rabbit Anti-HSF1 antibody (1:1000, 4356, Cell Signaling Technology, Inc., Danvers, MA, USA), Mouse anti-HSP70/HSPA1A antibody (1:1000, MAB1663, R&D Systems, Inc. Minneapolis, MN, USA), Rabbit anti-HSP90 Antibody (1:1000, #4874, Cell Signaling Technology, Inc., Danvers, MA, USA) or mouse anti-β-ACTIN (sc-47778, 1:5000, Santa Cruz Biotechnology, Dallas, TX, USA). Secondary antibodies against HRP-linked anti-rabbit immunoglobulins (1:10,000, 7074) and anti-mouse IgG (1:10,000, NXA931) secondary antibodies were purchased from Cell Signaling Technology (Danvers, MA, USA) and GE Healthcare (Cytiva, Marlborough, MA, USA), respectively.

4.5. GLI Reporter Assays

Stable GLI reporter AML cell lines were transduced by lentiviral constructs containing the *firefly luciferase* gene under the control of GLI transcriptional response elements and as internal control the *renilla luciferase* gene under the control of CMV promoter elements (Cignal™ Lenti Reporters, S-6030L, Qiagen, Venlo, The Netherlands) followed by puromycin (P7255, Sigma-Aldrich, St. Louis, MO, USA) and hygromycin (1287.1, Carl Roth GmbH, Karlsruhe, Germany) selection. Stable GLI reporter cells were treated with MBZ, GANT-61, PU-H71, VER-155008 or a solvent control, with the GLI promoter activity measured after 24 h using the Dual-GLO Luciferase Assay Kit (E2940, Promega, Madison, WI, USA) and the Infinite F200 PRO reader (Tecan, Männedorf, Switzerland). The firefly luciferase-mediated GLI promoter activity was normalized to the renilla luciferase-mediated CMV promoter activity.

4.6. Plasma Inhibitory Assay

OCI-AML3 reporter cells were plated at a ratio of 1:9 in serum-free medium plus plasma sample and incubated for 24 h at 37 °C. Before measurement, cells were washed three times with serum-free culture medium and the luciferase-mediated GLI promoter activity was measured in triplicates as described above.

4.7. Refolding Assay

MOLM-13^{luc+} cells stably expressing *firefly luciferase* were generated by lentiviral transduction using a luciferase-encoding vector kindly provided by Kristoffer Riecken [49]. The 1.5 million MOLM-13^{luc+} cells were incubated with 10 µM MBZ, 1 µM PU-H71, 25 µM VER-155008 or a solvent control at 37 °C for 30 min. Subsequently, cells were exposed to a heat-shock by incubation at 42 °C for 30 min, while the non-heat-shock control was incubated at 37 °C. Following heat-shock, cells were incubated at 37 °C and intracellular luciferase activity was measured on different time points (0, 30, 60, 120 min) using the Dual-GLO Luciferase Reagent (E2940, Promega, Madison, WI, USA) and the Infinite F200 PRO reader (Tecan, Männedorf, Switzerland).

4.8. Proliferation Assay

AML cells were incubated with different concentrations of MBZ alone or in combination with either GANT-61 or cytarabine for 3 or 7 days. Viable cell numbers were determined with the Trypan Blue dye exclusion method using the cell viability analyzer Vi-Cell ™ XR (Beckman Coulter, Brea, CA, USA).

4.9. Apoptosis Assay

AML cells were incubated with different concentrations of MBZ. Induction of apoptosis was measured after 48 h by flow cytometry using an APC-conjugated Annexin-V (AnxA100, MabTag GmbH, Friesoythe, Germany) and propidium iodide (P3566, Invitrogen, Thermo Fisher, Waltham, MA, USA) Data analysis was performed using the FACS Calibur (BD Biosciences, San Jose, CA, USA) and FlowJo V10 (Version 10.0.7, BD Life Sciences, FlowJo, LLC, Ashland, OR, USA) software.

4.10. Colony Formation Assay

AML cell lines were incubated with different concentrations of MBZ and/or GANT-61 and cultured in methylcellulose-based semi-solid media without or supplemented with growth factors, respectively (04230, Methocult H4230, Stemcell Technologies, Vancouver, BC, Canada). After seven days, the number of colonies was counted using an inverted microscope (Axiovert 25, Zeiss, Jena, Germany).

4.11. Cloning and Lentiviral Transduction

A pLKO.1-puro vectors encoding *GLI1* (TRCN0000020485, sequence 5′CCGGCCTGAT TATCTTCCTTCAGAACTCGAGTTCTGAAGGAAGATAATCAGGTTTTT-3′), or *scrambled*

shRNA (SHC002, non-target shRNA vector) were purchased from Sigma-Aldrich (St. Louis, MO, USA). The Lentiviral Gene Ontology Vector (LeGO) system was used for cloning and transfection into the AML cell lines (LeGO-G/Puro) [49]. Lentiviral particle containing supernatants were generated in HEK293T cells co-transfected with the plasmids LeGO-G/Puro (*GLI1* shRNA) or LeGO-G/Puro (*scrambled* shRNA) in combination with pMD2.G-VSV-G and psPAX2-Gag-Pol using calcium phosphate co-precipitation. THP-1 cells were either transduced with non-targeting shRNA (negative control) or with shRNA against *GLI1*. On day 3 after transduction, transduced cells were selected by addition of puromycin (2 µg/mL; Sigma-Aldrich, St. Louis, MO, USA) for 7 days prior to functional assays. The knock-down efficiency for GLI1 was determined using quantitative PCR analysis after seven days of puromycin selection. To generate the MOLM-13^{luc+} cells, MOLM-13 cells were transduced with a LeGO vector encoding for *firefly luciferase* using the same protocols. All work with lentiviral particles was done in a S2 facility after approval according to German law.

4.12. In Silico Modeling

All-atom molecular dynamic (MD) simulations were performed on models where MBZ was bound to HSP90′s ATP binding site using the AMBER software package [50]. A total of 6 independent simulations were performed that differed in the protein's crystal structure used (i.e., 2WI6, 2BT0 and 4W7T [51–53]) for model development and in the force field employed during the simulation. The proteins were modeled using the ff14SB and fb15 force fields [54,55], while MBZ was modeled using the gaff2 force field and RESP partial atomic charges [56]. The models were solvated using TIP3P or force-balanced water models, as appropriate for the protein force field. In total, 600 nanoseconds of simulation data were collected and analyzed. A complete description of the modeling can be found in reference [18].

4.13. Statistical Analysis

Data from the in vitro assays were statistically analyzed by the Welch's t-test using GraphPad Prism 7 (GraphPad Software, Inc., San Diego, CA). A p value less than 0.05 was considered to be statistically significant. The combination index (CI) and dose reduction index (DRI) were calculated using the CompuSyn program (Version 1.0, ComboSyn Inc., Paramus, NJ, USA) based on the Chou Talalay Method [57].

Supplementary Materials: The following are available online at https://www.mdpi.com/article/10.3390/ijms221910670/s1, Figure S1: Treatment with MBZ does not reduce GLI1 or GLI2 mRNA expression in AML cell lines, Figure S2: Treatment with ABZ does not reduce GLI promoter activity in AML reporter cell lines, Figure S3: Treatment with HSP70 or HSP90 inhibitors does not reduce GLI1 or GLI2 mRNA expression in AML cell lines, Figure S4: Mebendazole treatment does not affect HSP70 or HSP90 protein levels.

Author Contributions: Conceptualization, F.F., K.N.K., J.W. and W.F.; methodology, F.F. and J.M.; software, K.N.K.; validation, F.F., F.M., H.S., F.B., C.B., K.N.K., J.W. and W.F.; investigation, F.F., J.M., A.K. and K.N.K.; data curation, F.F. and F.M.; writing—original draft preparation, F.F., K.N.K., J.W. and W.F.; writing—review and editing, F.M., J.M., H.S., F.B., A.K. and C.B.; visualization, F.F. and K.N.K.; supervision, H.S., J.W. and W.F.; project administration, J.W. and W.F.; funding acquisition, J.W. and W.F. All authors have read and agreed to the published version of the manuscript.

Funding: This project was funded by the Erich und Gertrud Roggenbuck-Stiftung, the Federal Ministry for Education and Research and by the Ministry for Innovation, Science, Research, and Technology of the state Northrhine-Westfalia (research grant 13FH156IN6).

Institutional Review Board Statement: The study was conducted according to the guidelines of the Declaration of Helsinki, and approved by the local ethics committee (PV3469; Ethik Kommission der Ärztekammer, Hamburg, Germany).

Informed Consent Statement: Informed consent was obtained from all subjects involved in the study.

Acknowledgments: We would like to thank Vanessa Thaden, Gabi Vohwinkel and Julia Hinz, all Department of Oncology, Hematology and Bone Marrow Transplantation with Section Pneumology, Hubertus Wald University Cancer Center, University Medical Center Hamburg-Eppendorf, Hamburg, Germany for their technical support. The LeGO vectors were kindly provided by Kristoffer Riecken, Department for Stem Cell Transplantation at the University Medical Center Hamburg-Eppendorf. We would like to thank the Erich und Gertrud Roggenbuck-Stiftung for their financial support that allowed us to conduct this study. We would also like to thank Rudolf Berrendorf and Javed Razzaq for their continuous development and support of the UBRS's computing cluster. The UBRS's computer hardware was supported by the Federal Ministry for Education and Research and by the Ministry for Innovation, Science, Research, and Technology of the state Northrhine-Westfalia (research grant 13FH156IN6).

Conflicts of Interest: F.M. received support for meeting attendance from Servier, Incyte, Gilead, Jazz Pharmaceuticals, Novartis, Teva, Pfizer, Amgen, received research grant from Daiichi Sankyo and received speaker honorarium from Servier, outside of the submitted work. H.S. received a travel grant from Astellas GmbH and has an inventorship on patents held by Amgen Research (Munich, Germany) GmbH/Amgen Inc., outside of the submitted work. F.B. received travel grants from Daiichi Sankyo, Servier and Novartis and serves on advisory boards by Jazz. GmbH, Daiichi Sankyo and Servier, outside of the submitted work. C.B. reports personal fees from Sanofi Aventis, Merck KgA, Bristol-Myers Squibb, Merck Sharp & Dohme, Lilly Imclone, Bayer Healthcare, GSO Contract Research, AOK Rheinland-Hamburg, Novartis, outside the submitted work. W.F. reports a consultancy or advisory role for AbbVie, Amgen, ARIAD, Celgene, Jazz Pharmaceuticals, Novartis, Morphosys, and Pfizer; received research funding from Amgen; has patents, royalties, or other intellectual property from a patent on immunotherapy in AML obtained together with Amgen; and received travel support from Amgen, Daiichi Sankyo, Jazz Pharmaceuticals, and Servier, outside of the submitted work. No potential conflicts of interest were disclosed by the other authors. The funders had no role in the design of the study; in the collection, analyses, or interpretation of data; in the writing of the manuscript, or in the decision to publish the results.

Appendix A

Table A1. Primers used in this study.

Gene	Sense	Anti-Sense
GLI1	CTACATCAACTCCGGCCAAT	CGGCTGACAGTATAGGCAGA
GLI2	CCCCTACCGATTGACATGCG	GAAAGCCGGATCAAGGAGATG
GLI2-ALL	AACCCTGTCGCCATTCACAA	CCAGTGGCAGTTGGTCTCAT
GLI2-FL	TCAGCCTTTGGACACACACC	TGCACTTGTGGGGCTTCTC
GLI2-C-term	GCTGCAACAAAGCCTTCTCC	TTCTCTTTGAGCAGCGGTGT
GAPDH	GTCAGTGGTGGACCTGACCT	TGCTGTAGCCAAATTCGTTG

References

1. Jiang, J.; Hui, C. Hedgehog Signaling in Development and Cancer. *Dev. Cell* **2008**, *15*, 801–812. [CrossRef]
2. Aberger, F.; Hutterer, E.; Sternberg, C.; Del Burgo, P.J.; Hartmann, T.N. Acute Myeloid Leukemia-Strategies and Challenges for Targeting Oncogenic Hedgehog/GLI Signaling. *Cell Commun. Signal* **2017**, *15*, 8. [CrossRef] [PubMed]
3. Latuske, E.M.; Stamm, H.; Klokow, M.; Vohwinkel, G.; Muschhammer, J.; Bokemeyer, C.; Jücker, M.; Kebenko, M.; Fiedler, W.; Wellbrock, J. Combined Inhibition of GLI and FLT3 Signaling Leads to Effective Anti-Leukemic Effects in Human Acute Myeloid Leukemia. *Oncotarget* **2017**, *8*, 29187–29201. [CrossRef]
4. Teglund, S.; Toftgård, R. Hedgehog beyond Medulloblastoma and Basal Cell Carcinoma. *Biochim. Biophys. Acta-Rev. Cancer* **2010**, *1805*, 181–208. [CrossRef] [PubMed]
5. Dierks, C.; Beigi, R.; Guo, G.R.; Zirlik, K.; Stegert, M.R.; Manley, P.; Trussell, C.; Schmitt-Graeff, A.; Landwerlin, K.; Veelken, H.; et al. Expansion of Bcr-Abl-Positive Leukemic Stem Cells Is Dependent on Hedgehog Pathway Activation. *Cancer Cell* **2008**, *14*, 238–249. [CrossRef]
6. Cheng, J.; Gao, J.; Tao, K.; Yu, P. Prognostic Role of Gli1 Expression in Solid Malignancies: A Meta-Analysis. *Sci. Rep.* **2016**, *6*, 22184. [CrossRef]
7. Wellbrock, J.; Latuske, E.; Kohler, J.; Wagner, K.; Stamm, H.; Vettorazzi, E.; Vohwinkel, G.; Klokow, M.; Uibeleisen, R.; Ehm, P.; et al. Expression of Hedgehog Pathway Mediator GLI Represents a Negative Prognostic Marker in Human Acute Myeloid Leukemia and Its Inhibition Exerts Antileukemic Effects. *Clin. Cancer Res.* **2015**, *21*, 2388–2398. [CrossRef] [PubMed]

8. Wolska-Washer, A.; Robak, T. Glasdegib in the Treatment of Acute Myeloid Leukemia. *Future Oncol.* **2019**, *15*, 3219–3232. [CrossRef]
9. Guerini, A.E.; Triggiani, L.; Maddalo, M.; Bonù, M.L.; Frassine, F.; Baiguini, A.; Alghisi, A.; Tomasini, D.; Borghetti, P.; Pasinetti, N.; et al. Mebendazole as a Candidate for Drug Repurposing in Oncology: An Extensive Review of Current Literature. *Cancers* **2019**, *11*, 1284. [CrossRef]
10. WHO Informal Working Group on Echinococcosis. Guidelines for Treatment of Cystic and Alveolar Echinococcosis in Humans. *Bull. World Health Organ.* **1996**, *74*, 231–242.
11. Walf-Vorderwülbecke, V.; Pearce, K.; Brooks, T.; Hubank, M.; Van Den Heuvel-Eibrink, M.M.; Zwaan, C.M.; Adams, S.; Edwards, D.; Bartram, J.; Samarasinghe, S.; et al. Targeting Acute Myeloid Leukemia by Drug-Induced c-MYB Degradation. *Leukemia* **2018**, *32*, 882–889. [CrossRef]
12. Kinzler, K.W.; Bigner, S.H.; Bigner, D.D.; Trent, J.M.; Law, M.L.; O'Brien, S.J.; Wong, A.J.; Vogelstein, B. Identification of an Amplified, Highly Expressed Gene in a Human Glioma. *Science* **1987**, *236*, 70–73. [CrossRef] [PubMed]
13. Sadam, H.; Liivas, U.; Kazantseva, A.; Pruunsild, P.; Kazantseva, J.; Timmusk, T.; Neuman, T.; Palm, K. GLI2 Cell-Specific Activity Is Controlled at the Level of Transcription and RNA Processing: Consequences to Cancer Metastasis. *Biochim. Biophys. Acta-Mol. Basis Dis.* **2016**, *1862*, 46–55. [CrossRef] [PubMed]
14. Sasaki, H.; Nishizaki, Y.; Hui, C.C.; Nakafuku, M.; Kondoh, H. Regulation of Gli2 and Gli3 Activities by an Amino-Terminal Repression Domain: Implication of Gli2 and Gli3 as Primary Mediators of Shh Signaling. *Development* **1999**, *126*, 3915–3924. [CrossRef] [PubMed]
15. Zhao, X.; Ponomaryov, T.; Ornell, K.J.; Zhou, P.; Dabral, S.K.; Pak, E.; Li, W.; Atwood, S.X.; Whitson, R.J.; Chang, A.L.S.; et al. RAS/MAPK Activation Drives Resistance to Smo Inhibition, Metastasis, and Tumor Evolution in Shh Pathway-Dependent Tumors. *Cancer Res.* **2015**, *75*, 3623–3635. [CrossRef] [PubMed]
16. Chaudhry, P.; Singh, M.; Triche, T.J.; Guzman, M.; Merchant, A.A. GLI3 Repressor Determines Hedgehog Pathway Activation and Is Required for Response to SMO Antagonist Glasdegib in AML. *Blood* **2017**, *129*, 3465–3475. [CrossRef] [PubMed]
17. Dayan, A.D. Albendazole, Mebendazole and Praziquantel. Review of Non-Clinical Toxicity and Pharmacokinetics. *Acta Trop.* **2003**, *86*, 141–159. [CrossRef]
18. Fiedler, W.; Freisleben, F.; Wellbrock, J.; Kirschner, K. Mebendazole's Conformational Space and its Predicted Binding to Human Heat-Shock Protein 90. *ChemRxiv* **2021**, preprint.
19. Long, B.; Wang, L.-X.; Zheng, F.-M.; Lai, S.-P.; Xu, D.-R.; Hu, Y.; Lin, D.-J.; Zhang, X.-Z.; Dong, L.; Long, Z.-J.; et al. Targeting GLI1 Suppresses Cell Growth and Enhances Chemosensitivity in CD34+ Enriched Acute Myeloid Leukemia Progenitor Cells. *Cell. Physiol. Biochem.* **2016**, *38*, 1288–1302. [CrossRef]
20. Michaelis, M.; Agha, B.; Rothweiler, F.; Löschmann, N.; Voges, Y.; Mittelbronn, M.; Starzetz, T.; Harter, P.N.; Abhari, B.A.; Fulda, S.; et al. Identification of Flubendazole as Potential Anti-Neuroblastoma Compound in a Large Cell Line Screen. *Sci. Rep.* **2015**, *5*, 8202. [CrossRef]
21. Rimkus, T.K.; Carpenter, R.L.; Qasem, S.; Chan, M.; Lo, H.W. Targeting the Sonic Hedgehog Signaling Pathway: Review of Smoothened and GLI Inhibitors. *Cancers* **2016**, *8*, 22. [CrossRef]
22. Larsen, A.R.; Bai, R.Y.; Chung, J.H.; Borodovsky, A.; Rudin, C.M.; Riggins, G.J.; Bunz, F. Repurposing the Antihelmintic Mebendazole as a Hedgehog Inhibitor. *Mol. Cancer Ther.* **2015**, *14*, 3–13. [CrossRef]
23. Zhao, X.; Pak, E.; Ornell, K.J.; Murphy, M.F.P.; Mackenzie, E.L.; Chadwick, E.J.; Ponomaryov, T.; Kelleher, J.F.; Segal, R.A. A Transposon Screen Identifies Loss of Primary Cilia as a Mechanism of Resistance to SMO Inhibitors. *Cancer Discov.* **2017**, *7*, 1436–1439. [CrossRef]
24. Singh, M.; Chaudhry, P.; Merchant, A.A. Primary Cilia Are Present on Human Blood and Bone Marrow Cells and Mediate Hedgehog Signaling. *Exp. Hematol.* **2016**, *44*, 1181–1187. [CrossRef]
25. Rosenzweig, R.; Nillegoda, N.B.; Mayer, M.P.; Bukau, B. The Hsp70 Chaperone Network. *Nat. Rev. Mol. Cell Biol.* **2019**, *20*, 665–680. [CrossRef]
26. Taipale, M.; Jarosz, D.F.; Lindquist, S. HSP90 at the Hub of Protein Homeostasis: Emerging Mechanistic Insights. *Nat. Rev. Mol. Cell Biol.* **2010**, *11*, 515–528. [CrossRef]
27. Butler, L.M.; Ferraldeschi, R.; Armstrong, H.K.; Centenera, M.M.; Workman, P. Maximizing the Therapeutic Potential of HSP90 Inhibitors. *Mol. Cancer Res.* **2015**, *13*, 1445–1451. [CrossRef] [PubMed]
28. Morán Luengo, T.; Kityk, R.; Mayer, M.P.; Rüdiger, S.G.D. Hsp90 Breaks the Deadlock of the Hsp70 Chaperone System. *Mol. Cell* **2018**, *70*, 545–552. [CrossRef] [PubMed]
29. Dai, C.; Sampson, S.B. HSF1: Guardian of Proteostasis in Cancer. *Trends Cell Biol.* **2016**, *26*, 17–28. [CrossRef] [PubMed]
30. Im, C.N.; Yun, H.H.; Lee, J.H. Heat Shock Factor 1 Depletion Sensitizes A172 Glioblastoma Cells to Temozolomide via Suppression of Cancer Stem Cell-like Properties. *Int. J. Mol. Sci.* **2017**, *18*, 468. [CrossRef]
31. Kise, Y.; Takenaka, K.; Tezuka, T.; Yamamoto, T.; Miki, H. Fused Kinase Is Stabilized by Cdc37/Hsp90 and Enhances Gli Protein Levels. *Biochem. Biophys. Res. Commun.* **2006**, *351*, 78–84. [CrossRef]
32. Han, Y.; Wang, B.; Cho, Y.S.; Zhu, J.; Wu, J.; Chen, Y.; Jiang, J. Phosphorylation of Ci/Gli by Fused Family Kinases Promotes Hedgehog Signaling. *Dev. Cell* **2019**, *50*, 610–626. [CrossRef]
33. Nygren, P.; Fryknäs, M.; Ågerup, B.; Larsson, R. Repositioning of the Anthelmintic Drug Mebendazole for the Treatment for Colon Cancer. *J. Cancer Res. Clin. Oncol.* **2013**, *139*, 2133–2140. [CrossRef]

34. Simbulan-Rosenthal, C.M.; Dakshanamurthy, S.; Gaur, A.; Chen, Y.S.; Fang, H.B.; Abdussamad, M.; Zhou, H.; Zapas, J.; Calvert, V.; Petricoin, E.F.; et al. The Repurposed Anthelmintic Mebendazole in Combination with Trametinib Suppresses Refractory NRASQ61K Melanoma. *Oncotarget* **2017**, *8*, 12576–12595. [CrossRef] [PubMed]
35. Sasaki, J.I.; Ramesh, R.; Chada, S.; Gomyo, Y.; Roth, J.A.; Mukhopadhyay, T. The Anthelmintic Drug Mebendazole Induces Mitotic Arrest and Apoptosis by Depolymerizing Tubulin in Non-Small Cell Lung Cancer Cells. *Mol. Cancer Ther.* **2002**, *1*, 1201–1209. [PubMed]
36. Bai, R.Y.; Staedtke, V.; Aprhys, C.M.; Gallia, G.L.; Riggins, G.J. Antiparasitic Mebendazole Shows Survival Benefit in 2 Preclinical Models of Glioblastoma Multiforme. *Neuro-Oncology* **2011**, *13*, 974–982. [CrossRef]
37. Jamieson, C.; Martinelli, G.; Papayannidis, C.; Cortes, J.E. Hedgehog Pathway Inhibitors: A New Therapeutic Class for the Treatment of Acute Myeloid Leukemia. *Blood Cancer Discov.* **2020**, *1*, 134–145. [CrossRef]
38. Patil, V.M.; Bhelekar, A.; Menon, N.; Bhattacharjee, A.; Simha, V.; Abhinav, R.; Abhyankar, A.; Sridhar, E.; Mahajan, A.; Puranik, A.D.; et al. Reverse Swing-M, Phase 1 Study of Repurposing Mebendazole in Recurrent High-Grade Glioma. *Cancer Med.* **2020**, *9*, 4676–4685. [CrossRef]
39. Fernandez-Banares, F.; Gonzalez-Huix, F.; Xiol, X.; Catalá, I.; Miró, J.; López, N.; Casais, L. Marrow Aplasia during High Dose Mebendazole Treatment. *Am. J. Trop. Med. Hyg.* **1986**, *35*, 350–351. [CrossRef]
40. DiNardo, C.D.; Jonas, B.A.; Pullarkat, V.; Thirman, M.J.; Garcia, J.S.; Wei, A.H.; Konopleva, M.; Döhner, H.; Letai, A.; Fenaux, P.; et al. Azacitidine and Venetoclax in Previously Untreated Acute Myeloid Leukemia. *N. Engl. J. Med.* **2020**, *383*, 617–629. [CrossRef]
41. Braithwaite, P.A.; Roberts, M.S.; Allan, R.J.; Watson, T.R. Clinical Pharmacokinetics of High Dose Mebendazole in Patients Treated for Cystic Hydatid Disease. *Eur. J. Clin. Pharmacol.* **1982**, *22*, 161–169. [CrossRef]
42. Münst, G.J.; Karlaganis, G.; Bircher, J. Plasma Concentrations of Mebendazole during Treatment of Echinococcosis—Preliminary Results. *Eur. J. Clin. Pharmacol.* **1980**, *17*, 375–378. [CrossRef]
43. Pabst, C.; Krosl, J.; Fares, I.; Boucher, G.; Ruel, R.; Marinier, A.; Lemieux, S.; Hébert, J.; Sauvageau, G. Identification of Small Molecules That Support Human Leukemia Stem Cell Activity Ex Vivo. *Nat. Methods* **2014**, *11*, 436–442. [CrossRef]
44. Ye, J.; Coulouris, G.; Zaretskaya, I.; Cutcutache, I.; Rozen, S.; Madden, T.L. Primer-BLAST: A Tool to Design Target-Specific Primers for Polymerase Chain Reaction. *BMC Bioinform.* **2012**, *13*, 134. [CrossRef] [PubMed]
45. Untergasser, A.; Cutcutache, I.; Koressaar, T.; Ye, J.; Faircloth, B.C.; Remm, M.; Rozen, S.G. Primer3—New capabilities and interfaces. *Nucleic Acids Res.* **2012**, *40*, e115. Available online: https://primer3.ut.ee/ (accessed on 30 September 2021). [CrossRef] [PubMed]
46. Pfaffl, M.W. A New Mathematical Model for Relative Quantification in Real-Time RT–PCR. *Nucleic Acids Res.* **2001**, *29*, 2002–2007. [CrossRef]
47. Camacho Londoño, J.; Philipp, S.E. A Reliable Method for Quantification of Splice Variants Using RT-QPCR. *BMC Mol. Biol.* **2016**, *17*, 8. [CrossRef]
48. Freisleben, F.; Behrmann, L.; Thaden, V.; Muschhammer, J.; Bokemeyer, C.; Fiedler, W.; Wellbrock, J. Downregulation of GLI3 Expression Mediates Chemotherapy Resistance in Acute Myeloid Leukemia. *Int. J. Mol. Sci.* **2020**, *21*, 5084. [CrossRef] [PubMed]
49. Weber, K.; Mock, U.; Petrowitz, B.; Bartsch, U.; Fehse, B. Lentiviral Gene Ontology (LeGO) Vectors Equipped with Novel Drug-Selectable Fluorescent Proteins: New Building Blocks for Cell Marking and Multi-Gene Analysis. *Gene Ther.* **2010**, *17*, 511–520. Available online: http://www.lentigo-vectors.de/vectors.htm (accessed on 30 September 2021). [CrossRef] [PubMed]
50. Case, D.A.; Ben-Shalom, I.Y.; Brozell, S.R.; Cerutti, D.S.; Cheatham, T.E., III; Cruzeiro, V.W.D.; Darden, T.A.; Duke, R.E.; Ghoreishi, D.; Giambasu, G.; et al. Lessons learned from comparing molecular dynamics engines on the SAMPL5 dataset. *J. Comput.-Aided Mol. Des.* **2017**, *31*, 147–161.
51. Brough, P.A.; Barril, X.; Borgognoni, J.; Chene, P.; Davies, N.G.M.; Davis, B.; Drysdale, M.J.; Dymock, B.; Eccles, S.A.; Garcia-Echeverria, C.; et al. Combining Hit Identification Strategies: Fragment-Based and in Silico Approaches to Orally Active 2-Aminothieno[2,3−*d*]Pyrimidine Inhibitors of the Hsp90 Molecular Chaperone. *J. Med. Chem.* **2009**, *52*, 4794–4809. [CrossRef] [PubMed]
52. Dymock, B.W.; Barril, X.; Brough, P.A.; Cansfield, J.E.; Massey, A.; McDonald, E.; Hubbard, R.E.; Surgenor, A.; Roughley, S.D.; Webb, P.; et al. Novel, Potent Small-Molecule Inhibitors of the Molecular Chaperone Hsp90 Discovered through Structure-Based Design. *J. Med. Chem.* **2005**, *48*, 4212–4215. [CrossRef] [PubMed]
53. McBride, C.M.; Levine, B.; Xia, Y.; Bellamacina, C.; Machajewski, T.; Gao, Z.; Renhowe, P.; Antonios-McCrea, W.; Barsanti, P.; Brinner, K.; et al. Design, Structure-Activity Relationship, and in Vivo Characterization of the Development Candidate NVP-HSP990. *J. Med. Chem.* **2014**, *57*, 9124–9129. [CrossRef] [PubMed]
54. Maier, J.A.; Martinez, C.; Kasavajhala, K.; Wickstrom, L.; Hauser, K.E.; Simmerling, C. Ff14SB: Improving the Accuracy of Protein Side Chain and Backbone Parameters from Ff99SB. *J. Chem. Theory Comput.* **2015**, *11*, 3696–3713. [CrossRef] [PubMed]
55. Wang, L.-P.; McKiernan, K.A.; Gomes, J.; Beauchamp, K.A.; Head-Gordon, T.; Rice, J.E.; Swope, W.C.; Martínez, T.J.; Pande, V.S. Building a More Predictive Protein Force Field: A Systematic and Reproducible Route to AMBER-FB15. *J. Phys. Chem. B* **2017**, *121*, 4023–4039. [CrossRef]
56. Alenaizan, A.; Burns, L.A.; Sherrill, C.D. Python Implementation of the Restrained Electrostatic Potential Charge Model. *Int. J. Quantum Chem.* **2019**, *120*, e26035. [CrossRef]
57. Chou, T.C. Drug Combination Studies and Their Synergy Quantification Using the Chou-Talalay Method. *Cancer Res.* **2010**, *70*, 440–446. [CrossRef]

2. Darstellung der Publikationen mit Literaturverzeichnis

Die akute myeloische Leukämie (AML) ist eine Erkrankung des blutbildenden Systems, die durch eine klonale Expansion von abnormal differenzierten Blasten der myeloischen Linie gekennzeichnet ist. Sie entsteht auf dem Boden der onkogenen Transformationen einer hämatopoetischen Stammzelle oder einer Progenitorzelle mit wiedererlangten stammzellähnlichen Eigenschaften. Die Proliferation der unreifen Blasten resultiert in einer Verdrängung der normalen Hämatopoese mit Anämie, Hämorrhagien und schwerwiegenden Infektionen und führt unbehandelt innerhalb kürzester Zeit zum Tod (Short et al., 2018). Seit vielen Jahrzehnten stellt das 7+3-Chemotherapieschema (7 Tage Cytarabin und 3 Tage Daunorubicin) die Standardbehandlung dar, mit der in 60-85% der Erwachsenen jünger als 60 Jahre und in 40-60% der Patienten über 60 Jahren eine komplette Remission erzielt werden kann. Auch nach Erreichen einer kompletten Remission erleidet ein großer Teil der Patienten ein Rezidiv, sodass das Langzeitüberleben mit 35-45% bei Patienten unter 60 Jahren und nur 10-15% bei den Patienten mit 60 Jahren und niedrig schlecht ist (Döhner et al., 2017; Pabst et al., 2012).

Als Wurzel des Therapieversagens und von Rezidiven in der AML gelten leukämische Stammzellen (LSC), die in der Knochenmarksnische überleben und ein Reservoir für leukämische Blasten bilden (Batlle & Clevers, 2017; Bonnet & Dick, 1997; Lapidot et al., 1994). Diverse Studien konnten zeigen, dass der Nachweis einer starken stammzelltypischen Genexpression oder einer hohen Frequenz an LSC im Blut bei Erstdiagnose in hohem Maße prädiktiv für Rezidive und das klinische Outcome ist (Eppert et al., 2011; Gentles et al., 2010; Ho et al., 2016; Rocca et al., 2018; Shlush et al., 2017). Wie hämatopoetische Stammzellen besitzen auch LSC diverse Stammzell-Charakteristiken, die ihnen unter anderem die Fähigkeit zur Selbsterneuerung und ihre Widerstandfähigkeit gegenüber Therapien ermöglichen. Dazu zählen auch vielfältige Resistenzmechanismen wie beispielsweise Tumor Dormancy, Expression von Multidrug-Transportern und Apoptoseresistenz (Niu et al., 2022). Diese Eigenschaften werden durch hochkonservierte Stammzell-Signalwege vermittelt, unter anderem die Wnt/β-Catenin- (Hu et al., 2009; C. Zhao et al., 2007), Bmi-1- (Lessard & Sauvageau, 2003) und Hedgehog-Signalkasakade (Dierks et al., 2008; C. Zhao et al., 2009). Um langanhaltende Remissionen zu erreichen, ist es notwendig, diese malignen Stammzellen gezielt zu eliminieren.

Der Hedgehog-Signalweg (HH) ist eine hochkonservierte Signalkaskade, die eine entscheidende Rolle während der Embryogenese spielt und zudem an vielen grundlegenden Zellfunktionen, einschließlich Zelldifferenzierung, Proliferation und Stammzellerhaltung, beteiligt ist (Jiang & Hui, 2008). Der wichtigste Rezeptor für HH-Liganden ist Patched (Ptch), ein 12-Transmembranprotein. Nach der Ligandenbindung setzt Ptch SMO frei, ein rezeptorähnliches Protein mit sieben Transmembrandomänen, dessen Freisetzung letztlich zur Aktivierung der drei GLI-Zink-Finger-Transkriptionsfaktoren führt. Nach deren Aktivierung translozieren die GLI-Transkriptionsfaktoren in den Zellkern und induzieren die Expression von HH-Zielgenen. Die GLI-Transkriptionsfaktoren stellen über die Beeinflussung der zellulären Genexpression die zentralen Effektoren des HH-Signalwegs dar (Niewiadomski et al., 2019). Sie bestehen aus den drei Mitgliedern GLI1, GLI2 und GLI3 mit jeweils spezialisierten Funktionen und unterschiedlichen Regulationsmechanismen. GLI1 und GLI2 sind Transkriptionsaktivatoren, während GLI3 überwiegend in seiner Repressorform vorliegt und als starker Inhibitor der GLI-vermittelten Transkription fungiert (Jiang & Hui, 2008; Pan & Wang, 2007; H. Sasaki et al., 1997). Das Gleichgewicht zwischen den aktivierenden und suppressiven Formen der drei GLI-Transkriptionsfaktoren bestimmt die Gesamtexpression von HH-Zielgenen, einschließlich PTCH1 und GLI1(Aberger & Ruiz i Altaba, 2014). GLI1 wird in

ruhenden Zellen nicht exprimiert und fungiert nach HH-vermittelter Expression als positiver Feedback-Mechanismus (C. B. Bai et al., 2002). Im kanonischen HH-Signalweg reguliert SMO das Ausmaß der transkriptionellen GLI-Aktivität, indem es das Gleichgewicht zwischen einer Aktivierung durch GLI2 und einer Inhibition durch GLI3 in seiner Repressorform (GLI3R) verschiebt (Aberger & Ruiz i Altaba, 2014).

Wie oben beschrieben spielt der HH Signalweg jedoch auch eine zentrale Rolle in der Physiologie von leukämischen Stammzellen. Seine aberrante Aktivierung wurde darüber hinaus auch in zahlreichen weiteren Krebsentitäten gezeigt, darunter Karzinome der Prostata, Lunge, Brust und des Pankreas (Teglund & Toftgård, 2010). Aberrante Aktivierung des HH-Signalwegs kann durch den kanonischen Weg über Mutationen von SMO oder Ptch erfolgen, was unter anderem im Basalzellkarzinom und Medulloblastom gezeigt wurde (Raffel et al., 1997; Reifenberger et al., 2005; Xie et al., 1997, 1998). Oft erfolgt in Krebszellen jedoch die direkte Aktivierung der GLI-Transkriptionsfaktoren auf nicht-kanonischem Weg über Schnittstellen mit zahlreichen onkogenen Signalkaskaden, einschließlich FLT3/STAT5, RTK/RAF/MEK/ERK und PI3K/AKT/mTOR (Pietrobono et al., 2019). Diese intrinsische Aktivierung von Stammzell-Signalwegen ist eine mögliche Erklärung für eine zunehmende Unabhängigkeit der Krebsstammzellen von extrinsischen Signalen mit fortschreitender maligner Transformation (Batlle & Clevers, 2017).

Die klinische Relevanz zeigt sich dadurch, dass eine aktivierte GLI-Signalkaskade in verschiedenen Krebsarten mit einer schlechteren Prognose assoziiert ist (Cheng et al., 2016). Wir konnten in vorherigen Arbeiten zeigen, dass die Expression von GLI auch in der AML einen negativen prognostischen Faktor darstellt (Wellbrock et al., 2015). Dieser Effekt könnte unter anderem über eine erhöhte Widerstandsfähigkeit gegenüber Chemotherapie vermittelt werden. Mehrere Studien haben die Rolle einer aktivierten GLI-Signalkaskade bei der Entwicklung von Chemotherapieresistenz bei verschiedenen Krebsarten, einschließlich AML, Magen- und Ovarialkarzinomen, belegt (Kobune et al., 2009; Yoon et al., 2014; Zhang et al., 2018).

Es wurde mehrfach gezeigt, dass die Kombination von Cytarabin (Ara-C) mit dem SMO-Inhibitor Cyclopamin oder dem GLI-Inhibitor GANT-61 die Empfindlichkeit von AML-Zelllinien und primären $CD34^+$ AML-Zellen gegenüber Ara-C deutlich erhöht (Kobune et al., 2009; Liang et al., 2017; Long et al., 2016). Bei therapierefraktären AML-Patienten wurde gegenüber nicht refraktären Fällen eine signifikant höhere GLI1-Expression festgestellt. Darüber hinaus wurde eine hohe Expression von GLI1 mit einem erhöhten Risiko für rasche und wiederholte Rezidive in Verbindung gebracht. Die Autoren konnten die Resistenz einer multipel arzneimittelresistenten HL-60 AML-Zelllinie mit dem SMO-Inhibitor NVP-LDE225 aufheben. Die SMO-Inhibition führte zu einer verringerten Proteinexpression von MRP1, einem Membrantransporterprotein, das mit Arzneimittelresistenz und einer schlechten Prognose bei AML-Patienten assoziiert ist (Huang et al., 2019). Darüber hinaus führt ein aktivierter GLI-Signalweg zur Hochregulation verschiedener Medikamententransporter, darunter die ABC-Transporter ABCB1, ABCB2 und ABCG2, DNA-Reparaturmechanismen und wirkstoffmodifizierende Enzyme der UDP-Glucuronosyltransferase(UGT1A)-Familie (Chen et al., 2014; Meng et al., 2015; Zahreddine et al., 2014; Zhou et al., 2020).

Im Rahmen meiner Promotion setzte ich mich mit der zentralen Fragestellung auseinander, inwieweit der Hedgehog-Signalweg und insbesondere die GLI-Transkriptionsfaktoren zur Entstehung und Aufrechterhaltung von Chemotherapieresistenz in der AML beitragen und welche Mechanismen der Resistenzentwicklung zugrunde liegen. Zudem sollten neue Wege oder Wirkstoffe untersucht werden, um die GLI-Transkriptionsfaktoren zu inhibieren und damit

einer Resistenzentwicklung entgegenzuwirken. Die Ergebnisse meiner Studien konnte ich in zwei Erstautoren-Publikationen veröffentlichen, deren Inhalt ich im Folgenden kurz erläutern und diskutieren werde.

Um die Rolle des Hedgehog-Signalwegs und dessen Mechanismen bei der Entwicklung von Chemotherapieresistenz gegen Ara-C in der AML zu untersuchen, erzeugten wir Ara-C-resistente Varianten verschiedener AML-Zelllinien durch Langzeitkultivierung mit sukzessive steigenden Ara-C-Konzentrationen. Ara-C ist seit über vier Jahrzehnten der Kern der Standard-Induktionstherapie als Teil des 7+3-Schemas für Patienten, die für eine Hochdosis-Chemotherapie in Frage kommen (Döhner et al., 2017; Short et al., 2018). Die Ara-C-Resistenz wurde durch einen IC80-Wert (80%ige inhibitorische Konzentration) für das Zellwachstum über 10.000 nM definiert. Anschließend untersuchten wir die GLI-mRNA-Expression der resistenten Varianten im Vergleich zu ihrer jeweiligen parentalen Zelllinie. Bei der mRNA Expression von GLI1 oder GLI2 wurden keine signifikanten Veränderungen festgestellt. GLI3 mRNA war jedoch bei allen resistenten Varianten, deren parentale Zelllinie eine GLI3-Expression aufwies, nicht mehr nachweisbar. Darüber hinaus konnten wir mittels Western-Blot nachweisen, dass in den AML Zelllinien OCI-AML3 und OCI-AML5 auch auf Proteinebene signifikant niedrigere GLI3-Konzentrationen zu beobachten waren. Diese Herunterregulation scheint auch eine klinische Relevanz zu besitzen. Bereits in früheren Arbeiten stellten wir bei 74 % der AML-Patientenproben eine fehlende GLI3-Expression fest (Wellbrock et al., 2015). Im Einklang mit diesen Ergebnissen zeigte die genetische Analyse des AML-Datensatzes des Cancer Genome Atlas durch Chaudhry et al., dass die GLI3-Expression bei den meisten AML-Patienten epigenetisch stillgelegt ist (Chaudhry et al., 2017).

Um zu untersuchen, ob die Herunterregulation von GLI3 allein zu einer Chemotherapieresistenz führt, erzeugten wir GLI3-Knockdown-Zellen durch lentivirale Transduktion mit zwei verschiedenen GLI3-spezifischen short hairpin RNAs (shRNA). Bei gleichzeitiger Transduktion der beiden GLI3-spezifischen shRNAs wurde die GLI3-Expression in THP-1-Zellen auf 39,6 % (± 31,1 %) und in OCI-AML3-Zellen auf 53,7 % (± 31,4 %) im Vergleich zur Kontrolle reduziert. Trotz einer grenzwertigen Verringerung der GLI3 mRNA-Spiegel im Vergleich zur vollständigen Ausschaltung in resistenten Zelllinien konnten wir zeigen, dass die Herunterregulation von GLI3 mittels shRNA zu einer signifikant reduzierten Sensibilität der Zellen gegenüber Ara-C führte. Dieser Effekt war besonders deutlich in klonogenen Assays von AML-Zellen. Dies deutet darauf hin, dass die Herunterregulation von GLI3 leukämische Stamm- oder Vorläuferzellen spezifisch vor den zytotoxischen Wirkungen von Ara-C schützen könnte. Wie oben ausgeführt wurde der Zusammenhang zwischen aktiver HH-Signalkaskade und Chemotherapieresistenz bei AML und zahlreichen anderen Krebsarten gezeigt. Die Herunterregulation von GLI3 im Zusammenhang mit der Entwicklung einer Ara-C-Resistenz bei AML wurde bisher jedoch nie beschrieben.

Um den Mechanismus hinter der erhöhten Ara-C-Resistenz der Knockdown-Zelllinien zu verstehen, analysierten wir die Expression zahlreicher Gene, die am Ara-C-Stoffwechsel beteiligt oder im Kontext von Resistenzmechanismen beschrieben worden sind. Im Vergleich zum Wildtyp zeigten die GLI3-Knockdown-Zelllinien eine erhöhte Expression von SAMHD1, CDA und ABCC11 (MRP8). Die ATP-bindende Kassette C11 (ABCC11) gehört zur Familie der ATP-bindenden Kassettentransporter, die als Nukleotid-Efflux-Pumpe fungieren und die intrazellulären Konzentrationen mehrerer klinisch relevanter Nukleotidanaloga, einschließlich der zur Behandlung von Malignomen eingesetzten Fluoropyrimidine, verringern (Guo et al., 2003). Die Expression des Efflux-Transporters ABCC11 korreliert mit einer schlechten Prognose in der AML. Zellen, die mit ABCC11 transfiziert wurden, waren resistenter gegen Ara-C und wiesen geringere intrazelluläre Konzentrationen von Ara-C und seinen Metaboliten

auf (Guo et al., 2009). Intrazellulär wird Ara-C durch drei Phosphorylierungsschritte aktiviert, die zu seinem aktiven Metaboliten Cytidin-5′-triphosphat (Ara-CTP) führen, wobei die Phosphorylierung von Ara-C zu Ara-CMP durch die Desoxycytidin-Kinase (DCK) der geschwindigkeitsbestimmende Schritt bei seiner Aktivierung ist (Lamba, 2009). SAMHD1 ist eine Phosphohydrolase, die Desoxynukleosidtriphosphate (dNTP) in anorganisches Triphosphat und Desoxyribonukleoside spaltet (Franzolin et al., 2013). In leukämischen Zellen, die Ara-C ausgesetzt sind, reduziert SAMHD1 den Ara-CTP-Spiegel drastisch, indem es Ara-CTP zu inaktivem Ara-C hydrolysiert (Hollenbaugh et al., 2017). Die Inaktivierung von SAMHD1 führt in AML-Zellen zu einer deutlichen Sensibilisierung gegenüber den zytotoxischen Wirkungen von Ara-C in vitro und in vivo. Außerdem zeigte sich eine SAMHD1-Expression als ein negativer Prädiktor für das Ansprechen auf eine Ara-C-basierte Behandlung bei AML-Patienten (Schneider et al., 2017). Bei der Aktivierung von Ara-C konkurriert DCK mit Cytidindesaminase (CDA), die Ara-C irreversibel zu seinem inaktiven Uracil-Derivat Uracil-Arabinosid (Ara-U) deaminiert (Cohen, 1977). Ohta et al. zeigten, dass eine hohe CDA-Aktivität die Resistenz von U937 monozytoiden Leukämiezellen gegen Ara-C vermittelt (Ohta et al., 2004). In einem Ex-vivo-Zytotoxizitätstest mit AML-Patientenproben war die CDA-Expression in der Ara-C-sensitiven Gruppe im Vergleich zu den intermediär sensiblen oder resistenten Proben signifikant niedriger und erwies sich als ein starker Prädiktor für das Ansprechen auf Ara-C (Abraham et al., 2015). Bei AML-Patienten war eine hohe Aktivität und Expression von CDA mit einem schlechten initialen Ansprechen verbunden und prädiktiv für die Dauer der Remission (Jahns-Streubel et al., 1997; Schröder et al., 1998).

Wir konnten zeigen, dass die Herunterregulation von GLI3 einen Mechanismus für die Resistenz von AML-Zellen gegen Ara-C darstellt, den wir während der Resistenzbildung von AML-Zellen beobachten konnten. Zudem zeigte sich auch in Polymerase Chain Reaction (PCR)- bzw. Sequenzierungs-Daten primärer AML-Proben in einem Großteil der Zellen eine fehlende GLI3 Expression. In Anbetracht der übereinstimmenden Daten scheint die Herunterregulation von GLI3 in AML-Zellen von Vorteil zu sein. Eine Erklärung hierfür ist, dass GLI3 überwiegend in seiner Repressorform GLI3R vorliegt - dem wichtigsten Suppressor GLI-vermittelter Genexpression (Petrova et al., 2013). Für AML-Zellen scheint eine Ausschaltung dieses Suppressors eine zentrale Rolle zuzukommen. Besonders bei einer nicht-kanonischen Aktivierung der GLI-Transkriptionsfaktoren stellt eine intakte, aber nicht aktivierte kanonische HH-Signalkaskade über Bildung von GLI3R einen starken inhibitorischen Stimulus dar. So zeigt sich in einem Medulloblastom-Mausmodell, das durch die Expression von GLI2ΔN angetrieben wird, eine tumorsuppressive Rolle für GLI3R. GLI2ΔN ist eine konstitutiv aktive GLI2-Isoform, die zu einer überaktivierten GLI-Signalantwort führt (Han et al., 2009). Das primäre Zilium ist für die proteolytische Verarbeitung von GLI3 zu seiner Repressorform erforderlich (Chaudhry et al., 2017; Laclef et al., 2015). Erst nach Verlust der Zilien und daraus folgender Blockade der GLI3R-Bildung kann GLI2ΔN im Mausmodell früh Medulloblastome erzeugen (Han et al., 2009). Ein entsprechender Mechanismus wurde auch im Basalzellenkarzinom beobachtet. Dort verstärkte die Ablation der Zilien das Wachstum von GLI2-induzierten Tumoren deutlich (Wong et al., 2009). Der volle Effekt einer nicht-kanonischen Überaktivierung der HH-Signalkaskade auf dem Level der GLI-Transkriptionsfaktoren kann in der Zelle folglich nur zum Tragen kommen, wenn die Bildung von GLI3R durch Verlust der Zilie blockiert wird. Interessanterweise fehlen die primären Zilien bei einem großen Teil der AML-Zellen (Singh et al., 2016). GLI3R hat insbesondere dann eine suppressive Rolle, wenn eine nicht-kanonische GLI-Aktivierung in Abwesenheit einer kanonischen Aktivierung vorliegt. Eine simultane kanonische HH-Aktivierung führt aufgrund einer reduzierten Bildung von GLI3R zu keiner Suppression (Han et al., 2009; Wong et al., 2009). Durch die in der AML weit verbreitete Herunterregulation von GLI3 bzw. Verhinderung der GLI3 Bildung durch Verlust des primären Ziliums liegt der

Schluss nahe, dass in einem Teil der AML-Zellen eine nicht-kanonische GLI-Aktivierung vorliegt. Interessanterweise wird die Stärke der GLI-Aktivität in AML-Zelllinien weniger von SMO und mehr von der Menge des GLI3 Suppressors beeinflusst (Chaudhry et al., 2017). Hierbei muss allerdings bedacht werden, dass in Zelllinien aufgrund Ihrer reduzierten Abhängigkeit von äußeren Stimuli zur Selbsterhaltung möglicherweise vorwiegend intrinsische Signalaktivierung vorliegt, die die Realität von Interaktionen der AML-Zellen in der Knochenmarksnische nicht vollständig abbilden. Damit eignen sie sich nur begrenzt für Rückschlüsse der im Patienten vorliegenden Signalmechanismen in der AML.

Das Vorliegen einer dysfunktionalen kanonischen HH-Signalkaskade in einem Teil von AML-Zellen hätte weitreichende klinische Implikationen für Inhibitoren des Signalwegs. Inhibitoren von SMO, wie der für die AML klinisch zugelassene HH Inhibitor Glasdegib (Jamieson et al., 2020), wirken über einen intakten kanonischen HH-Signalweg. So zeigten Chaudhry et al., dass die Expression von GLI3 und die Bildung von GLI3R für die Wirksamkeit von SMO-Hemmern erforderlich ist (Chaudhry et al., 2017). Zudem können SMO-Inhibitoren zwar die kanonische Aktivierung von GLI1 und GLI2 reduzieren, die nachfolgende Aktivierung der GLI-Transkriptionsfaktoren auf nicht-kanonischem Wege können sie jedoch nicht verhindern. Damit übereinstimmend konnte in vorherigen Arbeiten unserer Arbeitsgruppe gezeigt werden, dass die Behandlung von GLI-Reporter-AML-Zelllinien mit dem SMO-Inhibitor Cyclopamin nicht zu einer Verringerung der GLI-Promotoraktivität führt (Latuske et al., 2017). Dennoch zeigten einige Studien die Wirksamkeit von SMO-Inhibitoren in der AML (Kobune et al., 2009; Liang et al., 2017; Long et al., 2016). Darüber hinaus konnten in einer vorherigen Arbeit unserer Arbeitsgruppe erhöhte Spiegel von Desert Hedgehog (DHH), einem Liganden der HH-Signalkaskade, im Serum von AML-Patienten nachgewiesen werden. Diese wurden in Stromazellen des Knochenmarks nachgewiesen, was auf eine parakrine Stimulation des HH-Signalwegs in AML-Zellen hinweist (Wellbrock et al., 2015). Auch die Wirksamkeit des SMO-Inhibitors Glasdegib in der AML weist auf eine große Bedeutung der kanonischen HH-Signalkaskade hin (Heuser et al., 2021). Ein großes Problem für die Wirksamkeit von SMO-Inhibitoren bei fortgeschrittener Therapiedauer ist, dass die Herunterregulation von GLI3 bzw. Blockade der GLI3 über ziliäre Ablation einen Resistenzmechanismus sowohl gegen SMO-Inhibitoren als auch, wie in dieser Arbeit gezeigt, gegen Ara-C-basierte Chemotherapie darstellt. Zudem könnte aufgrund des damit einhergehenden Verlusts der kanonischen HH-Signalkaskade die Relevanz von nicht-kanonischer HH-Aktivierung möglicherweise mit zunehmender Therapieresistenz in der AML zunehmen.

Neben der bekannten Aktivierung von GLI über andere onkogene Signalwege, überprüften wir, ob eine nicht-kanonische Aktivierung der GLI-Signalkaskade über die Expression der GLI2ΔN-Isoform vorliegt. GLI2ΔN ist eine konstitutiv aktive GLI2-Isoform, der die aminoterminale Repressordomäne fehlt (Sadam et al., 2016) und die die Fähigkeit besitzt, Zielgene im Vergleich zur GLI2-FullLength (GLI2FL) um ein Mehrfaches stärker zu induzieren (H. Sasaki et al., 1999). Die Expression von GLI2ΔN führt selbst in Gegenwart von SMO-Inhibitoren zu einer konstitutiv aktiven GLI-Signalkaskade, was einen wichtigen Mechanismus für die Resistenz gegen SMO-Inhibitoren in Krebszellen darstellt (X. Zhao et al., 2015). Daher analysierten wir die Expression von GLI2ΔN und GLI2FL in Proben von 47 neu diagnostizierten AML-Patienten mittels quantitativer PCR (qPCR). Die GLI2-Expression wurde in 16 der 47 Proben (34 %) nachgewiesen. Die mRNA-Expression von GLI2ΔN war 29,5-mal höher als die mRNA-Expression von GLI2FL. Darüber hinaus waren die Proteinkonzentrationen von GLI2ΔN in den untersuchten AML-Zelllinien deutlich höher als die von GLI2FL, wie mittels Western-Blot festgestellt wurde. Dies deutet darauf hin, dass GLI2ΔN im Vergleich zu GLI2FL die überwiegend exprimierte Isoform in der AML ist. Dies stellt einen neuen Mechanismus zur nicht-kanonischen GLI-Aktivierung in der AML dar.

Aufgrund der in der AML vorhandenen nicht-kanonischen HH-Aktivierung über Schnittstellen mit anderen Signalwegen, Resistenzmechanismen gegenüber SMO-Inhibitoren und der konstitutiv aktiven GLI2ΔN Isoform wäre ein therapeutischer Ansatz, der direkt auf die GLI-Transkriptionsfaktoren abzielt, das Mittel der Wahl. Obwohl jedoch bereits mehrere GLI-Inhibitoren entdeckt wurden (Sabol et al., 2018), wird derzeit keiner davon klinisch eingesetzt.

Bei der Untersuchung potenzieller Kandidaten für klinisch verfügbare GLI-Inhibitoren mittels GLI Reporter Zelllinien konnten wir zeigen, dass das Anthelminthikum Mebendazol (MBZ) zu einer starken dosisabhängigen Reduktion der GLI-Promoter-Aktivität in AML-Zellen führt. MBZ ist ein Breitspektrum-Benzimidazol, das seit mehreren Jahrzehnten in der Human- und Veterinärmedizin zur Behandlung einer Reihe von parasitären Wurminfektionen eingesetzt wird (Dayan, 2003). In den letzten Jahren wurde MBZ als vielversprechender Kandidat für Drug Repurposing in der Onkologie bekannt, sprich der Umnutzung zugelassener Medikamente zur Behandlung anderer Erkrankungen. In mehreren Studien konnten bei MBZ erhebliche In-vitro- und In-vivo-antitumorale Effekte beobachtet werden (Guerini et al., 2019). Neben dem Neuroblastom wurden hämatologische Malignome - darunter Leukämie, Lymphome und multiple Myelome - als die Krebsentitäten identifiziert, die am empfindlichsten auf eine Behandlung mit dem MBZ-Analogon Flubendazol reagieren, wie ein Screening von 321 Zelllinien aus 26 Krebsentitäten zeigte (Michaelis et al., 2015). Die MBZ-Konzentration, die zur Hemmung der GLI-Promotoraktivität erforderlich ist, lag in unseren Versuchen innerhalb der klinisch erreichbaren Konzentrationen. Die mittlere inhibitorische Konzentration (IC50) betrug nach 48 Stunden bei den getesteten AML-Zelllinien zwischen 32 ± 20 und 267 ± 71 nM. In der Vergangenheit wurde gezeigt, dass die langfristige, wiederholte Verabreichung von Mebendazol zu signifikant höheren Plasmaspiegeln im Vergleich zu einer Einzeldosis führt, was möglicherweise auf den enterohepatischen Kreislauf zurückzuführen ist (Braithwaite et al., 1982). Die erreichten Plasmaspiegel variieren stark zwischen den Individuen, wobei in einer Studie eine maximale Plasmakonzentration von 0,017-0,134 µM nach einer Einzeldosis von 1,5 g und bis zu 0,5 µM nach wiederholter Verabreichung von 1 g festgestellt wurde (Münst et al., 1980). In einer anderen Studie wurden 12 Patienten mit chronischer Echinokokkose mit einer einmaligen oder wiederholten Dosis von 10 mg/kg behandelt. Die Verabreichung einer Einzeldosis führte zu einer maximalen Plasmakonzentration von durchschnittlich 0,24 µM (zwischen 0,06 und 1,69 µM), während die wiederholte Verabreichung zu einer maximalen Konzentration von 0,47 µM und einer Area under the curve (AUC) führte, die fünfmal höher war als nach einer Einzeldosis (Braithwaite et al., 1982). Darüber hinaus gibt es bereits verschiedene Ansätze, um die Bioverfügbarkeit von oralem MBZ zu verbessern, wodurch eine Steigerung der Bioverfügbarkeit in einer Studie um den Faktor 2,12 (Chaudhary et al., 2016). und in einer weiteren Arbeit von 11% auf 41% (Zimmermann et al., 2018) erreicht werden konnte. Mittels Selbst-Nanoemulgierenden Drug-Delivery-Systemen (SNEDDS) konnte die AUC von MBZ um den Faktor 10 gesteigert werden (Sumimoto et al., 2022). Aufgrund des neu geweckten Interesses an MBZ zur Behandlung von Tumoren werden neue Darreichungsformen erprobt, unter anderem eine Mikroemulsion für intranasale Applikation zur Behandlung des Glioblastoms oder subkutane Implantate bei murinem triple-negativem Mamakarzinom. Beide Darreichungsformen von MBZ führten im Tiermodell zu einer verbesserten Überlebenszeit gegenüber der Kontrolle, während für die subkutanen Implantate im murinen triple-negativen Mammakarzinom sogar eine Überlegenheit gegenüber der oralen Gabe von MBZ gezeigt werden konnte (Kefayat et al., 2022; Mena-Hernández et al., 2020).

Um zu verstehen, wie MBZ die transkriptionelle Aktivität der GLI-Transkriptionsfaktoren reduziert, analysierten wir deren Expression auf Protein- und mRNA-Ebene. MBZ führte zu einer deutlichen Abnahme der GLI1 und GLI2 Proteinlevel, während sich die Level von GLI1/GLI2 mRNA nicht reduzierte. Da MBZ seine Wirkung auf der Proteinebene - und nicht

auf transkriptionellen Ebene - auszuüben schien, stellten wir die Hypothese auf, dass MBZ die GLI-Proteinkonzentration über Förderung deren proteasomalen Abbaus reduzierte. Daher analysierten wir den Einfluss des 26s-Proteasom-Inhibitors Bortezomib (BTZ) auf die GLI-Proteinlevel und Signalaktivität in AML-Zellen nach MBZ-Behandlung. Die Behandlung mit BTZ konnte die MBZ-vermittelte Hemmung der GLI-Promotoraktivität vollständig aufheben. In Übereinstimmung mit diesen Ergebnissen konnte durch BTZ die Wirkung von MBZ auf die GLI1- und GLI2-Proteinspiegel deutlich reduziert werden, wie mittels Western-Blot-Analyse gezeigt werden konnte. Diese Ergebnisse stützten die These, dass MBZ den proteasomalen Abbau von GLI1 und GLI2 vermittelt.

Hitzeschockproteine wirken als molekulare Chaperone, die an der Faltung, Aktivierung und dem Zusammenbau einer Vielzahl von Proteinen beteiligt sind. Heat Shock Protein 70 (HSP70) spielt eine Rolle in zahlreichen Prozessen der intrazellulären Proteinfaltung und -stabilisierung, während Heat Shock Protein 90 (HSP90) ausschließlich bei einer Auswahl von Client-Substraten beteiligt ist (Rosenzweig et al., 2019; Taipale et al., 2010). Für die Bindung an HSP90 benötigen seine Client-Proteine andere Chaperone und Co-Chaperone, da sie nicht direkt von HSP90 gebunden werden können. Bestimmte Client-Proteine, wie z.B. Transkriptionsfaktoren, müssen zunächst von HSP70 und seinem Co-Chaperon HSP40 gebunden werden, bevor sie an HSP90 übergeben werden können (Taipale et al., 2010). Es wird angenommen, dass HSP70 und HSP90 als zentrales Chaperonsystem fungieren, das die Stabilität, den Transport und den Abbau von Signalproteinen reguliert (Rosenzweig et al., 2019; Taipale et al., 2010) und somit die Aktivität einer Vielzahl von Proteinkinasen, Transkriptionsfaktoren und Steroidhormonrezeptoren aufrechterhält (Taipale et al., 2010). Eine Unterbrechung der HSP70/HSP90-Chaperonkaskade führt zur Fehlfaltung und zum Abbau dieser Client-Proteine (Butler et al., 2015). So beschrieben Walf-Vorderwülbecke et al. in der AML, dass MBZ den proteasomalen Abbau des Transkriptionsfaktors c-MYB durch Hemmung von HSP70 fördert (Walf-Vorderwülbecke et al., 2018). Die Abhängigkeit der Stabilität der GLI-Proteine von der enzymatischen Aktivität der Hitzeschockproteine wurde zuvor nicht beschrieben. Um die Rolle der Proteindestabilisierung durch HSP-Hemmung bei der Abnahme der GLI-Proteinlevel zu untersuchen, behandelten wir AML-Zellen mit niedermolekularen Inhibitoren von HSP70 (VER-155008) bzw. HSP90 (PU-H71). Inkubation von AML-Zellen mit dem jeweiligen Inhibitor führte zu einer signifikanten Verringerung der GLI1- und GLI2-Proteinspiegel in der Western-Blot-Analyse. Die simultane Hemmung von HSP70 und HSP90 durch die Kombination beider Wirkstoffe verstärkte die Wirkung nochmals erheblich. In Übereinstimmung mit den durch MBZ vermittelten Effekten sanken die mRNA-Spiegel von GLI1 und GLI2 nicht. MBZ hatte keinen Einfluss auf die Proteinexpression von HSP70 oder HSP90.

Um zu untersuchen, ob MBZ einen direkten Inhibitor der enzymatischen Aktivität der HSP-Chaperon-Maschinerie in AML-Zellen darstellt, etablierten wir einen in-vitro Renaturierungsversuch in AML-Zellen. Hierfür erzeugten wir eine MOLM-13-Zelllinie, die konstitutiv eine Firefly-Luciferase exprimiert (MOLM-13luc$^+$) und identifizierten die optimalen Bedingungen für den „Hitzeschock“ (Wärmeexposition). Nach dem Hitzeschock wurde die Zelllinie erneut bei 37°C inkubiert und die Stärke des durch die Luciferase erzeugten Lichts in einem Luminometer als Rückschluss auf die gesamte intrazelluläre enzymatische Aktivität im Zeitverlauf gemessen. Nach Exposition von Zellen gegenüber thermischem Stress hängt die Rückfaltung der hitzedenaturierten Firefly-Luciferase und die Regeneration der enzymatischen Aktivität von der kooperativen Chaperonaktivität von HSP70 und HSP90 ab (Morán Luengo et al., 2018). Nach einem Hitzeschock erholte sich das Luciferasesignal in MOLM-13luc$^+$ ohne Inhibitor. Die Inkubation von AML-Zellen mit MBZ oder spezifischen HSP-Inhibitoren beeinträchtigte die Wiederherstellung des Signals erheblich, was auf eine

direkte funktionelle Hemmung der HSP70/HSP90-vermittelten Rückfaltung der Luciferase durch MBZ hindeutet. Die starke Empfindlichkeit der GLI Proteine gegenüber der Hemmung von HSP70 und HSP90 deutet darauf hin, dass die GLI-Transkriptionsfaktoren für die Proteinfaltung und -stabilität stark auf die HSP70/HSP90-Chaperonkaskade angewiesen sind. Heat Shock Factor 1 (HSF1) ist der wichtigste Transkriptionsfaktor der Hitzeschockfamilie und zentraler Vermittler der Heat-Shock-Reaktion, einer zellulären Anpassungsreaktion auf unter anderem thermischen oder proteotoxischen Stress (Cyran & Zhitkovich, 2022). HSF1 war nach MBZ-Behandlung von AML-Zellen stark an Serin 326 phosphoryliert, was einen aktiven Zustand von HSF1 anzeigt. Dies ist ein Hinweis darauf, dass in den untersuchten Zellen proteotoxischer Stress durch MBZ-vermittelte Störung der Proteinfaltungsmechanismen vorliegt. In Kooperation mit Dr. Karl Kirschner der Hochschule Bonn-Rhein-Sieg (Insitut für Visual Computing) erfolgte eine in-silico Analyse der möglichen Interaktion von MBZ an die ATP-Bindungsstelle von HSP90. Mittels computergestützter Simulation konnten zwei stabile Bindungspositionen identifiziert werden, die mit großer Wahrscheinlichkeit experimentell beobachtet werden können. Eine ausführliche Analyse der neun Bindungsposen ist in Referenz (Fiedler et al., 2022) zu finden (W. Fiedler, F. Freisleben, J. Wellbrock, K.N. Kirschner, "Mebendazole's Conformational Space and Its Predicted Binding to Human Heat-Shock Protein 90", J. Chem. Inf. Model. 2022, 62, 15, 3604–3617).

Wir konnten die zuvor beschriebenen antileukämischen Effekte durch MBZ bestätigen. Die Behandlung von AML-Zelllinien und primären AML-Proben mit verschiedenen MBZ-Konzentrationen führte zu einer dosisabhängigen Wirkung auf die Proliferation, Koloniebildung und Apoptose. Wir konnten zeigen, dass in AML-Zellen die Kombination von MBZ mit dem niedermolekularen GLI-Inhibitor GANT-61 zu synergistischen anti-leukämischen Effekten führt. Dies könnte in Zukunft als potenzielle Behandlungsstrategie eingesetzt werden, um die Wirksamkeit einer pharmakologischen HH-Blockade zu erhöhen. Mehrere HH-Inhibitoren befinden sich in der Entwicklung für die AML-Behandlung, sodass HH-Inhibitoren als eine neue Klasse von Therapeutika angesehen werden können (Jamieson et al., 2020). MBZ ist ein vielversprechender Kandidat, um die Wirkung dieser Wirkstoffe zu potenzieren und ihren therapeutischen Erfolg zu maximieren. Um zu untersuchen, ob MBZ die Sensibilität der AML-Zelllinien MV4-11, MOLM-13 und OCI-AML3 gegenüber Cytarabin erhöhen kann, berechneten wir die Dose-Reduction-Index-Werte (DRI) für Cytarabin in der Wirkstoffkombination mit Mebendazol. Hierfür analysierten wir die Proliferationsdaten computergestützt nach der Chou-Talalay-Methode (CompuSyn), um DRI-Werte für die getestete Wirkstoffkombination mit Ara-C und MBZ bei konstantem Dosisverhältnis zu berechnen (Chou, 2010). Die DRI-Werte geben den Faktor an, um den die Dosis eines Medikaments in einer Kombination reduziert werden kann, um die gleiche Wirkstärke zu erzielen wie die Monotherapie des Medikaments. DRI-Werte > 1 gelten als günstig im Hinblick auf die prognostizierte Verringerung der Toxizität einer Arzneimitteltherapie. Mittels hoher DRI-Werte konnten wir zeigen, dass MBZ die AML-Zelllinien gegenüber Cytarabin sensibilisierte. Diese mögliche Dosisreduktion könnte die Toxizität der Therapie bei gleichbleibender antileukämischer Wirkung verringern. Das wäre ein möglicher Ansatz, um eine verbesserte Behandlung für ältere Patienten zu erreichen, bei welchen eine Hochdosis-Chemotherapie nicht in Frage kommt. Die Prognose für ältere, nicht für intensive Therapie geeignete Patienten ist mit den derzeitigen Behandlungen weiterhin schlecht. Glücklicherweise hat sich die Prognose für diese Patienten in den letzten Jahren durch die Einführung neuer zielgerichteter Wirkstoffe wie Bcl-2-, FLT3- und IDH1/2-Inhibitoren verbessert. Vor allem die Kombination von Azacitidin und Venetoclax hat sich bei älteren, für intensive Chemotherapie ungeeigneten AML-Patienten zu einem weit verbreiteten Behandlungsschema entwickelt, das im Vergleich zu hypomethylierenden Wirkstoffen allein zu einem längeren Gesamtüberleben führt (DiNardo et al., 2020; Short & Kantarjian, 2021). Allerdings sind nicht alle neuen

Behandlungsmethoden kurativ und die Behandlungsmöglichkeiten für Patienten, die auf diese Therapien nicht mehr ansprechen, sind spärlich. Daher könnte MBZ aufgrund seines sehr günstigen Toxizitätsprofils (Pantziarka et al., 2014; Patil et al., 2020) eine wertvolle therapeutische Option bei der Behandlung älterer Patienten darstellen.

Um weiter zu untersuchen, ob MBZ ein klinisch geeignetes Therapeutikum zur Hemmung von GLI ist, etablierten wir einen modifizierten Plasma-Inhibitory-Assay (mPIA). Hierbei wird eine das GLI-Luciferase-Promotor-Transgen tragende Indikatorzelllinie mit dem Plasma von Patienten vor und nach Wirkstoffverabreichung inkubiert. Anschließend wurde überprüft, inwieweit die im Plasma enthaltene Wirkstoffmenge einen Effekt auf die transkriptionelle Aktivität von GLI in der Indikatorzelllinie ausübt. So lassen sich Rückschlüsse auf die biologisch aktive Plasmakonzentration ziehen. Wir behandelten zwei refraktäre AML-Patienten mit einer MBZ-Monotherapie nach deren ausführlicher Aufklärung und Einwilligung in einem Off-Label-Setting. Während der Therapie entnahmen wir regelmäßig Blutproben über den Verlauf von bis zu 17 Tagen. Die genauen Patientencharakteristika lassen sich der Originalarbeit entnehmen. Darüber hinaus nahm ein 62-jähriger männlicher gesunder Proband MBZ in einer Dosis von 50 mg/kg, verteilt auf zwei Einnahmen zum Zeitpunkt 0 h und 12 h, ein. Die Blutentnahme erfolgte nach 4 h und 24 h. In allen Fällen zeigten die mPIA-Ergebnisse über eine deutliche Reduktion der GLI-Promoter-Aktivität in der Indikatorzelllinie eine biologisch aktive Plasmakonzentration an. In Übereinstimmung mit früheren Studien zu MBZ-Plasmaspiegeln führte die wiederholte Verabreichung des Medikaments bei den beiden Patienten zu einer stärkeren Hemmwirkung als eine Einzeldosis. Zudem erfolgte eine klinische Überwachung des Verlaufs beider Patienten unter MBZ-Monotherapie. Bei einem der beiden Patienten konnte unter MBZ-Therapie ein deutlicher und kontinuierlicher Rückgang der leukämischen Blasten im peripheren Blut, sowie eine rasche Verringerung der GLI2-Proteinspiegel in Blastenlysaten peripherer leukämischen Blutzellen beobachtet werden. Zusammenfassend deuten unsere Ergebnisse darauf hin, dass die orale Verabreichung von MBZ geeignet ist, um in der klinischen Anwendung spürbare therapeutische Effekte zu erzielen. Dies unterstreicht das außergewöhnliche Potenzial von MBZ als zukünftige therapeutische Option für die Behandlung verschiedener Krebsarten.

Neben den beschriebenen Effekten sei darauf hingewiesen, dass für MBZ eine Vielzahl anderer Mechanismen identifiziert wurden, die sowohl hemmende Wirkungen auf die GLI-Signalübertragung vermitteln als auch krebshemmende Wirkungen erzeugen können. Zu den beobachteten krebshemmenden Wirkungen von MBZ gehören die Induktion einer Anti-Tumor-Immunantwort, die Sensibilisierung für Strahlen- und Chemotherapie, die Hemmung der Angiogenese, die Induktion von Apoptose und die Hemmung der Proliferation (Guerini et al., 2019). Es wurde gezeigt, dass MBZ mehrere wichtige Signalkinasen hemmt, darunter VEGFR2, FAK, die GTPasen Rho-A und Rac1 (Guerini et al., 2019), ABL, JNK3 und KIT (Nygren et al., 2013). Darüber inhibiert MBZ die Kinasen BRAF und MEK durch Blockierung ihrer ATP-Bindungstasche (Simbulan-Rosenthal et al., 2017). MBZ hemmt die Tubulin-Depolymerisation in verschiedenen Tumorentitäten, einschließlich nicht-kleinzelligem Lungenkrebs und Glioblastom (R.-Y. Bai et al., 2011; J.-I. Sasaki et al., 2002). In AML-Zellen führte MBZ in Konzentrationen von bis zu 10 µM jedoch nicht zu einer Mikrotubuli-Depolymerisation (Walf-Vorderwülbecke et al., 2018). In unserer Arbeit konnten wir sehen, dass MBZ ebenfalls den Abbau von FLT3 induziert (Daten nicht gezeigt), dessen Überaktivierung einen wichtigen Stimulus für nicht-kanonische GLI-Aktivierung darstellt (Latuske et al., 2017). Es sind weitere Untersuchungen notwendig, um die vielfältigen Wirkungen von MBZ auf Krebszellen und auch auf die GLI-Transkriptionsfaktoren zu identifizieren.

Trotz der vielversprechenden Ergebnisse von MBZ in vitro und in Tierversuchen konnte in den Phase 2 Studien bei high-grade Gliomen oder Krebs des Gastrointestinaltrakts bisher kein Vorteil durch MBZ im klinischen Kontext gezeigt werden (Mansoori et al., 2021; Patil et al., 2022). Ein Grund könnte die schwierige und interindividuell stark unterschiedliche Bioverfügbarkeit von MBZ sein. Weitere klinische Studien stehen noch aus, unter anderem im metastasiertem kolorektalem Karzinom (ClinicalTrials.gov Identifier: NCT03925662). Weitere Forschung ist notwendig, um aufgrund der schlechten und unterschiedlichen Bioverfügbarkeit neue und zuverlässigere Darreichungsformen zu etablieren, bevor MBZ im klinischen Alltag angewendet werden kann.

In einer Phase 2 Studie (BRIGHT 1003) zeigte die Kombination des SMO Inhibitors Glasdegib mit niedrigdosiertem Ara-C (Low Dose Ara-C, LDAC) in der AML einen deutlichen Gesamtüberlebensvorteil (Heuser et al., 2021; ClinicalTrials.gov Identifier: NCT01546038), was zur Zulassung von Glasdegib führte. Diese vielversprechenden Ergebnisse sollen in der aktuell laufenden BRIGHT AML 1019 Phase III Studie mit LDAC bestätigt und ebenfalls mit intensiver Chemotherapie im 7+3 Schema überprüft werden (Cortes et al., 2019; ClinicalTrials.gov Identifier: NCT03416179). Im Pankreaskarzinom waren klinische Studien mit SMO-Inhibitoren in Kombination mit Chemotherapie nicht erfolgreich (Catenacci et al., 2015; De Jesus-Acosta et al., 2020). Eine mögliche Ursache könnte ein nicht-kanonischer Aktivierungsweg der HH-Signalkaskade in Pankreaszellen darstellen. Gleichzeitig wurde gezeigt, dass der Mechanismus einer Chemotherapieresistenz über Herunterregulation von GLI3 in der AML ebenfalls einen bekannten Resistenzmechanismus gegen SMO-Inhibition darstellt (Chaudhry et al., 2017). Die klinische Relevanz dieses geteilten Resistenzmechanismus muss im klinischen Umfeld überprüft werden.

Zusammenfassend unterstützt diese Arbeit die vielversprechenden Ergebnisse durch Glasdegib in Kombination mit Cytarabin in der AML und liefert Erklärungs- und Forschungsansätze, um diese Therapiestrategie in Zukunft effektiver zu gestalten. GLI3 wurde als relevanter Mediator einer Chemotherapieresistenz in der AML identifiziert und mehrere klinisch relevante, zugrundeliegende Resistenzgene nachgewiesen. Die Physiologie der HH-Aktivierung in der AML wurde tiefergehend beschrieben und ein neuer Mechanismus einer nicht-kanonischen GLI-Aktivierung über GLI2ΔN in der AML erstmals identifiziert. Zudem wurden Erklärungsansätze für ein mangelndes Ansprechen von SMO-Inhibitoren in anderen Krebsentitäten und mögliche Resistenzmechanismen aufgezeigt. Mit der Identifikation von MBZ als starker Inhibitor des GLI-Signalwegs konnte ein weiteres Element seiner komplexen krebshemmenden Wirkung beschrieben werden. Weitere Untersuchungen und eine Optimierung der pharmakologischen Eigenschaften sind jedoch notwendig, bevor MBZ im breiten klinischen Umfeld zur Anwendung kommen kann.

3. Zusammenfassungen

3.1. Zusammenfassung (Deutsch)

Die akute myeloische Leukämie (AML) ist eine maligne Erkrankung des blutbildenden Systems und entsteht auf dem Boden einer onkogenen Transformation einer hämatopoetischen Stamm- oder Progenitorzelle im Knochenmark. Die Standardbehandlung stellt ein intensives Chemotherapieschema dar. Selbst nach initialem Ansprechen erleidet ein großer Teil der Patienten einen Rückfall, sodass die Prognose weiterhin schlecht ist. Als Ursache des Therapieversagens und von Rezidiven gelten Leukämische Stammzellen (LSC), die in der Knochenmarksnische überleben und ein Reservoir für leukämische Blasten bilden. Die Stammzelleigenschaften der LSC, einschließlich einer hohen Therapieresistenz, werden über Stammzell-Signalwege vermittelt, unter anderem dem Hedgehog-Signalweg (HH). Eine aberrante Aktivierung des Hedgehog-Signalwegs (HH) wird bei vielen Neoplasien, einschließlich AML, beobachtet. Die GLI-Transkriptionsfaktoren sind die wichtigsten nachgeschalteten Effektoren der HH-Signalkaskade, indem sie die Transkription von Zielgenen regulieren. Im Rahmen dieser Promotion wurde untersucht, inwieweit die GLI-Transkriptionsfaktoren zur Entstehung und Aufrechterhaltung von Chemotherapieresistenz in der AML beitragen und welche Mechanismen der Resistenzentwicklung zugrunde liegen. Zudem sollten neue Wege oder Wirkstoffe untersucht werden, um die GLI-Transkriptionsfaktoren zu inhibieren und so einer Resistenzentwicklung entgegenzuwirken. Hierfür erzeugten wir Cytarabin(Ara-C)-resistente Varianten von AML-Zelllinien durch langfristige Kultivierung mit Ara-C. Die Expression von Mitgliedern der HH-Signalkaskade wurde anschließend untersucht. Im Vergleich zu den parentalen Zelllinien war die GLI3-Expression in allen resistenten Varianten vollständig unterdrückt. Wir erzeugten GLI3-Knockdown-AML-Zelllinien mittels shRNA. Der Knockdown von GLI3 reduzierte die Wirkung von Ara-C auf die AML-Zellen. Darüber hinaus analysierten wir die Expression verschiedener Gene, die am Stoffwechsel und Transport von Ara-C beteiligt sind. Die Herunterregulation von GLI3 führte zu einer Hochregulierung der Resistenzgene SAMHD1, CDA und ABCC11, von denen jedes als prädiktiver Marker für das Ansprechen auf Ara-C in der AML identifiziert worden ist. Die Herunterregulation von GLI3 stellt somit einen potenziellen Mechanismus dar, um eine Chemotherapieresistenz in der AML zu induzieren. Es ist bekannt, dass die Herunterregulation von GLI3 ebenfalls einen bekannten Resistenzmechanismus gegen SMO-Inhibitoren, wie das für die AML zugelassene Glasdegib, darstellt. Bei SMO-Inhibitoren handelt es sich um die derzeit einzige klinische zugelassene Wirkstoffklasse zur Hemmung des HH-Signalweges. Zudem können SMO-Inhibitoren nur die kanonische HH-Aktivierung, nicht jedoch nicht-kanonische HH-Aktivierung inhibieren. Durch qPCR-Analyse von Proben 47 neu diagnostizierter AML-Patienten konnten wir zeigen, dass die Expression der GLI2ΔN-Isoform eine weit verbreitete Form der nicht-kanonischen GLI-Aktivierung in AML-Zellen darstellt. Ein Inhibitor, der direkt auf die GLI-Transkriptionsfaktoren abzielt, wäre daher die bessere Wahl. Allerdings ist bisher kein klinischer GLI-Inhibitor verfügbar. Mebendazol (MBZ) ist ein seit Jahrzehnten zugelassenes und gut verträgliches Anthelminthikum. Wir konnten MBZ als potenten Inhibitor der HH-Signalkaskade identifizieren. Wir zeigten, dass MBZ in der Lage ist, das HSP70/HSP90 Chaperonesystem zu hemmen und so die Proteinfehlfaltung von GLI1 und GLI2 und deren Abbau über das 26s-Proteasom zu induzieren. Zwei Patienten mit refraktärer AML wurden im Rahmen einer Off-Label-Behandlung mit MBZ behandelt. Wir konnten in einem modifizierten Plasma-Inhibitory-Assay eine biologisch aktive Plasmakonzentration im Blut der Patienten nachweisen, die die GLI-Aktivität einer Indikatorzelllinie in-vitro reduzieren konnte. Darüber hinaus zeigte einer der Patienten einen Rückgang der Anzahl der Blasten im peripheren Blut unter Therapie. Daher ist MBZ ein bereits zugelassener und vielversprechender GLI-Inhibitor, dessen Wirksamkeit in der klinischen Praxis geprüft werden sollte.

3.2. Zusammenfassung (Englisch)

Acute myeloid leukemia (AML) is a malignant disease of the hematopoietic system and develops due to an oncogenic transformation of a hematopoietic stem or progenitor cell in the bone marrow. The standard treatment is an intensive chemotherapy regimen. Even after initial response, a large proportion of patients relapse, so the prognosis remains poor. Leukemic stem cells (LSCs), which survive in the bone marrow niche and form a reservoir for leukemic blasts, are the cause of treatment failure and relapse. The stem cell properties of LSCs, such as high resistance to therapy, are mediated by stem cell signaling pathways, including the Hedgehog (HH) pathway. Aberrant activation of the Hedgehog signaling (HH) pathway is observed in many neoplasms, including AML. The GLI transcription factors are the key downstream effectors of the HH signaling cascade by regulating the expression of target genes. This doctoral thesis investigated if the GLI transcription factors contribute to the development and maintenance of chemotherapy resistance in AML and the mechanisms underlying resistance development. In addition, we aimed to investigate new approaches or agents to inhibit GLI transcription factors and thus counteract resistance development. For this purpose, we generated cytarabine (Ara-C)-resistant variants of AML cell lines by long-term cultivation with Ara-C. The expression of members of the HH signaling cascade was subsequently examined. Compared with the parental cell lines, GLI3 expression was completely silenced in all resistant variants. We generated GLI3 knockdown AML cell lines using shRNA. Knockdown of GLI3 reduced the effect of Ara-C on AML cells. In addition, we analyzed the expression of several genes involved in Ara-C metabolism and transport. Downregulation of GLI3 resulted in upregulation of the resistance genes SAMHD1, CDA, and ABCC11, each of which has been identified as a predictive marker for response to Ara-C in AML. Thus, downregulation of GLI3 represents a potential mechanism to induce chemotherapy resistance in AML. It is known that downregulation of GLI3 is also a known mechanism of resistance to SMO inhibitors, such as Glasdegib, which has been approved for AML. SMO inhibitors are currently the only clinically approved class of HH pathway inhibitors. Moreover, SMO inhibitors can only inhibit canonical HH activation, but not non-canonical HH activation. By qPCR analysis of samples from 47 newly diagnosed AML patients, we demonstrated that expression of the GLI2ΔN isoform is a common form of noncanonical GLI activation in AML cells. Therefore, an inhibitor that directly targets the GLI transcription factors would be a better choice. However, no clinical GLI inhibitor is yet available. Mebendazole (MBZ) is a well-tolerated anthelmintic that has been approved for decades. We identified MBZ as a potent inhibitor of the HH signaling cascade. We demonstrated that MBZ can inhibit the HSP70/HSP90 chaperone system, promoting protein misfolding of GLI1 and GLI2 and their degradation via the 26s proteasome. Two patients with refractory AML were treated with MBZ in an off-label setting. In a modified plasma inhibitory assay, we detected a biological active plasma concentration in the blood of the patients, which was able to reduce the GLI activity of an indicator cell line in vitro. In addition, one of the patients showed to a decrease in the number of blasts in peripheral blood under therapy. Therefore, MBZ is an already approved and promising GLI inhibitor whose effectiveness should be tested in clinical practice.

4. Literaturverzeichnis

1. Aberger, F., & Ruiz i Altaba, A. (2014). Context-dependent signal integration by the GLI code: The oncogenic load, pathways, modifiers and implications for cancer therapy. *Seminars in Cell and Developmental Biology*, *33*, 93–104. https://doi.org/10.1016/j.semcdb.2014.05.003
2. Abraham, A., Varatharajan, S., Karathedath, S., Philip, C., Lakshmi, K. M., Jayavelu, A. K., Mohanan, E., Janet, N. B., Srivastava, V. M., Shaji, R. V., Zhang, W., Abraham, A., Viswabandya, A., George, B., Chandy, M., Srivastava, A., Mathews, V., & Balasubramanian, P. (2015). RNA expression of genes involved in cytarabine metabolism and transport predicts cytarabine response in acute myeloid leukemia. *Pharmacogenomics*, *16*(8), 877–890. https://doi.org/10.2217/pgs.15.44
3. Bai, C. B., Auerbach, W., Lee, J. S., Stephen, D., & Joyner, A. L. (2002). Gli2, but not Gli1, is required for initial Shh signaling and ectopic activation of the Shh pathway. *Development*, *129*(20), 4753–4761.
4. Bai, R.-Y., Staedtke, V., Aprhys, C. M., Gallia, G. L., & Riggins, G. J. (2011). Antiparasitic mebendazole shows survival benefit in 2 preclinical models of glioblastoma multiforme. *Neuro-Oncology*, *13*(9), 974–982. https://doi.org/10.1093/neuonc/nor077
5. Batlle, E., & Clevers, H. (2017). Cancer stem cells revisited. *Nature Medicine*, *23*(10), 1124–1134. https://doi.org/10.1038/nm.4409
6. Bonnet, D., & Dick, E. (1997). Human acute myeloid leukemia is organized as a hierarchy that originates from a primitive hematopoietic cell. *Nature Medicine*, *3*(7), 730–737. http://www.nature.com/naturemedicine
7. Braithwaite, P. A., Roberts, M. S., Allan, R. J., & Watson, T. R. (1982). Clinical Pharmacokinetics of High Dose Mebendazole in Patients Treated for Cystic Hydatid Disease. *Eur J Clin Pharmacol*, *22*, 161–169.
8. Butler, L. M., Ferraldeschi, R., Armstrong, H. K., Centenera, M. M., & Workman, P. (2015). Maximizing the therapeutic potential of HSP90 inhibitors. *Molecular Cancer Research*, *13*(11), 1445–1451. https://doi.org/10.1158/1541-7786.MCR-15-0234
9. Catenacci, D. V. T., Junttila, M. R., Karrison, T., Bahary, N., Horiba, M. N., Nattam, S. R., Marsh, R., Wallace, J., Kozloff, M., Rajdev, L., Cohen, D., Wade, J., Sleckman, B., Lenz, H. J., Stiff, P., Kumar, P., Xu, P., Henderson, L., Takebe, N., … Kindler, H. L. (2015). Randomized phase Ib/II study of gemcitabine plus placebo or vismodegib, a hedgehog pathway inhibitor, in patients with metastatic pancreatic cancer. *Journal of Clinical Oncology*, *33*(36), 4284–4292. https://doi.org/10.1200/JCO.2015.62.8719
10. Chaudhary, S., Garg, T., Rath, G., Murthy, R. R., & Goyal, A. K. (2016). Enhancing the bioavailability of mebendazole by integrating the principles solid dispersion and nanocrystal techniques, for safe and effective management of human echinococcosis. *Artificial Cells, Nanomedicine and Biotechnology*, *44*(3), 937–942. https://doi.org/10.3109/21691401.2014.1000493
11. Chaudhry, P., Singh, M., Triche, T. J., Guzman, M., & Merchant, A. A. (2017). GLI3 repressor determines Hedgehog pathway activation and is required for response to SMO antagonist glasdegib in AML. *Blood*, *129*(26), 3465–3475. https://doi.org/10.1182/blood-2016-05-718585
12. Chen, Y., Bieber, M. M., & Teng, N. N. H. (2014). Hedgehog signaling regulates drug sensitivity by targeting ABC transporters ABCB1 and ABCG2 in epithelial ovarian cancer. *Molecular Carcinogenesis*, *53*(8), 625–634. https://doi.org/10.1002/mc.22015
13. Cheng, J., Gao, J., & Tao, K. (2016). Prognostic role of Gli1 expression in solid malignancies: A meta-analysis. *Scientific Reports*, *6*(22184). https://doi.org/10.1038/srep22184

14. Chou, T. C. (2010). Drug Combination Studies and Their Synergy Quantification Using the Chou-Talalay method. *Cancer Research*, *70*(2), 440–446. https://doi.org/10.1158/0008-5472.CAN-09-1947
15. Cohen, S. S. (1977). The mechanisms of lethal action of arabinosyl cytosine (araC) and arabinosyl adenine (araA). *Cancer*, *40*, 509–518. https://doi.org/10.1002/1097-0142(197707)40:1+<509::AID-CNCR2820400717>3.0.CO;2-8
16. Cortes, J. E., Dombret, H., Merchant, A., Tauchi, T., Dirienzo, C. G., Sleight, B., Zhang, X., Leip, E. P., Shaik, N., Bell, T., Chan, G., & Sekeres, M. A. (2019). Glasdegib plus intensive/nonintensive chemotherapy in untreated acute myeloid leukemia: BRIGHT AML 1019 Phase III trials. *Future Oncology*, *15*(31), 3531–3545. https://doi.org/10.2217/fon-2019-0373
17. Cyran, A. M., & Zhitkovich, A. (2022). Heat Shock Proteins and HSF1 in Cancer. *Frontiers in Oncology*, *12*(860320). https://doi.org/10.3389/fonc.2022.860320
18. Dayan, A. D. (2003). Albendazole, mebendazole and praziquantel. Review of non-clinical toxicity and pharmacokinetics. *Acta Tropica*, *86*(2–3), 141–159. https://doi.org/10.1016/S0001-706X(03)00031-7
19. De Jesus-Acosta, A., Sugar, E. A., O'Dwyer, P. J., Ramanathan, R. K., Von Hoff, D. D., Rasheed, Z., Zheng, L., Begum, A., Anders, R., Maitra, A., McAllister, F., Rajeshkumar, N. V., Yabuuchi, S., de Wilde, R. F., Batukbhai, B., Sahin, I., & Laheru, D. A. (2020). Phase 2 study of vismodegib, a hedgehog inhibitor, combined with gemcitabine and nab-paclitaxel in patients with untreated metastatic pancreatic adenocarcinoma. *British Journal of Cancer*, *122*(4), 498–505. https://doi.org/10.1038/s41416-019-0683-3
20. Dierks, C., Beigi, R., Guo, G. R., Zirlik, K., Stegert, M. R., Manley, P., Trussell, C., Schmitt-Graeff, A., Landwerlin, K., Veelken, H., & Warmuth, M. (2008). Expansion of Bcr-Abl-Positive Leukemic Stem Cells Is Dependent on Hedgehog Pathway Activation. *Cancer Cell*, *14*(3), 238–249. https://doi.org/10.1016/j.ccr.2008.08.003
21. DiNardo, C. D., Jonas, B. A., Pullarkat, V., Thirman, M. J., Garcia, J. S., Wei, A. H., Konopleva, M., Döhner, H., Letai, A., Fenaux, P., Koller, E., Havelange, V., Leber, B., Esteve, J., Wang, J., Pejsa, V., Hájek, R., Porkka, K., Illés, Á., … Pratz, K. W. (2020). Azacitidine and Venetoclax in Previously Untreated Acute Myeloid Leukemia. *New England Journal of Medicine*, *383*(7), 617–629. https://doi.org/10.1056/nejmoa2012971
22. Döhner, H., Estey, E., Grimwade, D., Amadori, S., Appelbaum, F. R., Dombret, H., Ebert, B. L., Fenaux, P., Larson, R. A., Levine, R. L., Lo-Coco, F., Naoe, T., Niederwieser, D., Ossenkoppele, G. J., Sanz, M., Sierra, J., Tallman, M. S., Tien, H.-F., Wei, A. H., & Bloomfield, C. D. (2017). Diagnosis and management of AML in adults: 2017 ELN recommendations from an international expert panel. *Blood*, *129*(4), 424–447. https://doi.org/10.1182/blood-2016-08
23. Eppert, K., Takenaka, K., Lechman, E. R., Waldron, L., Nilsson, B., van Galen, P., Metzeler, K. H., Poeppl, A., Ling, V., Beyene, J., Canty, A. J., Danska, J. S., Bohlander, S. K., Buske, C., Minden, M. D., Golub, T. R., Jurisica, I., Ebert, B. L., & Dick, J. E. (2011). Stem cell gene expression programs influence clinical outcome in human leukemia. *Nature Medicine*, *17*(9), 1086–1094. https://doi.org/10.1038/nm.2415
24. Fiedler, W., Freisleben, F., Wellbrock, J., & Kirschner, K. N. (2022). Mebendazole's Conformational Space and Its Predicted Binding to Human Heat-Shock Protein 90. *Journal of Chemical Information and Modeling*, *62*(15), 3604–3617. https://doi.org/10.1021/acs.jcim.2c00290
25. Franzolin, E., Pontarin, G., Rampazzo, C., Miazzi, C., Ferraro, P., Palumbo, E., Reichard, P., & Bianchi, V. (2013). The deoxynucleotide triphosphohydrolase

SAMHD1 is a major regulator of DNA precursor pools in mammalian cells. *Proceedings of the National Academy of Sciences of the United States of America*, *110*(35), 14272–14277. https://doi.org/10.1073/pnas.1312033110
26. Gentles, A. J., Plevritis, S. K., Majeti, R., & Alizadeh, A. A. (2010). Association of a Leukemic Stem Cell Gene Expression Signature With Clinical Outcomes in Acute Myeloid Leukemia. *JAMA*, *304*(24), 2706–2715. www.jama.com
27. Guerini, A. E., Triggiani, L., Maddalo, M., Bonù, M. L., Frassine, F., Baiguini, A., Alghisi, A., Tomasini, D., Borghetti, P., Pasinetti, N., Bresciani, R., Magrini, S. M., & Buglione, M. (2019). Mebendazole as a candidate for drug repurposing in oncology: An extensive review of current literature. *Cancers*, *11*(1284). https://doi.org/10.3390/cancers11091284
28. Guo, Y., Köck, K., Ritter, C. A., Chen, Z., Grube, M., Jedlitschky, G., Illmer, T., Ayres, M., Beck, J. F., Siegmund, W., Ehninger, G., Gandhi, V., Kroemer, H. K., Kruh, G. D., & Schaich, M. (2009). Expression of ABCC-type Nucleotide Exporters in Blasts of Adult Acute Myeloid Leukemia: Relation to Long-term survival. *Clinical Cancer Research*, *15*(5), 1762–1769. https://doi.org/10.1158/1078-0432.CCR-08-0442
29. Guo, Y., Kotova, E., Chen, Z.-S., Lee, K., Hopper-Borge, E., Belinsky, M. G., & Kruh, G. D. (2003). MRP8, ATP-binding cassette C11 (ABCC11), is a cyclic nucleotide efflux pump and a resistance factor for fluoropyrimidines 2′,3′-dideoxycytidine and 9′-(2′-phosphonylmethoxyethyl)adenine. *Journal of Biological Chemistry*, *278*(32), 29509–29514. https://doi.org/10.1074/jbc.M304059200
30. Han, Y.-G., Kim, H. J., Dlugosz, A. A., Ellison, D. W., Gilbertson, R. J., & Alvarez-Buylla, A. (2009). Dual and opposing roles of primary cilia in medulloblastoma development. *Nature Medicine*, *15*(9), 1062–1065. https://doi.org/10.1038/nm.2020
31. Heuser, M., Smith, B. D., Fiedler, W., Sekeres, M. A., Montesinos, P., Leber, B., Merchant, A., Papayannidis, C., Pérez-Simón, J. A., Hoang, C. J., O'Brien, T., Ma, W. W., Zeremski, M., O'Connell, A., Chan, G., & Cortes, J. E. (2021). Clinical benefit of glasdegib plus low-dose cytarabine in patients with de novo and secondary acute myeloid leukemia: long-term analysis of a phase II randomized trial. *Annals of Hematology*, *100*, 1181–1194. https://doi.org/10.1007/s00277-021-04465-4
32. Ho, T. C., LaMere, M., Stevens, B. M., Ashton, J. M., Myers, J. R., O'Dwyer, K. M., Liesveld, J. L., Mendler, J. H., Guzman, M., Morrissette, J. D., Zhao, J., Wang, E. S., Wetzler, M., Jordan, C. T., & Becker, M. W. (2016). Evolution of acute myelogenous leukemia stem cell properties after treatment and progression. *Blood*, *128*(13), 1671–1678. https://doi.org/10.1182/blood-2016-02-695312
33. Hollenbaugh, J. A., Shelton, J., Tao, S., Amiralaei, S., Liu, P., Lu, X., Goetze, R. W., Zhou, L., Nettles, J. H., Schinazi, R. F., & Kim, B. (2017). Substrates and inhibitors of SAMHD1. *PLoS ONE*, *12*(1). https://doi.org/10.1371/journal.pone.0169052
34. Hu, Y., Chen, Y., Douglas, L., & Li, S. (2009). β-Catenin is essential for survival of leukemic stem cells insensitive to kinase inhibition in mice with BCR-ABL-induced chronic myeloid leukemia. *Leukemia*, *23*(1), 109–116. https://doi.org/10.1038/leu.2008.262
35. Huang, K., Sun, Z., Ding, B., Jiang, X., Wang, Z., Zhu, Y., & Meng, F. (2019). Suppressing hedgehog signaling reverses drug resistance of refractory acute myeloid leukemia. *OncoTargets and Therapy*, *12*, 7477–7488. https://doi.org/10.2147/OTT.S216628
36. Jahns-Streubel, G., Reuter, C., Auf Der Landwehr, U., Unterhalt, M., Schleyer, E., Wörmann, B., Büchner, T., & Hiddemann, W. (1997). Activity of Thymidine Kinase and of Polymerase a as Well as Activity and Gene Expression of Deoxycytidine Deaminase in Leukemic Blasts Are Correlated With Clinical Response in the Setting of Granulocyte-Macrophage Colony-Stimulating Factor-Based Priming Before and

During TAD-9 Induction Therapy in Acute Myeloid Leukemia. *Blood*, *90*(5), 1968–1976.
37. Jamieson, C., Martinelli, G., Papayannidis, C., & Cortes, J. E. (2020). Hedgehog Pathway Inhibitors: A New Therapeutic Class for the Treatment of Acute Myeloid Leukemia. *Blood Cancer Discovery*, *1*(2), 134–145. https://doi.org/10.1158/2643-3230.bcd-20-0007
38. Jiang, J., & Hui, C. chung. (2008). Hedgehog Signaling in Development and Cancer. *Developmental Cell*, *15*(6), 801–812. https://doi.org/10.1016/j.devcel.2008.11.010
39. Kefayat, A., Hosseini, M., Ghahremani, F., Jolfaie, N. A., & Rafienia, M. (2022). Biodegradable and biocompatible subcutaneous implants consisted of pH-sensitive mebendazole-loaded/folic acid-targeted chitosan nanoparticles for murine triple-negative breast cancer treatment. *Journal of Nanobiotechnology*, *20*(169). https://doi.org/10.1186/s12951-022-01380-2
40. Kobune, M., Takimoto, R., Murase, K., Iyama, S., Sato, T., Kikuchi, S., Kawano, Y., Miyanishi, K., Sato, Y., Niitsu, Y., & Kato, J. (2009). Drug resistance is dramatically restored by hedgehog inhibitors in CD34+ leukemic cells. *Cancer Science*, *100*(5), 948–955. https://doi.org/10.1111/j.1349-7006.2009.01111.x
41. Laclef, C., Anselme, I., Besse, L., Catala, M., Palmyre, A., Baas, D., Paschaki, M., Pedraza, M., Métin, C., Durand, B., & Schneider-Maunoury, S. (2015). The role of primary cilia in corpus callosum formation is mediated by production of the Gli3 repressor. *Human Molecular Genetics*, *24*(17), 4997–5014. https://doi.org/10.1093/hmg/ddv221
42. Lamba, J. K. (2009). Genetic factors influencing cytarabine therapy. *Pharmacogenomics*, *10*(10), 1657–1674. https://doi.org/10.2217/pgs.09.118
43. Lapidot, T., Sirard, C., Vormoor, J., Murdoch, B., Hoang, T., Caceres-Cortes, J., Minden, M., Paterson, B., Caligiuri, M. A., & Dick, J. E. (1994). A cell initiating human acute myeloid leukaemia after transplantation into SCID mice. *Nature*, *362*, 645–648.
44. Latuske, E.-M., Stamm, H., Klokow, M., Vohwinkel, G., Muschhammer, J., Bokemeyer, C., Jücker, M., Kebenko, M., Fiedler, W., & Wellbrock, J. (2017). Combined inhibition of GLI and FLT3 signaling leads to effective anti-leukemic effects in human acute myeloid leukemia. *Oncotarget*, *8*(17), 29187–29201. www.impactjournals.com/oncotarget
45. Lessard, J., & Sauvageau, G. (2003). Bmi-1 determines the proliferative capacity of normal and leukaemic stem cells. *Nature*, *423*, 255–260. www.nature.com/nature
46. Liang, H., Zheng, Q. L., Fang, P., Zhang, J., Zhang, T., Liu, W., Guo, M., Robinson, C. L., Chen, S. B., Chen, X. P., Chen, F. P., & Zeng, H. (2017). Targeting the PI3K/AKT pathway via GLI1 inhibition enhanced the drug sensitivity of acute myeloid leukemia cells. *Scientific Reports*, *7*(40361). https://doi.org/10.1038/srep40361
47. Long, B., Wang, L. X., Zheng, F. M., Lai, S. P., Xu, D. R., Hu, Y., Lin, D. J., Zhang, X. Z., Dong, L., Long, Z. J., Tong, X. Z., & Liu, Q. (2016). Targeting GLI1 suppresses cell growth and enhances chemosensitivity in CD34 + enriched acute myeloid leukemia progenitor cells. *Cellular Physiology and Biochemistry*, *38*(4), 1288–1302. https://doi.org/10.1159/000443075
48. Mansoori, S., Fryknäs, M., Alvfors, C., Loskog, A., Larsson, R., & Nygren, P. (2021). A phase 2a clinical study on the safety and efficacy of individualized dosed mebendazole in patients with advanced gastrointestinal cancer. *Scientific Reports*, *11*(8981). https://doi.org/10.1038/s41598-021-88433-y
49. Mena-Hernández, J., Jung-Cook, H., Llaguno-Munive, M., García-López, P., Ganem-Rondero, A., López-Ramírez, S., Barragán-Aroche, F., Rivera-Huerta, M., & Mayet-

Cruz, L. (2020). Preparation and Evaluation of Mebendazole Microemulsion for Intranasal Delivery: an Alternative Approach for Glioblastoma Treatment. *AAPS PharmSciTech*, *21*(264). https://doi.org/10.1208/s12249-020-01805-x
50. Meng, E., Hanna, A., Samant, R. S., & Shevde, L. A. (2015). The impact of hedgehog signaling pathway on DNA repair mechanisms in human cancer. *Cancers*, *7*, 1333–1348. https://doi.org/10.3390/cancers7030839
51. Michaelis, M., Agha, B., Rothweiler, F., Löschmann, N., Voges, Y., Mittelbronn, M., Starzetz, T., Harter, P. N., Abhari, B. A., Fulda, S., Westermann, F., Riecken, K., Spek, S., Langer, K., Wiese, M., Dirks, W. G., Zehner, R., Cinatl, J., Wass, M. N., & Cinatl, J. (2015). Identification of flubendazole as potential anti-neuroblastoma compound in a large cell line screen. *Scientific Reports*, *5*(8202). https://doi.org/10.1038/srep08202
52. Morán Luengo, T., Kityk, R., Mayer, M. P., & Rüdiger, S. G. D. (2018). Hsp90 Breaks the Deadlock of the Hsp70 Chaperone System. *Molecular Cell*, *70*(3), 545-552.e9. https://doi.org/10.1016/j.molcel.2018.03.028
53. Münst, G. J., Karlaganis, G., & Bircher, J. (1980). Plasma Concentrations of Mebendazole During Treatment of Echinococcosis. *Eur. J. Clin. Pharmacol*, *17*, 375–378.
54. Niewiadomski, P., Niedziółka, S. M., Markiewicz, Ł., Uśpieński, T., Baran, B., & Chojnowska, K. (2019). Gli proteins: Regulation in development and cancer. *Cells*, *8*(147). https://doi.org/10.3390/cells8020147
55. Niu, J., Peng, D., & Liu, L. (2022). Drug Resistance Mechanisms of Acute Myeloid Leukemia Stem Cells. *Frontiers in Oncology*, *12*. https://doi.org/10.3389/fonc.2022.896426
56. Nygren, P., Fryknäs, M., Ågerup, B., & Larsson, R. (2013). Repositioning of the anthelmintic drug mebendazole for the treatment for colon cancer. *Journal of Cancer Research and Clinical Oncology*, *139*(12), 2133–2140. https://doi.org/10.1007/s00432-013-1539-5
57. Ohta, T., Hori, H., Ogawa, M., Miyahara, M., Kawasaki, H., Taniguchi, N., & Komada, Y. (2004). Impact of cytidine deaminase activity on intrinsic resistance to cytarabine in carcinoma cells. *Oncology Reports*, *12*(5), 1115–1120. https://doi.org/10.3892/or.12.5.1115
58. Pabst, T., Vellenga, E., van Putten, W., Schouten, H. C., Graux, C., Vekemans, M.-C., Biemond, B., Sonneveld, P., Passweg, J., Verdonck, L., Legdeur, M.-C., Theobald, M., Jacky, E., Bargetzi, M., Maertens, J., Ossenkoppele, G. J., & Löwenberg, B. (2012). Favorable effect of priming with granulocyte colony-stimulating factor in remission induction of acute myeloid leukemia restricted to dose escalation of cytarabine. *Blood*. https://doi.org/10.1182/blood-2011
59. Pan, Y., & Wang, B. (2007). A novel protein-processing domain in Gli2 and Gli3 differentially blocks complete protein degradation by the proteasome. *Journal of Biological Chemistry*, *282*(15), 10846–10852. https://doi.org/10.1074/jbc.M608599200
60. Pantziarka, P., Bouche, G., Meheus, L., Sukhatme, V., & Sukhatme, V. P. (2014). Repurposing Drugs in Oncology (ReDO) - Mebendazole as an anti-cancer agent. *Ecancermedicalscience*, *8*(443). https://doi.org/10.3332/ecancer.2014.443
61. Patil, V. M., Bhelekar, A., Menon, N., Bhattacharjee, A., Simha, V., Abhinav, R., Abhyankar, A., Sridhar, E., Mahajan, A., Puranik, A. D., Purandare, N., Janu, A., Ahuja, A., Krishnatry, R., Gupta, T., & Jalali, R. (2020). Reverse swing-M, phase 1 study of repurposing mebendazole in recurrent high-grade glioma. *Cancer Medicine*, *9*(13), 4676–4685. https://doi.org/10.1002/cam4.3094

62. Patil, V. M., Menon, N., Chatterjee, A., Tonse, R., Choudhari, A., Mahajan, A., Puranik, A. D., Epari, S., Jadhav, M., Pathak, S., Peelay, Z., Walavalkar, R., Muthuluri, H. K., Krishna, M. R., Chandrasekharan, A., Pande, N., Gupta, T., Banavali, S., & Jalali, R. (2022). Mebendazole plus lomustine or temozolomide in patients with recurrent glioblastoma: A randomised open-label phase II trial. *EClinicalMedicine*, *49*(101449). https://doi.org/10.1016/j
63. Petrova, R., Garcia, D. R., & Joyner, A. L. (2013). Titration of GLI3 repressor activity by sonic hedgehog signaling is critical for maintaining multiple adult neural stem cell and astrocyte functions. *Journal of Neuroscience*, *33*(44), 17490–17505. https://doi.org/10.1523/JNEUROSCI.2042-13.2013
64. Pietrobono, S., Gagliardi, S., & Stecca, B. (2019). Non-canonical Hedgehog Signaling Pathway in Cancer: Activation of GLI Transcription Factors Beyond Smoothened. *Frontiers in Genetics*, *10*(556). https://doi.org/10.3389/fgene.2019.00556
65. Raffel, C., Jenkins, R. B., Frederick, L., Hebrink, D., Alderete, B., Fults, D. W., & David James, C. (1997). Sporadic Medulloblastomas Contain PTCH Mutations1. *Cancer Research*, *57*, 842–845. http://aacrjournals.org/cancerres/article-pdf/57/5/842/2465694/cr0570050842.pdf
66. Reifenberger, J., Wolter, M., Knobbe, C. B., Köhler, B., Schönicke, A., Scharwächter, C., Kumar, K., Blaschke, B., Ruzicka, T., & Reifenberger, G. (2005). Somatic mutations in the PTCH, SMOH, SUFUH and TP53 genes in sporadic basal cell carcinomas. *British Journal of Dermatology*, *152*, 43–51. https://doi.org/10.1111/j.1365-2133.2005.06353.x
67. Rocca, R., Costa, G., Ngankeu, A., Aqeilan, R. I., Croce, C. M., Bertoni, F., Alcaro, S., & Trapasso, F. (2018). Leukaemic stem cell load at diagnosis predicts the development of relapse in young acute myeloid leukaemia patients. *British Journal of Haematology*, *183*(3), 512–516. https://doi.org/10.1111/bjh.14989
68. Rosenzweig, R., Nillegoda, N. B., Mayer, M. P., & Bukau, B. (2019). The Hsp70 chaperone network. *Nature Reviews Molecular Cell Biology*, *20*(11), 665–680. https://doi.org/10.1038/s41580-019-0133-3
69. Sabol, M., Trnski, D., Musani, V., Ozretić, P., & Levanat, S. (2018). Role of GLI transcription factors in pathogenesis and their potential as new therapeutic targets. *International Journal of Molecular Sciences*, *19*(2562). https://doi.org/10.3390/ijms19092562
70. Sadam, H., Liivas, U., Kazantseva, A., Pruunsild, P., Kazantseva, J., Timmusk, T., Neuman, T., & Palm, K. (2016). GLI2 cell-specific activity is controlled at the level of transcription and RNA processing: Consequences to cancer metastasis. *Biochimica et Biophysica Acta - Molecular Basis of Disease*, *1862*(1), 46–55. https://doi.org/10.1016/j.bbadis.2015.10.008
71. Sasaki, H., Hui, C., Nakafuku, M., & Kondoh, H. (1997). A binding site for Gli proteins is essential for HNF-3βfloor plate enhancer activity in transgenics and can respond to Shh in vitro. *Development*, *124*(7), 1313–1322.
72. Sasaki, H., Nishizaki, Y., Hui, C., Nakafuku, M., & Kondoh, H. (1999). Regulation of Gli2 and Gli3 activities by an amino-terminal repression domain: implication of Gli2 and Gli3 as primary mediators of Shh signaling. *Development*, *126*(17), 3915–3924.
73. Sasaki, J.-I., Ramesh, R., Chada, S., Gomyo, Y., Roth, J. A., & Mukhopadhyay, T. (2002). The Anthelmintic Drug Mebendazole Induces Mitotic Arrest and Apoptosis by Depolymerizing Tubulin in Non-Small Cell Lung Cancer Cells. *Molecular Cancer Therapeutics*, *1*(13), 1201–1209. http://aacrjournals.org/mct/article-pdf/1/13/1201/2221503/gd1302001201.pdf
74. Schneider, C., Oellerich, T., Baldauf, H. M., Schwarz, S. M., Thomas, D., Flick, R., Bohnenberger, H., Kaderali, L., Stegmann, L., Cremer, A., Martin, M., Lohmeyer, J.,

Michaelis, M., Hornung, V., Schliemann, C., Berdel, W. E., Hartmann, W., Wardelmann, E., Comoglio, F., … Cinatl, J. (2017). SAMHD1 is a biomarker for cytarabine response and a therapeutic target in acute myeloid leukemia. *Nature Medicine*, *23*(2), 250–255. https://doi.org/10.1038/nm.4255

75. Schröder, J. K., Kirch, C., Seeber, S., & Schütte, J. (1998). Structural and functional analysis of the cytidine deaminase gene in patients with acute myeloid leukaemia. *British Journal of Haematology*, *103*, 1096–1103. https://doi.org/10.1046/j.1365-2141.1998.01084.x
76. Shlush, L. I., Mitchell, A., Heisler, L., Abelson, S., Ng, S. W. K., Trotman-Grant, A., Medeiros, J. J. F., Rao-Bhatia, A., Jaciw-Zurakowsky, I., Marke, R., McLeod, J. L., Doedens, M., Bader, G., Voisin, V., Xu, C., McPherson, J. D., Hudson, T. J., Wang, J. C. Y., Minden, M. D., & Dick, J. E. (2017). Tracing the origins of relapse in acute myeloid leukaemia to stem cells. *Nature*, *547*(7661), 104–108. https://doi.org/10.1038/nature22993
77. Short, N. J., & Kantarjian, H. (2021). When Less Is More: Reevaluating the Role of Intensive Chemotherapy for Older Adults With Acute Myeloid Leukemia in the Modern Era. *Journal of Clinical Oncology*, *39*(28), 3104–3108. https://doi.org/10.1200/JCO.21
78. Short, N. J., Rytting, M. E., & Cortes, J. E. (2018). Acute myeloid leukaemia. *The Lancet*, *392*(10147), 593–606. https://doi.org/10.1016/S0140-6736(18)31041-9
79. Simbulan-Rosenthal, C. M., Dakshanamurthy, S., Gaur, A., Chen, Y.-S., Fang, H.-B., Abdussamad, M., Zhou, H., Zapas, J., Calvert, V., Petricoin, E. F., Atkins, M. B., Byers, S. W., & Rosenthal, D. S. (2017). The repurposed anthelmintic mebendazole in combination with trametinib suppresses refractory NRAS Q61K melanoma. *Oncotarget*, *8*(8), 12576–12595. www.impactjournals.com/oncotarget/
80. Singh, M., Chaudhry, P., & Merchant, A. A. (2016). Primary cilia are present on human blood and bone marrow cells and mediate Hedgehog signaling. *Experimental Hematology*, *44*(12), 1181–1187. https://doi.org/10.1016/j.exphem.2016.08.009
81. Sumimoto, Y., Okawa, S., Inoue, T., Masuda, K., Maruyama, M., & Higaki, K. (2022). Extensive improvement of oral bioavailability of mebendazole, a brick dust, by polymer-containing SNEDDS preparation: Disruption of high crystallinity by utilizing its counter ion. *European Journal of Pharmaceutics and Biopharmaceutics*, *172*, 213–227. https://doi.org/10.1016/j.ejpb.2022.02.002
82. Taipale, M., Jarosz, D. F., & Lindquist, S. (2010). HSP90 at the hub of protein homeostasis: Emerging mechanistic insights. *Nature Reviews Molecular Cell Biology*, *11*(7), 515–528. https://doi.org/10.1038/nrm2918
83. Teglund, S., & Toftgård, R. (2010). Hedgehog beyond medulloblastoma and basal cell carcinoma. *Biochimica et Biophysica Acta - Reviews on Cancer*, *1805*(2), 181–208. https://doi.org/10.1016/j.bbcan.2010.01.003
84. Walf-Vorderwülbecke, V., Pearce, K., Brooks, T., Hubank, M., Van Den Heuvel-Eibrink, M. M., Zwaan, C. M., Adams, S., Edwards, D., Bartram, J., Samarasinghe, S., Ancliff, P., Khwaja, A., Goulden, N., Williams, G., De Boer, J., & Williams, O. (2018). Targeting acute myeloid leukemia by drug-induced c-MYB degradation. *Leukemia*, *32*(4), 882–889. https://doi.org/10.1038/leu.2017.317
85. Wellbrock, J., Latuske, E., Kohler, J., Wagner, K., Stamm, H., Vettorazzi, E., Vohwinkel, G., Klokow, M., Uibeleisen, R., Ehm, P., Riecken, K., Loges, S., Thol, F., Schubert, C., Amling, M., Jucker, M., Bokemeyer, C., Heuser, M., Krauter, J., & Fiedler, W. (2015). Expression of hedgehog pathway mediator GLI represents a negative prognostic marker in human acute myeloid leukemia and its inhibition exerts Antileukemic effects. *Clinical Cancer Research*, *21*(10), 2388–2398. https://doi.org/10.1158/1078-0432.CCR-14-1059

86. Wong, S. Y., Seol, A. D., So, P. L., Ermilov, A. N., Bichakjian, C. K., Epstein, E. H., Dlugosz, A. A., & Reiter, J. F. (2009). Primary cilia can both mediate and suppress Hedgehog pathway-dependent tumorigenesis. *Nature Medicine*, *15*(9), 1055–1061. https://doi.org/10.1038/nm.2011
87. Xie, J., Johnson, R. L., Zhang, X., Bare, J. W., Waldman, F. M., Cogen, P. H., Menon, A. G., Warren, R. S., Chen, L.-C., Scott, M. P., & Epstein, E. H. (1997). Mutations of the PATCHED Gene in Several Types of Sporadic Extracutaneous Tumors. *Cancer Research*, *57*, 2369–2372. http://aacrjournals.org/cancerres/article-pdf/57/12/2369/2463642/cr0570122369.pdf
88. Xie, J., Murone, M., Luoh, S.-M., Ryan, A., Gu, Q., Zhang, C., Bonifas, J. M., Lamk, C.-W., Hynes, M., Goddard, A., Rosenthal, A., Epstein, E. H., & De Sauvage, F. J. (1998). Activating Smoothened mutations in sporadic basal-cell carcinoma. *NATURE*, *391*, 90–92. http://www.nature.com
89. Yoon, C., Park, D. J., Schmidt, B., Thomas, N. J., Lee, H. J., Kim, T. S., Janjigian, Y. Y., Cohen, D. J., & Yoon, S. S. (2014). CD44 expression denotes a subpopulation of gastric cancer cells in which Hedgehog signaling promotes chemotherapy resistance. *Clinical Cancer Research*, *20*(15), 3974–3988. https://doi.org/10.1158/1078-0432.CCR-14-0011
90. Zahreddine, H. A., Culjkovic-Kraljacic, B., Assouline, S., Gendron, P., Romeo, A. A., Morris, S. J., Cormack, G., Jaquith, J. B., Cerchietti, L., Cocolakis, E., Amri, A., Bergeron, J., Leber, B., Becker, M. W., Pei, S., Jordan, C. T., Miller, W. H., & Borden, K. L. B. (2014). The sonic hedgehog factor GLI1 imparts drug resistance through inducible glucuronidation. *Nature*, *511*(7507), 90–93. https://doi.org/10.1038/nature13283
91. Zhang, W., Yu, F., Wang, Y., Zhang, Y., Meng, L., & Chi, Y. (2018). Rab23 promotes the cisplatin resistance of ovarian cancer via the Shh-Gli-ABCG2 signaling pathway. *Oncology Letters*, *15*, 5155–5160. https://doi.org/10.3892/ol.2018.7949
92. Zhao, C., Blum, J., Chen, A., Kwon, H. Y., Jung, S. H., Cook, J. M., Lagoo, A., & Reya, T. (2007). Loss of β-Catenin Impairs the Renewal of Normal and CML Stem Cells In Vivo. *Cancer Cell*, *12*(6), 528–541. https://doi.org/10.1016/j.ccr.2007.11.003
93. Zhao, C., Chen, A., Jamieson, C. H., Fereshteh, M., Abrahamsson, A., Blum, J., Kwon, H. Y., Kim, J., Chute, J. P., Rizzieri, D., Munchhof, M., VanArsdale, T., Beachy, P. A., & Reya, T. (2009). Hedgehog signalling is essential for maintenance of cancer stem cells in myeloid leukaemia. *Nature*, *458*(7239), 776–779. https://doi.org/10.1038/nature07737
94. Zhao, X., Ponomaryov, T., Ornell, K. J., Zhou, P., Dabral, S. K., Pak, E., Li, W., Atwood, S. X., Whitson, R. J., Chang, A. L. S., Li, J., Oro, A. E., Chan, J. A., Kelleher, J. F., & Segal, R. A. (2015). RAS/MAPK activation drives resistance to Smo inhibition, metastasis, and tumor evolution in Shh pathway-dependent tumors. *Cancer Research*, *75*(17), 3623–3635. https://doi.org/10.1158/0008-5472.CAN-14-2999-T
95. Zhou, X.-T., Ding, J., Li, H. Y., Zuo, J. L., Ge, S. Y., Jia, H. L., & Wu, J. (2020). Hedgehog signalling mediates drug resistance through targeting TAP1 in hepatocellular carcinoma. *Journal of Cellular and Molecular Medicine*, *24*(7), 4298–4311. https://doi.org/10.1111/jcmm.15090
96. Zimmermann, S. C., Tichý, T., Vávra, J., Dash, R. P., Slusher, C. E., Gadiano, A. J., Wu, Y., Jančařík, A., Tenora, L., Monincová, L., Prchalová, E., Riggins, G. J., Majer, P., Slusher, B. S., & Rais, R. (2018). N-Substituted Prodrugs of Mebendazole Provide Improved Aqueous Solubility and Oral Bioavailability in Mice and Dogs. *Journal of Medicinal Chemistry*, *61*(9), 3918–3929. https://doi.org/10.1021/acs.jmedchem.7b01792

5. Erklärung des Eigenanteils

Originalarbeit 1: Downregulation of GLI3 Expression Mediates Chemotherapy Resistance in Acute Myeloid Leukemia; Freisleben et al., Int. J. Mol. Sci. 2020, 21(14), 5084

Konzeptualisierung	Fabian Freisleben, Walter Fiedler, Jasmin Wellbrock
Datenerhebung / Methoden	Fabian Freisleben, Jana Muschhammer, Vanessa Thaden
Datenvalidierung	Fabian Freisleben, Walter Fiedler, Jasmin Wellbrock, Jana Muschhammer, Vanessa Thaden.
Datenanalyse	Fabian Freisleben, Jasmin Wellbrock
Betreuung	Jasmin Wellbrock, Walter Fiedler, Lena Behrmann, Carsten Bokemeyer
Schreiben	
Erster Entwurf	Fabian Freisleben, Walter Fiedler, Jasmin Wellbrock
Durchsicht / Bearbeitung	Lena Behrmann, Vanessa Thaden, Jana Muschhammer, Carsten Bokemeyer
Visualisierung / Grafiken	Fabian Freisleben, Walter Fiedler, Jasmin Wellbrock

Originalarbeit 2: Mebendazole Mediates Proteasomal Degradation of GLI Transcription Factors in Acute Myeloid Leukemia; Freisleben et al., Int. J. Mol. Sci. 2021, 22(19), 10670

Konzeptualisierung	Fabian Freisleben, Karl N. Kirschner, Jasmin Wellbrock, Walter Fiedler
Datenerhebung / Methoden	Fabian Freisleben, Jana Muschhammer, Alexander Krispien, Karl N. Kirschner
Software	Karl N. Kirschner (molekulare Bindungsanalyse), Fabian Freisleben (Evaluation Wirkstoffkombinationen mittels CompuSyn)
Datenvalidierung	Fabian Freisleben, Franziska Modemann, Hauke Stamm, Franziska Brauneck, Carsten Bokemeyer, Karl N. Kirschner, Jasmin Wellbrock, Walter Fiedler
Datenanalyse	Fabian Freisleben, Franziska Modemann
Betreuung	Hauke Stamm, Jasmin Wellbrock and Walter Fiedler
Schreiben	
Erster Entwurf	Fabian Freisleben, Karl N. Kirschner, Jasmin Wellbrock, Walter Fiedler
Durchsicht / Bearbeitung	Franziska Modemann, Jana Muschhammer, Hauke Stamm, Franziska Brauneck, Alexander Krispien, Carsten Bokemeyer
Visualisierung / Grafiken	Fabian Freisleben, Karl N. Kirschner

6. Danksagung

Zuerst möchte ich mich ganz besonders bei PD Dr. Jasmin Wellbrock und Prof. Walter Fiedler für die Betreuung und Unterstützung bedanken, die ihr mir während meiner Promotion zuteil habt werden lassen. Euer offenes Ohr und eure Unterstützung bei Herausforderungen waren mir eine große Hilfe. Ich konnte immer eigene Ideen einbringen, wobei ihr mich unterstützt und mich mit wertvollen Ratschlägen und eurer jahrelangen Expertise begleitet habt. Eure Begeisterung für die Forschung ist ansteckend und hat mir sehr viel Spaß bereitet. Ihr standet in wichtigen Momenten hinter mir und habt euch für mich eingesetzt. Ich bin sehr dankbar dafür, euch als meine wissenschaftlichen Mentoren gehabt zu haben.

Ein großer Dank geht auch an Jana Muschhammer, die mich in ein großes Arsenal an Methoden im Labor eingeführt hat. Ich werde die gemeinsamen qPCR-Marathons, unzähligen Prolis und die unterhaltsamen Gespräche nicht vergessen. Der Dank geht natürlich auch an Vanessa Thaden, die mich immer mit vollem Einsatz unterstützt hat. Eure Arbeit mit viel Liebe zum Detail und euer Engagement haben mir in einer Zeit geholfen, als ich selbst den Berg an Arbeit kaum bewältigen konnte.

Dr. Hauke Stamm, du hast mich in den Anfängen von dem unterstützt, was sich zu einem neuen vielversprechenden Projekt entwickeln sollte. Dein Vertrauen und deine Ratschläge haben mir sehr geholfen und den Grundstein für einen großen Teil dieser Arbeit gelegt. Dr. Franziska Modemann, der spannende fachliche Austausch und die enge Zusammenarbeit mit dir haben großen Spaß gemacht. An dieser Stelle möchte ich allen weiteren Mitgliedern der AG Akute Leukämien, meiner wissenschaftlichen Heimat in Hamburg, danken: Meinen Mitdoktoranden Alexander Krispien, Leonie Ramke und Nader Attar, und darüber hinaus Franziska Brauneck, Gabi Vohwinkel, Lena Behrmann, Zoran Knezevic und Frauke Fuchs. Ich habe sehr gerne mit euch zusammengearbeitet!

Dr. Karl N. Kirschner, die Kooperationen mit Ihnen hat sehr viel Spaß gemacht. Ihre Begeisterung für ihr Fach, Ihre große Hilfsbereitschaft und Ihre wertvollen Ratschläge haben das Projekt sehr bereichert.

Ein besonderer Dank geht an die deutsche José Carreras Stiftung (in Kooperation mit der Deutschen Gesellschaft für Hämatologie und Onkologie) für die Möglichkeiten, die ich durch Ihr Promotionsstipendien erhalten habe. Die finanzielle Unterstützung durch Ihre Stiftung war für mich von unschätzbarem Wert und hat mir ermöglicht, mich ein Jahr voll und ganz auf meine Forschung konzentrieren zu können. In diesem Jahr konnte ich den Grundstein für alle Ergebnisse und Möglichkeiten legen, die sich daraus ergeben haben.

Ein großer Dank geht auch an das Comprehensive Cancer Center Hamburg (CCCH) für die einzigartige Möglichkeit meine Arbeit dort im jährlichen wissenschaftlichen Retreat vorzustellen und die Auszeichnung und Förderung meiner Arbeit mittels des Hubertus-Wald-Preises. Ich war überwältigt von der Menge an positiver Rückmeldung.

Ohne meine Frau Claudi wäre diese Promotion nicht möglich gewesen. Danke für all deine Unterstützung in dieser Zeit. Dein Verständnis, wenn mich das Labor wieder verschluckt hatte, deine Ermutigung in schwierigen Phasen und deine grenzenlose Liebe waren das Fundament für diese Arbeit. Danke, dass du mich auf dieser Reise begleitet hast und mir durch dick und dünn immer zur Seite standest. Ich bin so glücklich, dich in meinem Leben zu haben - ich hätte mir keine bessere Partnerin wünschen können.

7. Lebenslauf

Lebenslauf aus datenschutzrechtlichen Gründen nicht enthalten

8. Eidesstattliche Versicherung

Ich versichere ausdrücklich, dass ich die Arbeit selbständig und ohne fremde Hilfe verfasst, andere als die von mir angegebenen Quellen und Hilfsmittel nicht benutzt und die aus den benutzten Werken wörtlich oder inhaltlich entnommenen Stellen einzeln nach Ausgabe (Auflage und Jahr des Erscheinens), Band und Seite des benutzten Werkes kenntlich gemacht habe.
Ferner versichere ich, dass ich die Dissertation bisher nicht einem Fachvertreter an einer anderen Hochschule zur Überprüfung vorgelegt oder mich anderweitig um Zulassung zur Promotion beworben habe.
Ich erkläre mich einverstanden, dass meine Dissertation vom Dekanat der Medizinischen Fakultät mit einer gängigen Software zur Erkennung von Plagiaten überprüft werden kann.

Unterschrift: .....